Geodesic Pathways through the Potential Energy Landscape of Liquid Crystal Formers

Layne Frechette

April 2015

Abstract

In this work, we explore the inherent dynamics of liquid crystal formers using geodesic theory. We locate geodesics (shortest paths) through the potential energy landscape ensembles of the isotropic liquid and nematic liquid crystal phases of a liquid crystal forming system. One expects that the differences in properties of these paths between the liquid and liquid crystal phases will yield insight into how molecular motion differs between these phases. What is found is that, while it yields results for the isotropic liquid phase which are consistent with previous studies on linear (diatomic) molecules [1],[2], the current formulation of geodesic theory for linear molecules does not correctly capture the inherent dynamics of liquid crystals, and a modification of the current theory is necessary in order to describe these dynamics.

Contents

1 Introduction

Traditionally, all matter has been classified as being in one of three states: solid, liquid, and gas. These classifications are based on the degree of order in a substance. The atoms or molecules that make up (crystalline) solids are arranged in regular and rather fixed patterns; those that make up fluids are arranged in more random fashions. However, certain substances exhibit phases which do not fit neatly into this simple classification - these are called *mesophases*. One interesting class of mesophases is *liquid crystal* phases. These phases are characterised by having high orientational order, but (varying degrees of) translational disorder. In this thesis, we will focus on the *nematic* liquid crystal phase, in which molecules posess a high degree of orientational order but are completely translationally disordered. For information on other liquid crystal phases, see [3].

It is interesting to consider how the motion of molecules in a normal liquid of linear molecules differs from that in a liquid crystal. In the nematic liquid crystal phase, rotational motion is much more restricted than it is in the liquid phase, as reflected by the very different rotational diffusion constants of these phases (see Appendix A.) In order to better understand molecular motion in liquid crystals, we analyze pathways through the potential energy landscape of a liquid-crystal forming system. The theory of shortest pathways (geodesics) through the potential energy landscapes of linear molecules has already been investigated [1],[2]. The conclusion of this study was that the shortest, most efficient pathways - which represent the "inherent dynamics" of the liquid (the dynamics that remain after filtering out thermal motion [1]) - are ones in which molecules execute just enough rotation to translate along their long axes through narrow "channels" in the liquid. However, one might expect that in the rotationally restricted liquid crystal phase, there would be even less molecular rotation compared to translation than in a normal liquid.

In this thesis, we shall first some of the phenomenology of liquid crystals and the model we use to simulate them. We will then discuss the potential energy landscape ensemble and geodesic theory for linear molecules. Next, we review the geodesic path-finding algorithm for linear molecules. Finally, we present our findings about geodesics through liquid crystal potential energy landscapes. In the appendices we include detailed results of a molecular dynamics simulation of our liquid crystal model, an analysis of the efficiency of part of our path-finding algorithm, and several key derivations.

1.1 Reduced Units

I have defined the quantities in this simulation in terms of the following units: σ_0, which defines the length scale; ϵ_0 which defines the energy scale; m, the mass of each of the molecules; and I, the moment of inertia of each of the molecules. All other units are defined in terms of these four units:

$$\begin{aligned}
r^* &= r/\sigma_0 && distance \\
E^* &= E/\epsilon_0 && energy \\
\rho^* &= \rho\sigma_0^3 && density \\
t^* &= \sqrt{\frac{\epsilon_0}{m\sigma_0^2}}t = t/\tau && time \\
T^* &= k_B T/\epsilon_0 && temperature \\
p^* &= p\sigma_0^3/\epsilon_0 && pressure \\
D_T^* &= D_T\sigma_0^{-2}\tau && translational\ diffusion\ constant \\
D_R^* &= D_R\tau && rotational\ diffusion\ constant
\end{aligned}$$

I used $\sigma_0 = \epsilon_0 = m = I = 1$ in my simulations. Additionally, I used $N = 256$ molecules for all simulations. For isotropic liquids I used $T^* = 1.00$, $\rho^* = 0.28$, and for nematic liquid crystals I used $T^* = 1.00$, $\rho^* = 0.34$.

2 Liquid Crystals

2.1 Phenomenology

In an *isotropic* liquid, molecules have no prefered direction of alignment. However, certain chemical species exhibit phases where the orientations of the constitutent molecules, which have an ellipsoidal or rod-like shape, tend to point in a single direction, called the *director*. This orientationally ordered phase is called a *nematic* phase. The degree of ordering in a nematic phase is characterized by a quantity called the *order parameter* S, which is defined as:

$$S = \frac{1}{N}\sum_{i=1}^{N}\left\langle \frac{3}{2}\cos^2\theta_i - \frac{1}{2}\right\rangle$$

where N is the number of molecules, θ_i is the angle that the ith molecule makes with the director, and $\langle\cdot\rangle$ represents an ensemble average.

2.2 The Gay-Berne Model

The Gay-Berne potential (see [4]) is a anisotropic, single-site model of ellipsoidal molecules. Its form is similar to that of the Lennard-Jones potential. Let $\vec{r}$ be the separation vector between two molecules, let $r = |\vec{r}|$, let $\hat{r} = \vec{r}/r$, and let $\hat{\Omega}_\alpha$ be the orientation vector of the αth molecule. This geometry in shown in Fig. 1. The potential between the ith and jth molecules is given by:

$$u(\vec{r}, \hat{\Omega}_i, \hat{\Omega}_j) = 4\epsilon^\nu(\hat{\Omega}_i, \hat{\Omega}_j)\epsilon'^\mu(\hat{r}, \hat{\Omega}_i, \hat{\Omega}_j) \times \left[\left(\frac{\sigma_0}{r - \sigma(\hat{r}, \hat{\Omega}_i, \hat{\Omega}_j) + \sigma_0} \right)^{12} - \left(\frac{\sigma_0}{r - \sigma(\hat{r}, \hat{\Omega}_i, \hat{\Omega}_j) + \sigma_0} \right)^{6} \right]$$

Where:

$$\epsilon(\hat{\Omega}_i, \hat{\Omega}_j) = \epsilon_0 \left[1 - \chi^2 (\hat{\Omega}_i \cdot \hat{\Omega}_j) \right]^{-1/2}$$

$$\epsilon'(\hat{r}, \hat{\Omega}_i, \hat{\Omega}_j) = 1 - \frac{\chi'}{2} \left[\frac{(\hat{r} \cdot \hat{\Omega}_i + \hat{r} \cdot \hat{\Omega}_j)^2}{1 + \chi'(\hat{\Omega}_i \cdot \hat{\Omega}_j)} + \frac{(\hat{r} \cdot \hat{\Omega}_i - \hat{r} \cdot \hat{\Omega}_j)^2}{1 - \chi'(\hat{\Omega}_i \cdot \hat{\Omega}_j)} \right]$$

$$\sigma(\hat{r}, \hat{\Omega}_i, \hat{\Omega}_j) = \sigma_0 \left(1 - \frac{\chi}{2} \left[\frac{(\hat{r} \cdot \hat{\Omega}_i + \hat{r} \cdot \hat{\Omega}_j)^2}{1 + \chi(\hat{\Omega}_i \cdot \hat{\Omega}_j)} + \frac{(\hat{r} \cdot \hat{\Omega}_i - \hat{r} \cdot \hat{\Omega}_j)^2}{1 - \chi(\hat{\Omega}_i \cdot \hat{\Omega}_j)} \right] \right)^{-1/2}$$

The quantities χ and χ' are anisotropy parameters which determine the range and strength of the interaction, respectively. They are given by:

$$\chi = \frac{(\sigma_\parallel/\sigma_\perp)^2 - 1}{(\sigma_\parallel/\sigma_\perp)^2 + 1}$$

$$\chi' = \frac{(\epsilon_s/\epsilon_e)^{1/\mu} - 1}{(\epsilon_s/\epsilon_e)^{1/\mu} + 1}$$

The quantity $\sigma_\parallel/\sigma_\perp$ is the ratio of the major axis of the Gay-Berne molecule to the minor axis, and the quantity ϵ_s/ϵ_e is the ratio of the depth of the potential well when two molecules are placed side-to-side to the depth of the potential well when two molecules are placed end-to-end.

In this project, I used the length and energy ratios found in the original paper by Gay and Berne [4]:

$$\sigma_\parallel/\sigma_\perp = 3 \implies \chi = 4/5$$

$$\epsilon_s/\epsilon_e = 5 \implies \chi' = \frac{\sqrt{3} - 1}{\sqrt{3} + 1}$$

$$\nu = 1$$

$$\mu = 2$$

The Gay-Berne model produces isotropic liquid and nematic liquid crystal phases, as well as smectic liquid crystal phases. The most easily changed parameter that controls the system's phase is the density. A phase diagram of the Gay-Berne model for the above choice of parameters, reproduced from [5], is shown in Fig. 2.

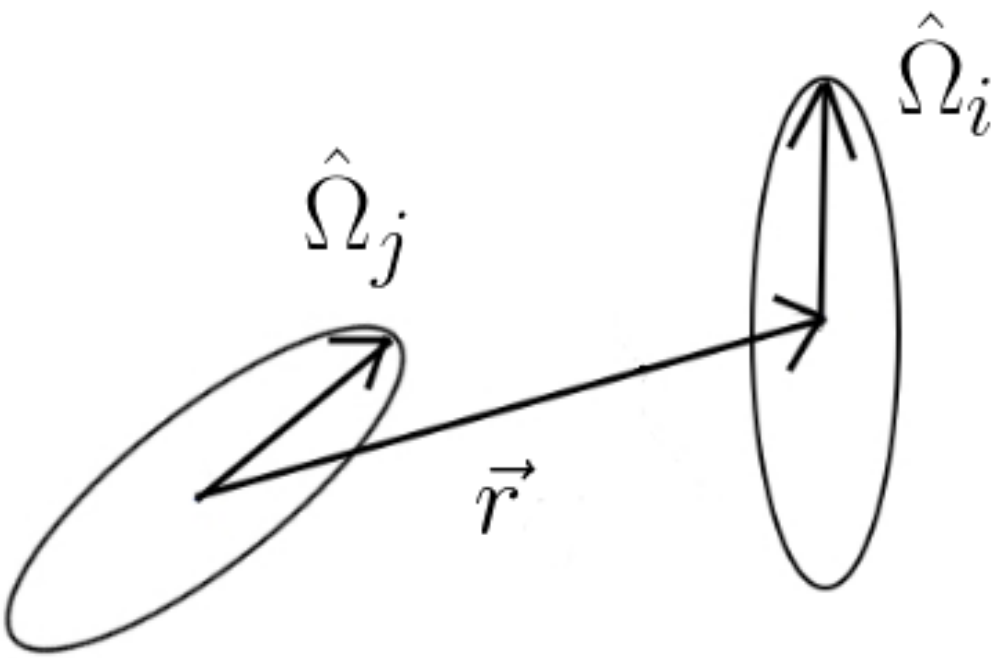

Figure 1: Geometry of a pair of ellipsoidal molecules.

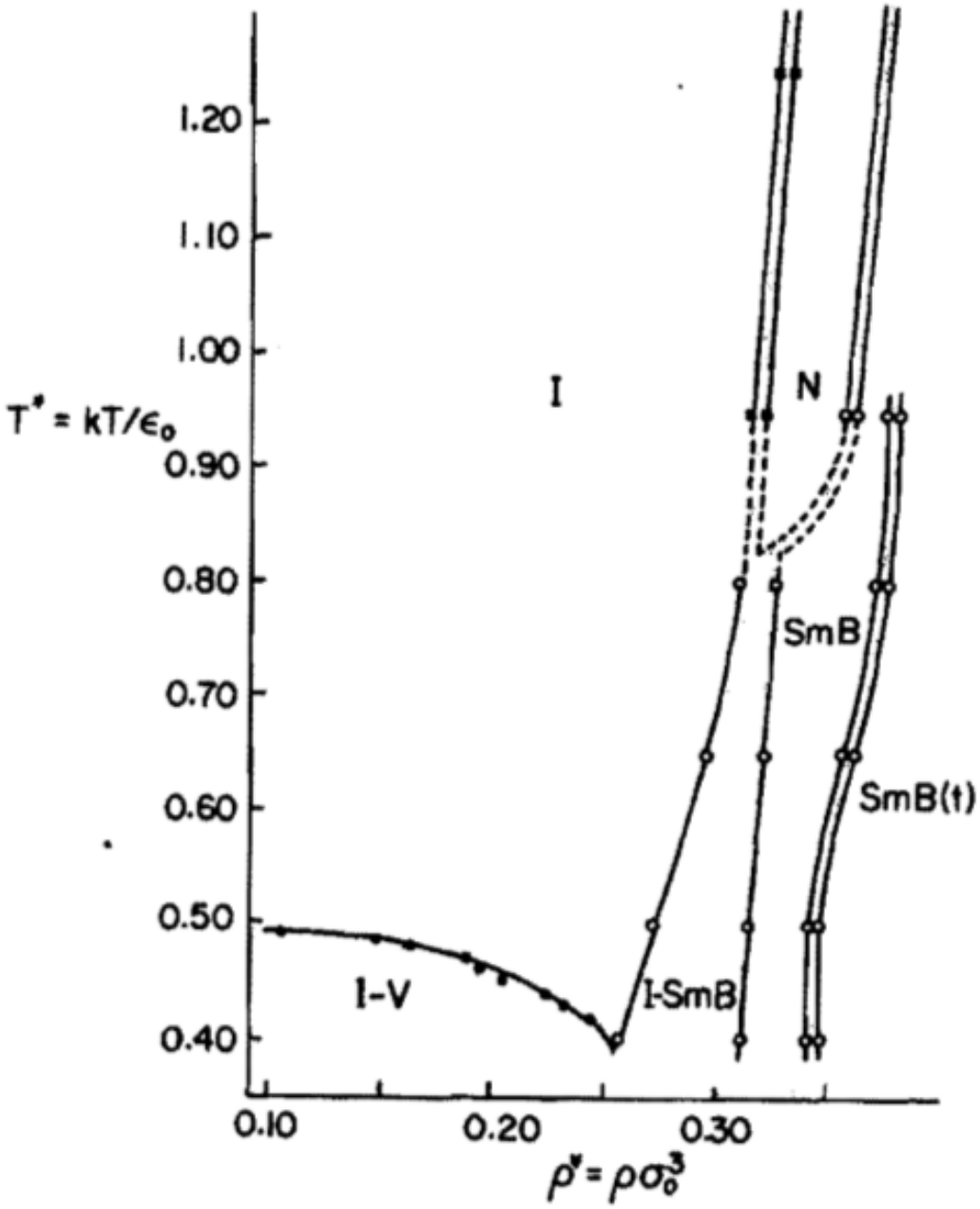

Figure 2: Phase diagram of the Gay-Berne fluid with parameters $\sigma_{\parallel}/\sigma_{\perp} = 3$, $\epsilon_s/\epsilon_e = 5$. The isotropic phase is labelled by I, and the nematic phase is labelled by N. Reprinted from [5].

3 The Potential Energy Landscape Ensemble and Geodesics

One common approach to understanding the dynamics of many-body systems is to locate special points on a system's potential energy landscape: things like energy minima and transition states. However, in many-body systems where the dynamics is dominated by slow diffusion, there are a multitude of energy minima and it is unclear how much information is gained by identifying these points. An alternative approach is to look at *pathways* through the potential energy landscape [6], [7].

3.1 The Potential Energy Landscape Ensemble

The pathways we are interested in are those through what is called the *potential energy landscape ensemble*. This is defined to be the collection of configuration space points, in a system with a constant number of particles N and constant volume V, which have a potential energy less than or equal to a certain *landscape energy*, E_L. Mathematically, this is written as[1]:

$$\{\widetilde{\mathbf{R}} \,|\, U(\widetilde{\mathbf{R}}) \leq E_L\}$$

All configurations satisfying this condition ("allowed" configurations) have equal probability. One can visualize this ensemble by picturing a potential energy landscape which is "filled up" with energy to some level E_L. The ensemble then consists of a "sea" of states all of which are equally allowed, interspersed with forbidden "islands" (which have $U(\widetilde{\mathbf{R}}) > E_L$). A visual representation of the ensemble is shown in figure 3.

3.2 The Path Integral Formulation of Diffusion

What do pathways through the potential energy landscape ensemble tell us? As it turns out, the *shortest* of these pathways, called *geodesics*, yield information about the inherent dynamics of the system. To understand why geodesics, which are *geometric* features of the potential energy landscape, yield information about *dynamics*, let us examine the path integral formulation of diffusion. Consider a particle diffusing in one dimension. It can be shown [8] that the probability density for the particle propagating from an initial position x_0 to a final position x in a time t (i.e. the *Green's function* for the particle) is given by:

$$G(x_0 \to x, t) = \int_{x_0,0}^{x,t} \mathcal{D}[x(\tau)] \exp\left[-\frac{1}{4D}\int_0^t \left(\frac{dx}{d\tau}\right)^2 d\tau\right]$$

Where $\mathcal{D}$ indicates integration over all possible paths, and D is the diffusion constant. If instead of a single particle moving in one dimension we have N particles each moving in three dimensions, then given a configuration space vector $\mathbf{R} = (\vec{r}_1, \ldots, \vec{r}_N)$, $\vec{r}_i \in \mathbb{R}^3$, the Green's function for propagating to this configuration from an initial configuration $\mathbf{R}_0$ in

[1] To refer to a configuration space vector of both positions and orientations for a system of linear molecules, we will use the notation $\widetilde{\mathbf{R}} = (\mathbf{R}, \hat{\mathbf{\Omega}})$, where $\mathbf{R}$ is the set of center-of-mass positions of the molecules and $\hat{\mathbf{\Omega}}$ is the set of molecular orientations.

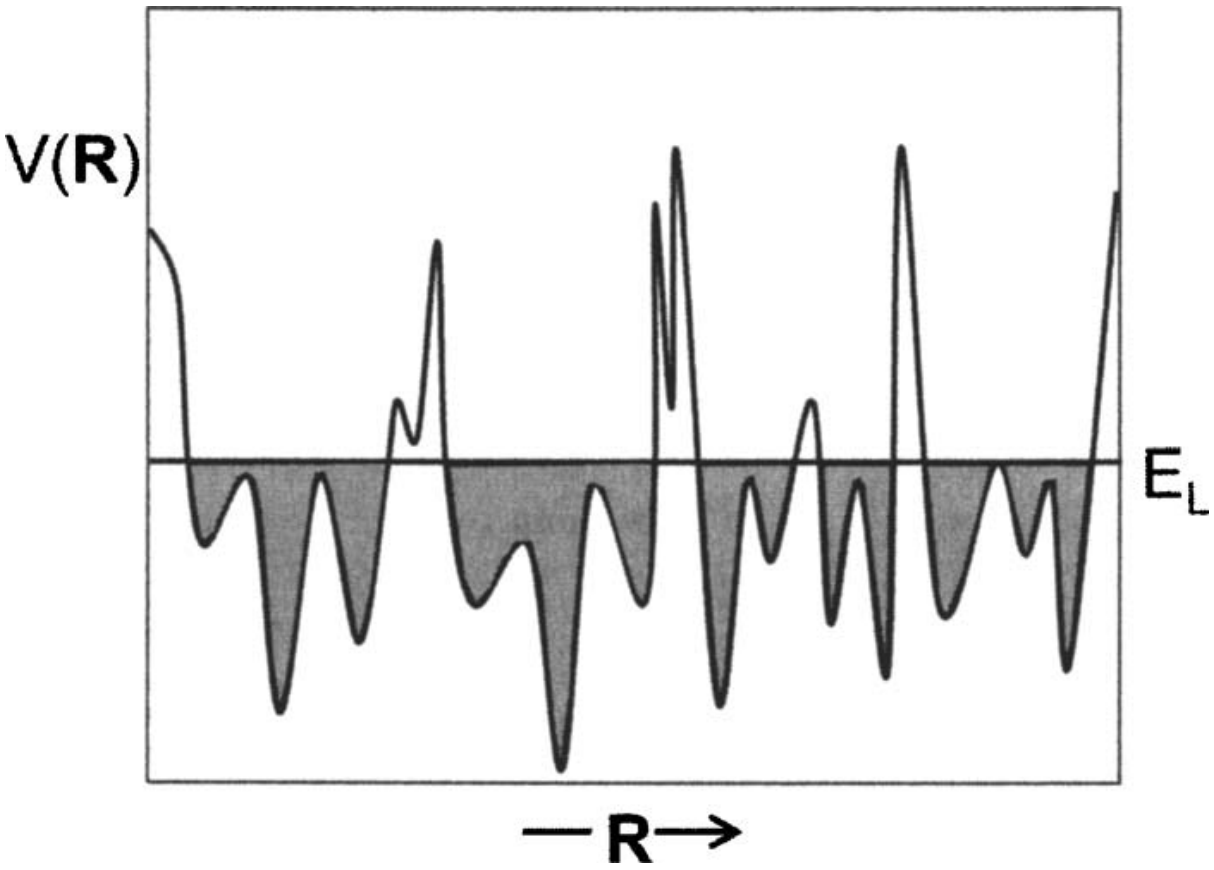

Figure 3: Visualization of the potential energy landscape ensemble. The shaded regions represent allowed configurations. Reprinted from [6].

a time t is given by:

$$G(\mathbf{R}_0 \to \mathbf{R}, t) = \int_{\mathbf{R}_0,0}^{\mathbf{R},t} \mathcal{D}[\mathbf{R}(\tau)] \exp\left[-\frac{1}{4D_T}\int_0^t \left(\frac{d\mathbf{R}}{d\tau}\right)^2 d\tau\right]$$

Where $(d\mathbf{R}/d\tau)^2 = \sum_{i=1}^{N}(d\vec{r}_i/d\tau)^2$ and D_T is the translational diffusion constant. For a system of linear molecules, we need to consider not only translational motion, but also rotational motion. We must therefore come up with a Green's function for rotational diffusion. It turns out (see Appendix C for a derivation) that, given an orientational configuration vector $\hat{\mathbf{\Omega}} = (\hat{\Omega}_1, \ldots, \hat{\Omega}_N)$, the Green's function for diffusion from an initial orientational configuration $\hat{\mathbf{\Omega}}_0$ to $\hat{\mathbf{\Omega}}$ in time t is:

$$G(\hat{\mathbf{\Omega}}_0 \to \hat{\mathbf{\Omega}}, t) = \int_{\hat{\mathbf{\Omega}}_0,0}^{\hat{\mathbf{\Omega}},t} \mathcal{D}[\hat{\mathbf{\Omega}}(\tau)] \exp\left[-\frac{1}{4D_R}\int_0^t \left(\frac{d\hat{\mathbf{\Omega}}}{d\tau}\right)^2 d\tau\right]$$

Where $(d\hat{\mathbf{\Omega}}/d\tau)^2 = \sum_{i=1}^{N}(d\hat{\Omega}_i/d\tau)^2$ and D_R is the rotational diffusion constant.

3.3 Geodesics

Let us consider the terms in the exponentials of the translational and rotational Green's functions. When diffusion is slow, the diffusion constants are small: $D_T, D_R \to 0$. This

tends to make the term in the exponential a large, negative number, which makes the paths' contribution to the Green's function small. The paths that contribute the most to the Green's function, therefore, are the ones for which integrals in the exponentials are small. These integrals are proportional to classical actions:

$$\int_0^t \left(\frac{d\mathbf{R}}{d\tau}\right)^2 d\tau \propto \int_0^t 2K_T(\tau)d\tau$$
$$\int_0^t \left(\frac{d\hat{\mathbf{\Omega}}}{d\tau}\right)^2 d\tau \propto \int_0^t 2K_R(\tau)d\tau$$

Where K_T and K_R are translational and rotational kinetic energies, respectively. Minimizing the integral of a quantity is equivalent to minimizing the integral of its square root; the time integral of the square root of the kinetic energy is proportional to a *kinematic path length* [7]:

$$l_T = \int_0^t \sqrt{2K_T(\tau)}d\tau$$
$$l_R = \int_0^t \sqrt{2K_R(\tau)}d\tau$$

So the dominant paths will be those that minimize these path lengths. These geodesic path lengths are denoted g_T, g_R.

3.4 Diffusion Constants from Geodesic Lengths

One can equate different expressions for the diffusion Green's functions to derive expressions for diffusion constants in terms of geodesic lengths. The translational and rotational diffusion constants are related to the corresponding geodesic lengths to the following formulae:

$$\frac{D_T}{D_{T\,0}} = \lim_{\Delta R\to\infty} \left(\frac{\Delta R}{g_T}\right)^2$$
$$\frac{D_R}{D_{R0}} = \lim_{\Delta\psi\to\infty} \frac{|\Delta\psi|^2}{[g_R/(L/2)]^2}$$

Here, the 0 subscripts denote high-temperature or low-density reference diffusion constants, ΔR is the Euclidean distance between the final and inital center-of-mass positions of two configurations, $\Delta\psi$ is the total angular distance between the initial and final orientations of all the molecules, and g_T and g_R are the translational and rotational geodesic lengths. These formulae, which are derived in Appendix D, illustrate the direct connection between the geometry and dynamics of a molecular liquid.

4 Geodesic Path-Finding Algorithm

How do we actually locate geodesics through the potential energy landscape ensemble? By the Kuhn-Tucker theorem, the geodesics will consist of unions of straight line segments (through the "sea" of allowed configurations) and segments along the boundaries of obstacles (the "islands") [7]. We can thus divide the path-finding algorithm into a part for calculating the free particle path and a part for calculating the path along the boundaries.

4.1 Endpoint Generation

To begin, we need to generate pairs of configuration space points between which to compute a path. This was done via molecular dynamics simulation (see Appendix A.) To obtain the endpoints for a given Euclidean distance, $\Delta\widetilde{R}$, 16 molecular dynamics trajectories, each with different, randomly seeded intial conditions, was run. From each of these trajectories, 4 endpoint pairs were chosen, giving a total of 64 endpoint pairs for each value of $\Delta\widetilde{R}$. To ensure that the pairs selected from each trajectory were statistically independent, the ending point of one pair and the start point of another were separated by 50τ along the trajectory.

4.2 Free Particle Motion

The motion in the allowed regions of configuration space is just free-particle motion:

$$\begin{aligned}\vec{r}_j(\tau) &= (1-\tau)\vec{r}_{j,0} + \tau\vec{r}_{j,f} \\ \hat{\Omega}_j(\tau) &= \frac{\sin[\Delta\psi_j(1-\tau)]\hat{\Omega}_{j,0} + \sin[\Delta\psi_j\tau]\hat{\Omega}_{j,f}}{\sin[\Delta\psi_j]} \\ j &= 1,\ldots,N\end{aligned}$$

Here, the 0 subscript denotes an initial value and the f subscript denotes a final value, $\Delta\psi_j$ is the angle between $\hat{\Omega}_{j,0}$ and $\hat{\Omega}_{j,f}$, and τ is a progress variable which ranges from 0 to 1. For a derivation, see [1]. In the algorithm we use, the system takes free particle steps of total length $5\times10^{-3}\sigma_0$ until it lands in a forbidden region, at which point we must deal with motion along the boundary as described below.

4.3 Motion Along Boundaries

To deal with motion along the boundary, we use a Newton-Raphson root-finding scheme, the details and derivation of which can be found in [1]. Basically, if the system takes a free-particle step and finds itself in a forbidden region, then a Newton-Raphson root search is used to take it to the point on the boundary the shortest distance away. Working out the magnitude and direction of this "escape step," one finds that the positions and orientations of the molecules must change in the following way:

$$\begin{aligned}\Delta\vec{r}_j &= -\left(\frac{I}{m}\right)\gamma\vec{F}_j \\ \Delta\hat{\Omega}_j &= (\cos(\Delta\psi_j)-1)\hat{\Omega}_{0,j} + \sin(\Delta\psi_j)\hat{G}_j^{\perp} \\ j &= 1,\ldots,N\end{aligned}$$

Where:

$$
\begin{aligned}
\sin(\Delta\psi_j) &= -\gamma \left| \hat{G}_j^{\perp} \right| \\
\cos(\Delta\psi_j) &= \sqrt{1 - \left(\gamma \left| \hat{G}_j^{\perp} \right| \right)^2} \\
\gamma &= \frac{\Delta U}{\left(\frac{I}{m}\right) F^2 + (G^{\perp})^2} \\
F^2 &= \sum_j \left| \vec{F}_j \right|^2 \\
(G^{\perp})^2 &= \sum_j \left| \vec{G}_j^{\perp} \right|^2 \\
\vec{F}_j &= \sum_{k \neq j} \vec{f}_k \\
\vec{G}_j^{\perp} &= \sum_{k \neq j} \vec{g}_k^{\perp} \\
(\vec{f}_k)_\mu &= -\frac{\partial U}{\partial r_{k,\mu}} \\
(\vec{g}_k)_\mu &= -\frac{\partial U}{\partial \Omega_{k,\mu}} \\
\vec{g}_k^{\perp} &= \vec{g}_k \cdot (\mathbb{1} - \hat{\Omega}_k \hat{\Omega}_k)
\end{aligned}
$$

Here, $m = 1$ is the mass of a molecule, $I = 1$ is the moment of inertia of a molecule, $\sqrt{I/m}$ is a quantity which is functionally equivalent to $L/2$, half the bond length, for a diatomic molecule in [1], and $\Delta U = E_L - U(\widetilde{\mathbf{R}})$ is the difference in potential energy between the configuration at its current "forbidden" location and the potential energy at the boundary. We have $\Delta U < 0$ and $U(\widetilde{\mathbf{R}}) > E_L$ for a forbidden configuration. In the equations for $\vec{F}_j$ and $\vec{G}_j^{\perp}$, the sum is over the forces and auxiliary torques from all the other molecules acting on molecule j. When the molecular positions and orientations are changed by the prescribed amounts $\Delta\vec{r}_j$ and $\Delta\hat{\Omega}_j$, the potential is lowered to the value of the landscape energy.[2]

4.4 Optimization

The algorithm described above is guaranteed to find paths which satisfy the Kuhn-Tucker theorem; however, this is a necessary but not sufficient condition for paths to be geodesics. In order to locate the "true" geodesics we optimize the paths found using the above algorithm by making Monte Carlo moves. A single configuration along the unoptimized "candidate geodesic" path is selected at random, and one of the molecules is selected at random. The position and orientation of the selected molecule are then perturbed by the following amounts:

[2]In practice, since these equations are linear approximations, it may take a few iterations to make the potential sufficiently close to the landscape energy. Thus this escape step procedure is repeated until the potential is within some tolerance of the landscape energy: $(U(\widetilde{\mathbf{R}}) - E_L)/|E_L| < \delta_E$. We set $\delta_E = 10^{-6}$ in this work.

$$\delta\vec{r} = 0.01\sigma_0$$
$$\delta\psi = \delta\vec{r}/\sqrt{I/m}$$

Where the rotation by $\delta\psi$ is performed about a an axis $\hat{v}$ perpendicular to the orientation vector, chosen randomly by generating a random unit vector $\hat{\lambda}$ on the surface of a sphere (see [9] for details) and then calculating:

$$\hat{v} = \hat{\Omega}_j \times \hat{\lambda}$$

Next, we apply apply the path-finding algorithm to compute the distance between the starting point and the perturbed configuration, and the distance between the perturbed configuration and the end point. If the sum of these distances is less than the original geodesic distance, then we take the union of the two paths to be the new geodesic path, and throw out the old one. Otherwise, we keep our original geodesic path. We repeat this process 10 times.

This algorithm is nearly identical to the one used in [1]. One significant difference, however, is that in [1] when a geodesic pathway through the perturbed configuration was unable to be located, i.e. the algorithm got "stuck," the entire optimization procedure was restarted. We do not do this - when the algorithm is unable to find a path through the perturbed configuration, we simply attempt a new trial move, and count the "unsuccessful" trial as a trial move. (That is, we make 10 trial moves regardless of whether a move successfully locates a path or not.)

In practice, these optimizations change the geodesic path lengths only slightly; see Appendix B for further discussion.

4.5 Path Lengths

To compute geodesic path lengths, we simply sum the distances between successive configurations along the geodesic path. Assuming that there are M total configurations, and N total molecules, the geodesic path lengths are computed as:

$$g_{trans} = \sum_{m=1}^{M-1} \sqrt{\sum_{i=1}^{N} (\vec{r}_{i,m+1} - \vec{r}_{i,m})^2}$$
$$g_{rot} = \sum_{m=1}^{M-1} \sqrt{\sum_{i=1}^{N} \frac{I}{m} \left(\arccos(\hat{\Omega}_{i,m+1} \cdot \hat{\Omega}_{i,m}) \right)^2}$$
$$g_{total} = \sum_{m=1}^{M-1} \sqrt{\sum_{i=1}^{N} \left[(\vec{r}_{i,m+1} - \vec{r}_{i,m})^2 + \frac{I}{m} \left(\arccos(\hat{\Omega}_{i,m+1} \cdot \hat{\Omega}_{i,m}) \right)^2 \right]}$$

To get the Euclidean distances between endpoint configurations, we simply use:

$$\Delta\widetilde{R} = \sqrt{\sum_{i=1}^{N}\left[(\vec{r}_{i,f}-\vec{r}_{i,0})^2 + \frac{I}{m}(\arccos\left(\hat{\Omega}_{i,f}\cdot\hat{\Omega}_{i,0}\right)\right)^2\right]}$$

$$\Delta\widetilde{R}_{trans} = \sqrt{\sum_{i=1}^{N}(\vec{r}_{i,f}-\vec{r}_{i,0})^2}$$

$$\Delta\widetilde{R}_{rot} = \sqrt{\sum_{i=1}^{N}\frac{I}{m}(\arccos\left(\hat{\Omega}_{i,f}\cdot\hat{\Omega}_{i,0}\right)\right)^2}$$

4.6 Implementation Details

All code was written in C. For pseudo-random number generation I used the Mersenne Twister implementation found in the GNU Scientific Library [10]. To seed the PRNG, I used "truly random" numbers generated from random.org [11].

5 Results

5.1 Order Parameter along Geodesics

The most significant discovery made in this study was how the order parameter changes as the system traverses a geodesic. In the liquid phase, the order parameter tends to fluctuate about a value close to zero; in the liquid crystal phase, the order parameter fluctuates about a value much closer to one. When one does a molecular dynamics simulation of the Gay-Berne model, this is what one sees (see Fig. 4.) This is also what ones sees along the course of a geodesic pathway between isotropic-phase endpoints. However, this is *not* what one sees along geodesic pathways between nematic-phase endpoints. Along these geodesics, the order parameter starts off at a "normal" nematic value (near 0.8, in this case), then decays to a low, "isotropic" value along the course of the geodesic, gradually climbing back up to its normal value at the final configuration (see Fig. 5.) What this indicates is that the shortest pathway between nematic-phase endpoints, in the potential energy landscape ensemble we have defined, is one which disorders and goes through a normal liquid phase.

But this does not correctly represent the dynamics of the nematic phase! If one wants to investigate molecular motion in an ordered nematic phase, it does not make sense to allow the system to go into a disordered isotropic phase. It appears that we missed an important piece of physics in setting up our problem: constraining the phase that the system can be in along the course of the geodesic. The potential energy landscape ensemble involves an *inequality* constraint: that the potential energy be less than or equal to a particular value. Compare this to, for example, the canonical ensemble, where the occupation of different energy states is controlled by an equality (namely that the temperature be constant.) A particular set of values N, V, and T in the canonical ensemble defines a unique phase; however, this is not the case for the potential energy landscape ensemble.

Particular values of N, V, and E_L in the potential energy landscape ensemble, though, can include configurations which are in different phases; this has been demonstrated for atomic liquids [7]. That this is so is perhaps not too surprising - ensembles tend to yield different thermodynamic results in the vicinity of phase transitions.

In order to keep the system in the nematic phase along the course of its geodesics, we plan to implement a constraint: that the order parameter have a fixed value along the course of the geodesics. We are currently working out how to include this constraint in our path-finding algorithm.

5.2 Geodesic Lengths & Ratios

The following geodesic lengths were calculated:

$$g_{total} = \int_0^t \sqrt{\sum_{j=1}^{N} m \left(\frac{d\vec{r}_j}{d\tau}\right)^2 + \sum_{j=1}^{N} I \left(\frac{d\hat{\Omega}_j}{d\tau}\right)^2}\, d\tau$$

$$g_T = \int_0^t \sqrt{\sum_{j=1}^{N} m \left(\frac{d\vec{r}_j}{d\tau}\right)^2}\, d\tau$$

$$g_R = \int_0^t \sqrt{\sum_{j=1}^{N} I \left(\frac{d\hat{\Omega}_j}{d\tau}\right)^2}\, d\tau$$

$$g_{z^b} = \int_0^t \sqrt{\sum_{j=1}^{N} m \left(\frac{dz_j^b}{d\tau}\right)^2}\, d\tau$$

$$g_{x^b,y^b} = \int_0^t \sqrt{\sum_{j=1}^{N} m \left(\frac{dx_j^b}{d\tau}\right)^2 + m \left(\frac{dy_j^b}{d\tau}\right)^2}\, d\tau$$

$$g_{R||\hat{n}} = \int_0^t \sqrt{\sum_{j=1}^{N} I \left(\frac{d\hat{\Omega}_j}{d\tau} \cdot \hat{n}\hat{n} \cdot \frac{d\hat{\Omega}_j}{d\tau}\right)}\, d\tau$$

$$g_{R\perp\hat{n}} = \int_0^t \sqrt{\sum_{j=1}^{N} I \left(\frac{d\hat{\Omega}_j}{d\tau} \cdot (1 - \hat{n}\hat{n}) \cdot \frac{d\hat{\Omega}_j}{d\tau}\right)}\, d\tau$$

From these lengths, we calculated the following ratios:

$$g_T/g_R$$
$$g_{z^b}/g_{x^b,y^b}$$
$$g_{R||\hat{n}}/g_{R\perp\hat{n}}$$

These are the ratio of translational to rotational length, the ratio of body-fixed z length to body-fixed x and y length, and the ratio of rotational length parallel to the director to the length perpendicular to the director. When these are compared to their equilibrium

contour-length equivalents, they ought to yield mechanistic information about the motion of ellipsoidal molecules in liquid and liquid crystal phases. The equilibrium predictions for the corresponding contour-length ratios are:

$$\begin{aligned} l_T/l_R &= \sqrt{3/2} \\ l_{z^b}/l_{x^b,y^b} &= 1/\sqrt{2} \\ l_{R||\hat{n}}/l_{R\perp\hat{n}} &= 1/\sqrt{2}\,(isotropic) \\ &= \sqrt{\frac{1-S}{2+S}}\,(nematic) \end{aligned}$$

where S is the order parameter in the nematic phase. Derivations of these equilibrium predictions can be found in appendix E.

It should be noted that, although 64 endpoint pairs for computing geodesics were generated for each Euclidean endpoint separation distance and for each phase (isotropic or nematic), a geodesic was not able to be located for every such pair; in some cases our path-finding algorithm failed.[3] The number of successfully located paths (and thus the number of paths averaged over) for each endpoint separation distance and each phase is shown in the table below:

$\Delta\widetilde{R}/\sigma_0$	Isotropic	Nematic
25	63	64
50	61	57
100	61	57
150	56	61
200	56	62
300	50	60
400	56	61
500	59	54

The converged ($\Delta\widetilde{R} = 500\sigma_0$) geodesic ratios, for the optimized paths, are shown below:

	Isotropic	Nematic	Equilibrium value
g_T/g_R	1.918 ± 0.00169	1.723 ± 0.00235	1.225
$g_{z^b}/g_{x^b,y^b}$	1.013 ± 0.00186	1.211 ± 0.00253	0.707
$g_{R\|\|\hat{n}}/g_{R\perp\hat{n}}$	0.705 ± 0.00150	0.462 ± 0.0110	0.707/0.275

The ± indicates standard error. The equilibrium nematic value of $g_{R||\hat{n}}/g_{R\perp\hat{n}}$ (to the right of the slash) used an order parameter of $S = 0.789$. Plots of these ratios, versus their equilibrium predictions, for different values of the endpoint separation, are shown in Figs. 6-8.[4]

I also checked that the ratios of different geodesic lengths to the total endpoint separation distance converged. The results are shown in Figs. 9-15.

[3] If the algorithm failed to travel more than $1.0 \times 10^{-8}\sigma_0$ from its previous location for 1000 steps in a row, then the algorithm was said to have "failed."

[4] Due to time constraints, optimized paths for $\Delta\widetilde{R} = 200\sigma_0, 400\sigma_0$ were not calculated, so length ratios for these values do not appear in the figures.

There are several observations to be made about the above results. Let us begin with the caveat that we cannot draw any real conclusions from the nematic results, since we know that the dynamics are incorrect.

The fact that g_T/g_R is greater than the equilibrium prediction is consistent with Daniel Jacobson's result for diatomic molecules [1]: along geodesics, linear molecules perform just enough rotation to allow them to slide (translate) through narrow "channels." Plots of the bond length-normalized diatomic ratios, compared with the equivalent isotropic Gay-Berne ratio, are shown in Figs. 16 and 17.

Next, we see that the ratio of body-fixed z motion to body-fixed x and y motion is larger than the equilibrium prediction (in both the isotropic and nematic phases.) This tells us that the molecules of a Gay-Berne fluid tend to translate in a direction parallel to their long axis, in accord with our picture of molecules threading their way through narrow channels.

The ratio of rotational motion parallel to the director to rotational motion perpendicular to the director exhibits interesting behavior. For the isotropic case, the geodesic ratio is identical to the equilibrium prediction. This is as it should be - in the isotropic phase, one does not have a well-defined director (in the sense that the molecules do not tend to line up in a particular direction - one can still calculate an instantaneous director as an eigenvector of the Q tensor, but it is essentially an arbitrary axis) and so we would not expect the geodesic result to differ from the equilibrium prediction.

Examining the convergence of $g_{R||\hat{n}}/g_{R\perp\hat{n}}$ in the nematic case, we see that the geodesic result agrees, more or less, with the equilibrium prediction for small $\Delta\widetilde{R}$, but as $\Delta\widetilde{R}$ increases, the nematic ratio converges to a value larger than that of the equilibrium prediction. Thus, $d\hat{\Omega}/dt$ is parallel to the director more often than one expects. But this means (see Fig. 18) that $\hat{\Omega}$ is spending more time perpendicular to the director, contrary to the notion that molecules in the nematic phase spend most of their time nearly parallel to the director! This behavior makes sense in light of the fact that the order parameter along the nematic geodesic decays to an isotropic value.[5]

5.3 Diffusion Constants

The geodesic predictions for the diffusion constants, using the lengths of the optimized paths for $\Delta\widetilde{R} = 500\sigma_0$, are:

$$\frac{D_T^{iso*}}{D_{T\,0}^*} \approx 0.374 \quad \frac{D_T^{nem*}}{D_{T\,0}^*} \approx 0.239$$
$$\frac{D_R^{iso*}}{D_{R\,0}^*} \approx 0.00417 \quad \frac{D_R^{nem*}}{D_{R\,0}^*} \approx 0.00206$$

The reference diffusion constants were obtained by performing a molecular dynamics simulation (see Appendix A) of the Gay-Berne fluid at low density: $\rho^* = 0.05$, $T^* = 1.0$.

[5] In fact, this was the first hint that something might be wrong with the nematic geodesics.

They were found to be:

$$D^*_{T\,0} \approx 1.480$$
$$D^*_{R\,0} \approx 0.657$$

This allows us to determine the geodesic predictions for the diffusion constants. I have compared the geodesic predictions with the MD results in the table below:

	Geodesic	MD
D_T^{iso*}	0.553	0.109
D_T^{nem*}	0.353	0.0518
D_R^{iso*}	0.00274	0.0568
D_R^{nem*}	0.00136	0.00881

It is also useful to compare the ratios of diffusion constants in the nematic and isotropic phases. The geodesic predictions for these ratios and the corresponding MD results are given below:

	Geodesic	MD
D_T^{iso*}/D_T^{nem*}	1.57	2.10
D_R^{iso*}/D_R^{nem*}	2.02	6.45

As can be seen, the geodesic predictions are not great. This is likely because the diffusion constants do not differ by orders of magnitude, which is the regime where we would expect geodesic predictions of diffusion constants to be highly accurate. Additionally, since the geodesics we found for the nematic phase do not accurately represent the dynamics, we would expect neither the nematic diffusion constants nor the ratio of isotropic to nematic diffusion constants to be correct.

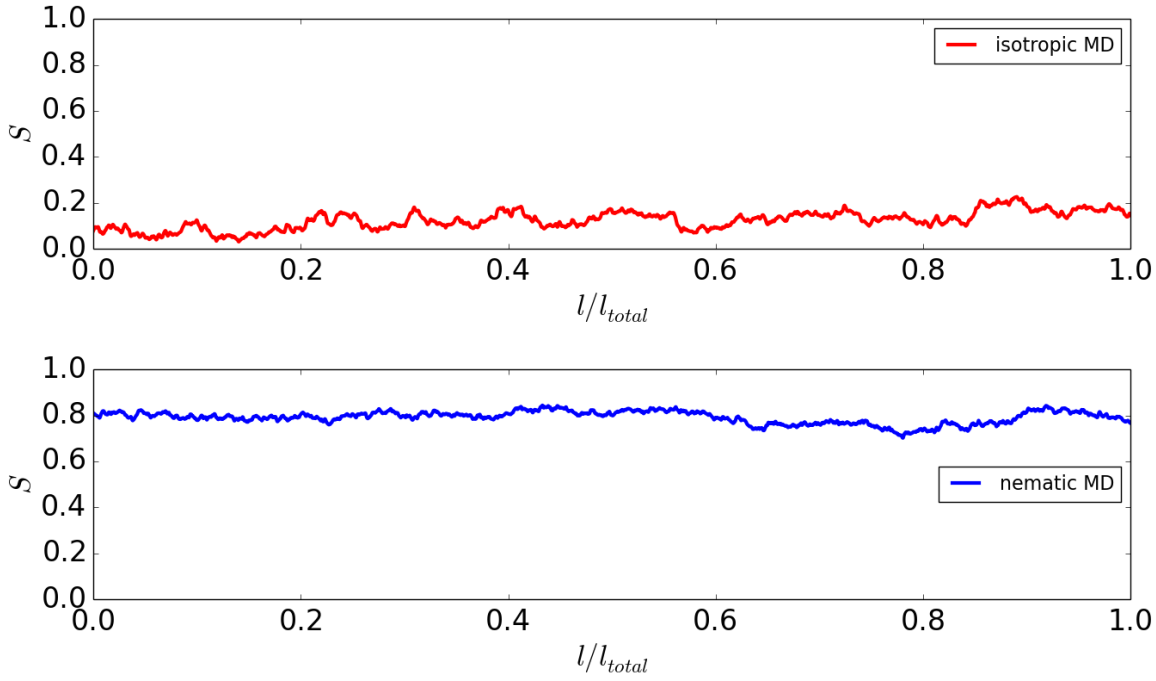

Figure 4: Order parameter during a molecular dynamics simulation. l represents the distance the system has travelled along its trajectory. This data was taken during the data collection phase of an isotropic MD run and a nematic MD run (see Appendix A.)

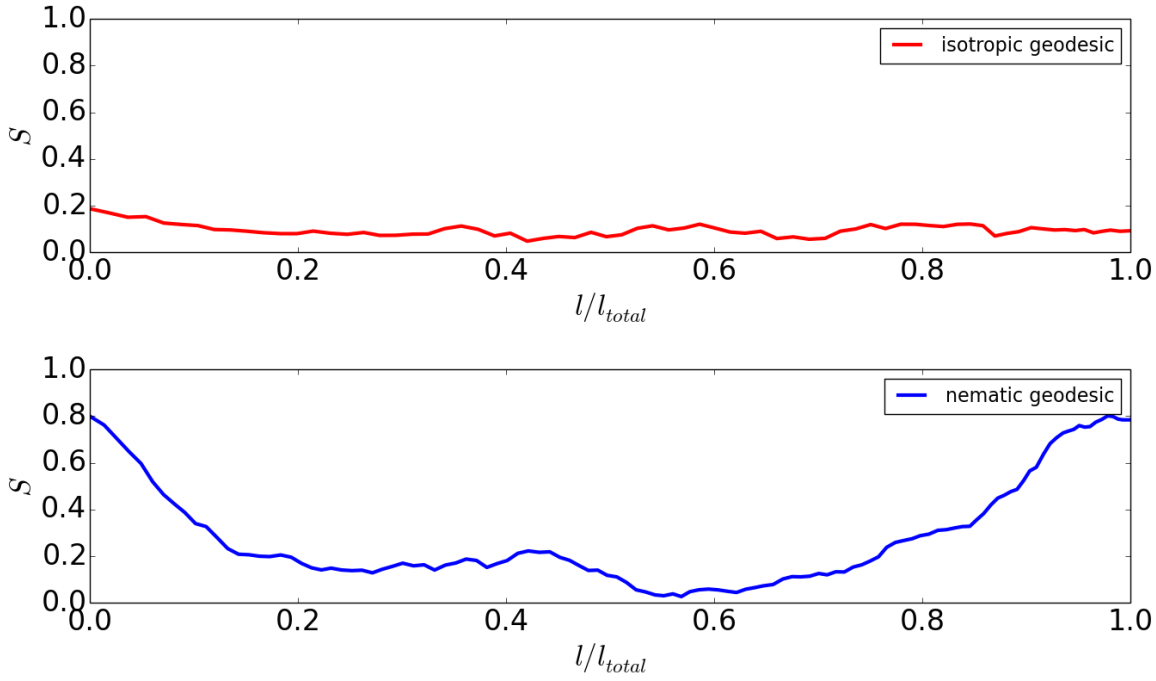

Figure 5: Order parameter along the course of a single (unoptimized) geodesic between Euclidean endpoints separated by $\Delta\widetilde{R} = 500\sigma_0$. l represents the distance the system has travelled along the geodesic.

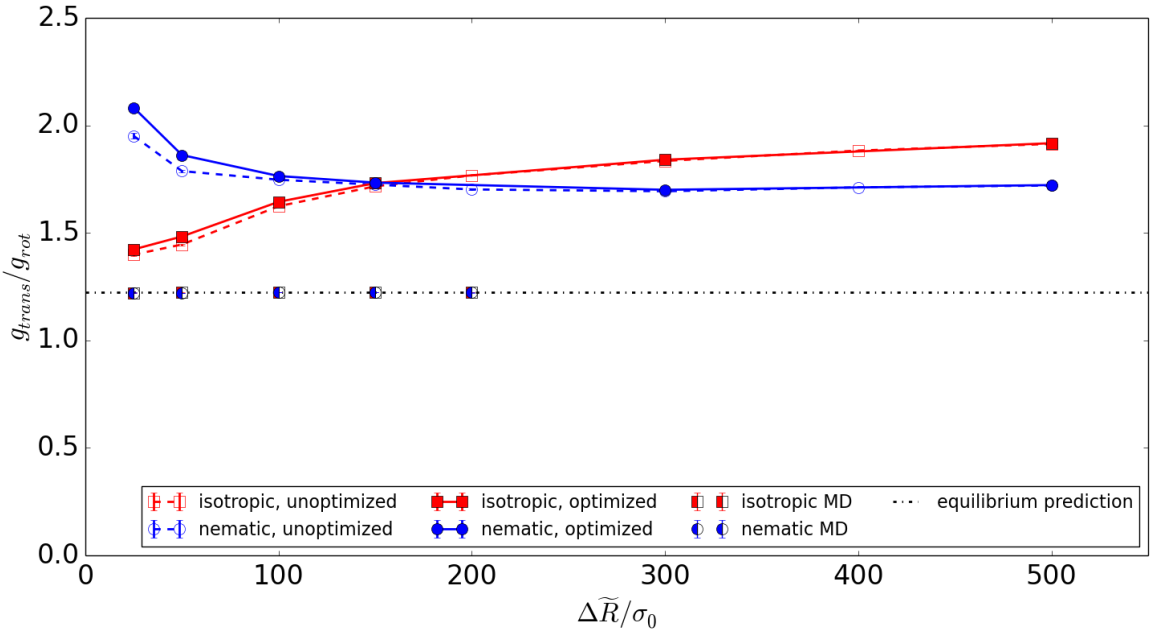

Figure 6: Ratio of translational to rotational geodesic lengths. The isotropic and nematic MD points overlap.

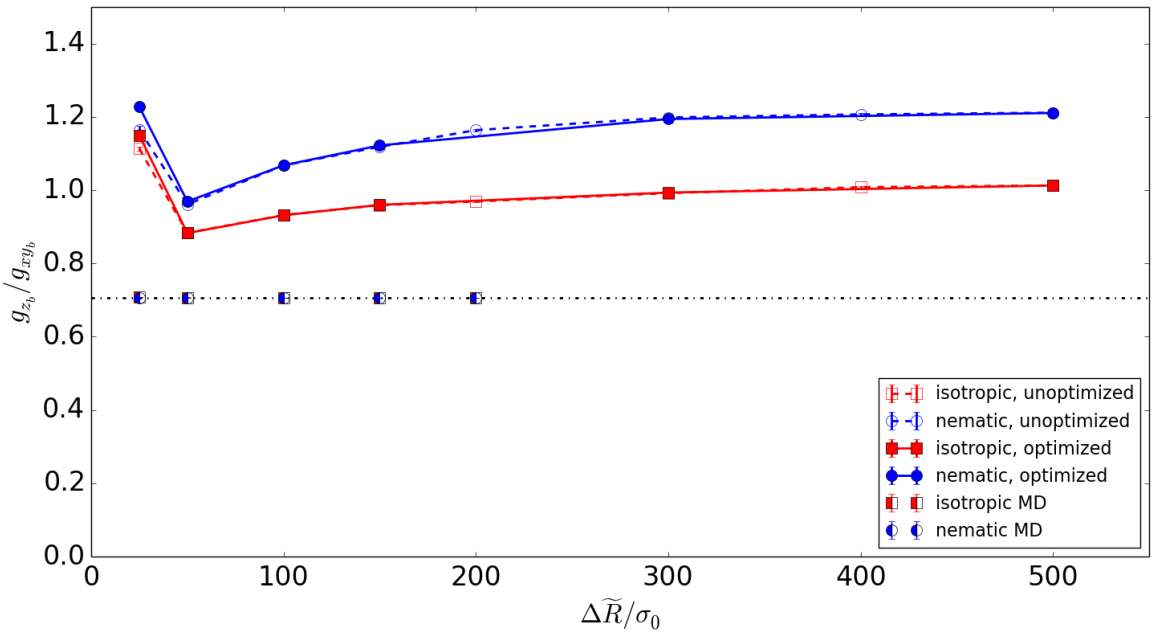

Figure 7: Ratio of body-fixed z to x, y translational geodesic lengths. The isotropic and nematic MD points overlap.

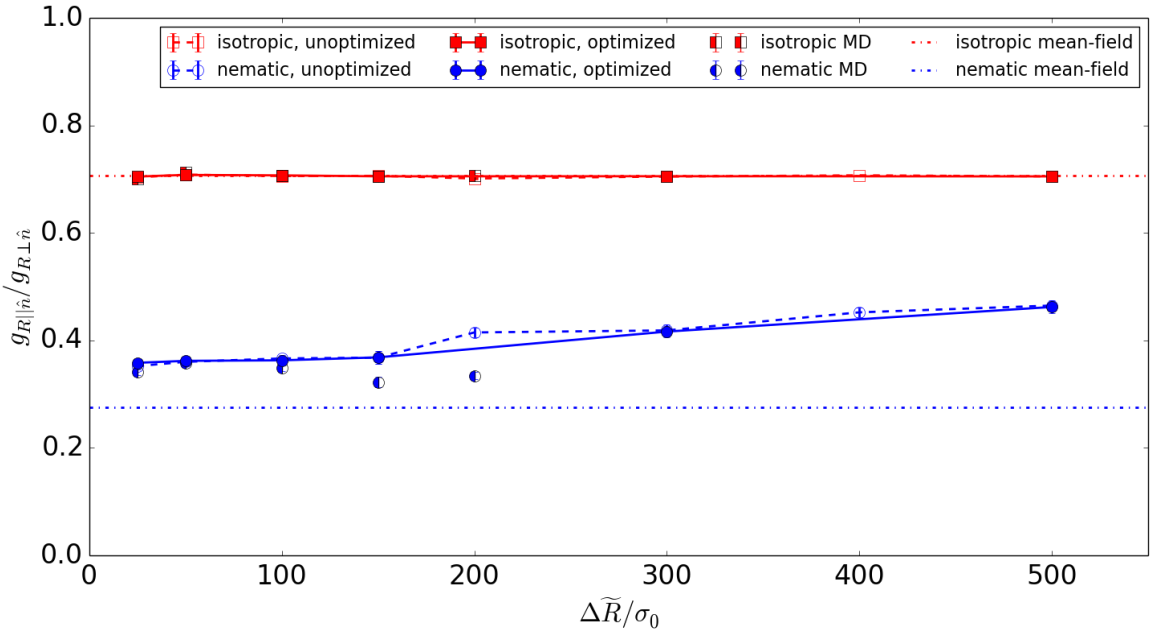

Figure 8: Ratio of parallel-to-director to perpendicular-to-director rotational geodesic lengths. As can be seen, the mean-field result is a decent predictor of the molecular dynamics ratios, but it is not perfect.

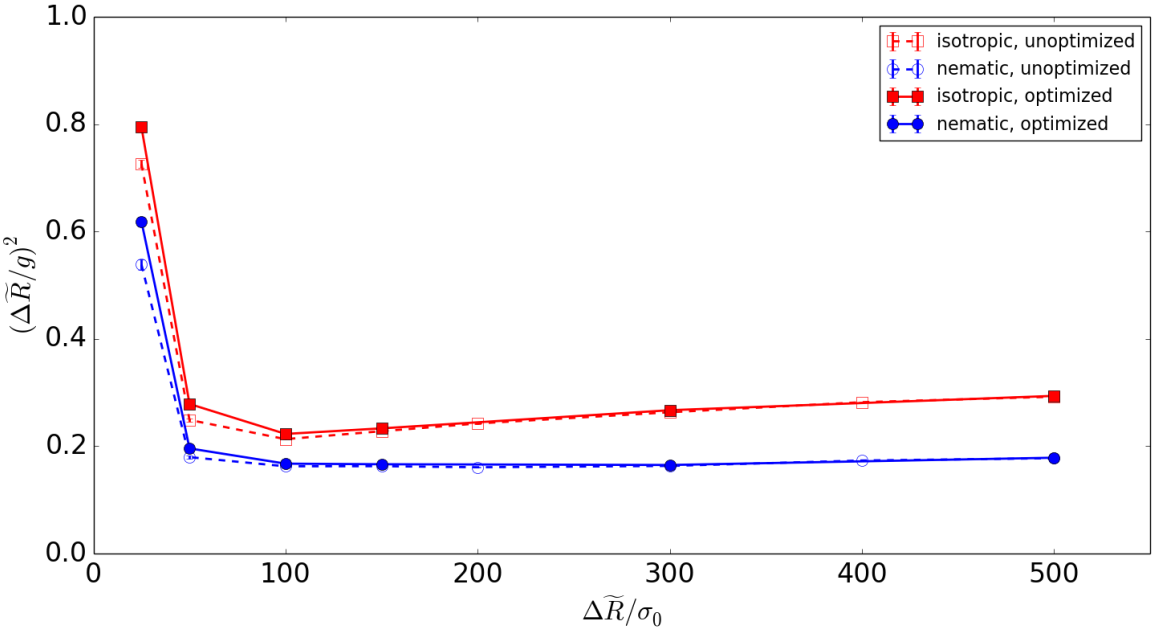

Figure 9: Convergence of total geodesic lengths with respect to $\Delta\widetilde{R}$.

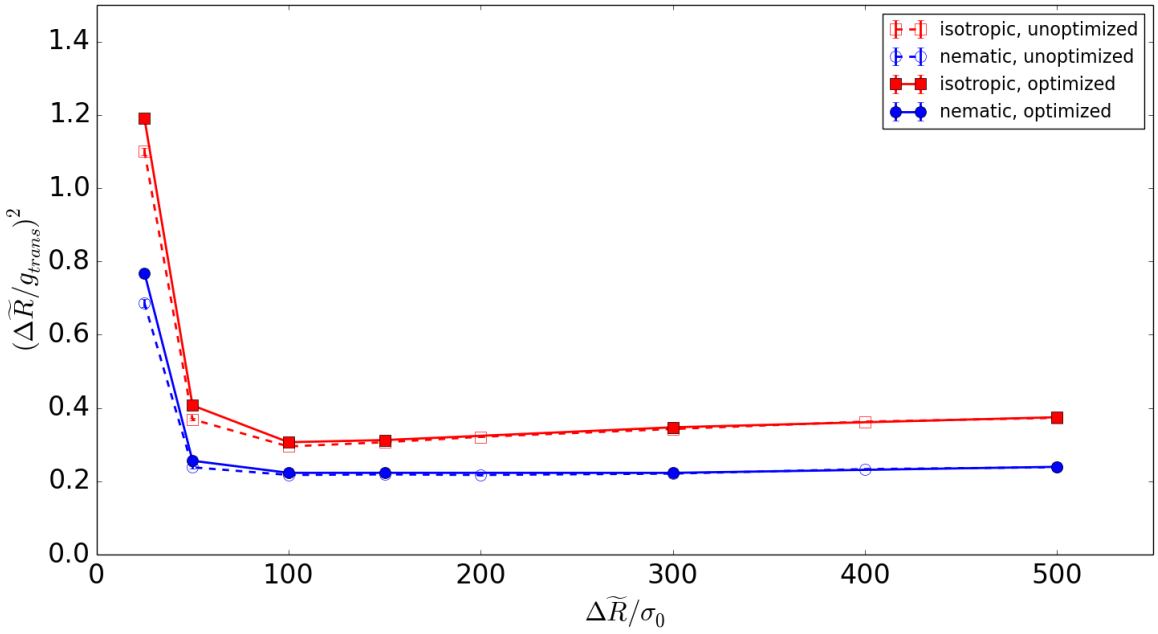

Figure 10: Convergence of translational geodesic lengths with respect to $\Delta\widetilde{R}$.

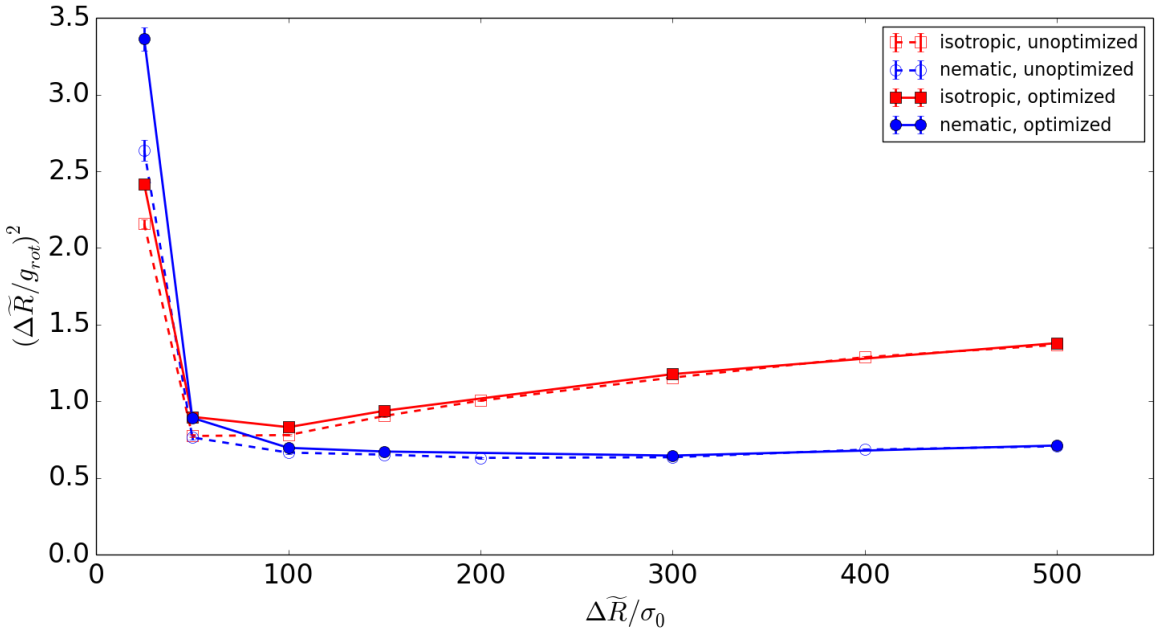

Figure 11: Convergence of rotational geodesic lengths with respect to $\Delta\widetilde{R}$.

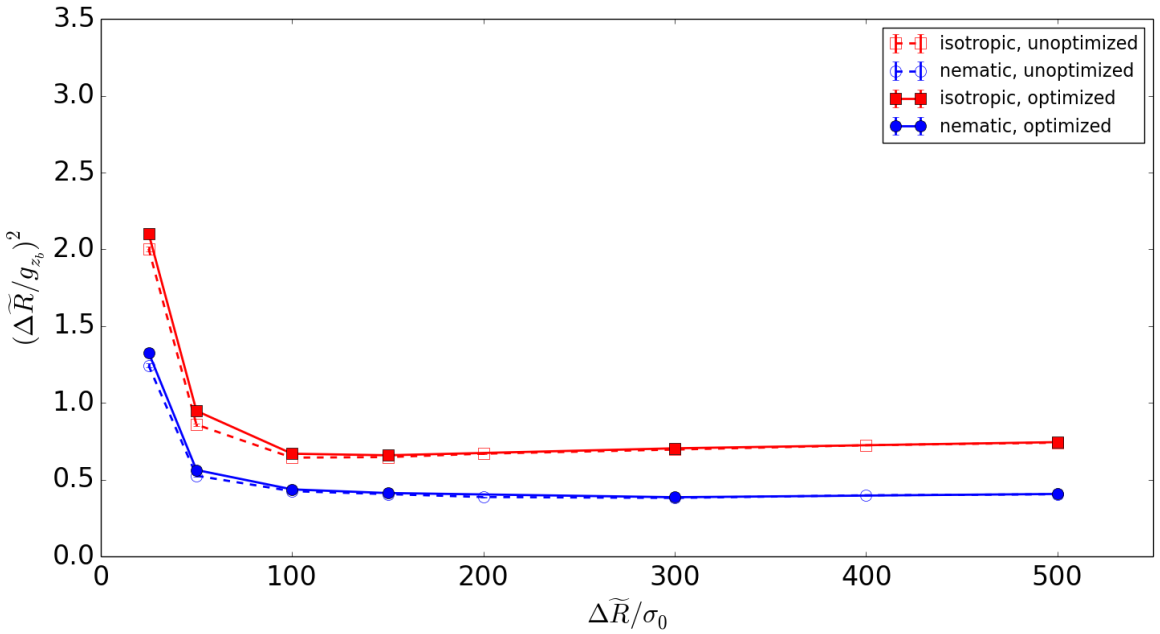

Figure 12: Convergence of body-fixed z translational geodesic lengths with respect to $\Delta\widetilde{R}$.

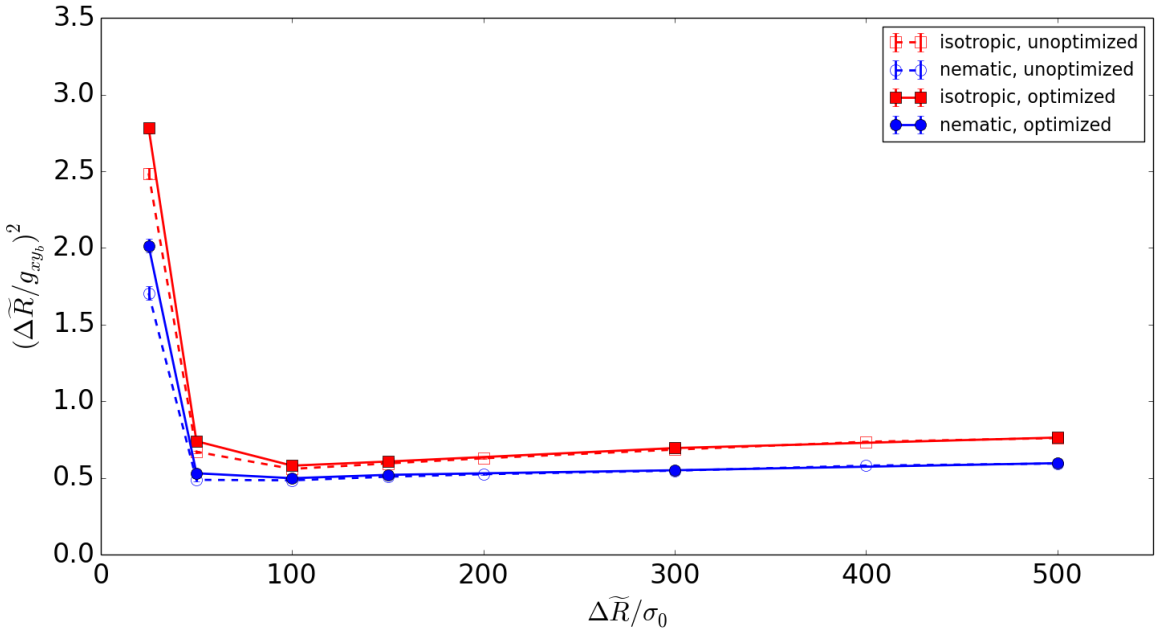

Figure 13: Convergence of body-fixed x, y translational geodesic lengths with respect to $\Delta\widetilde{R}$.

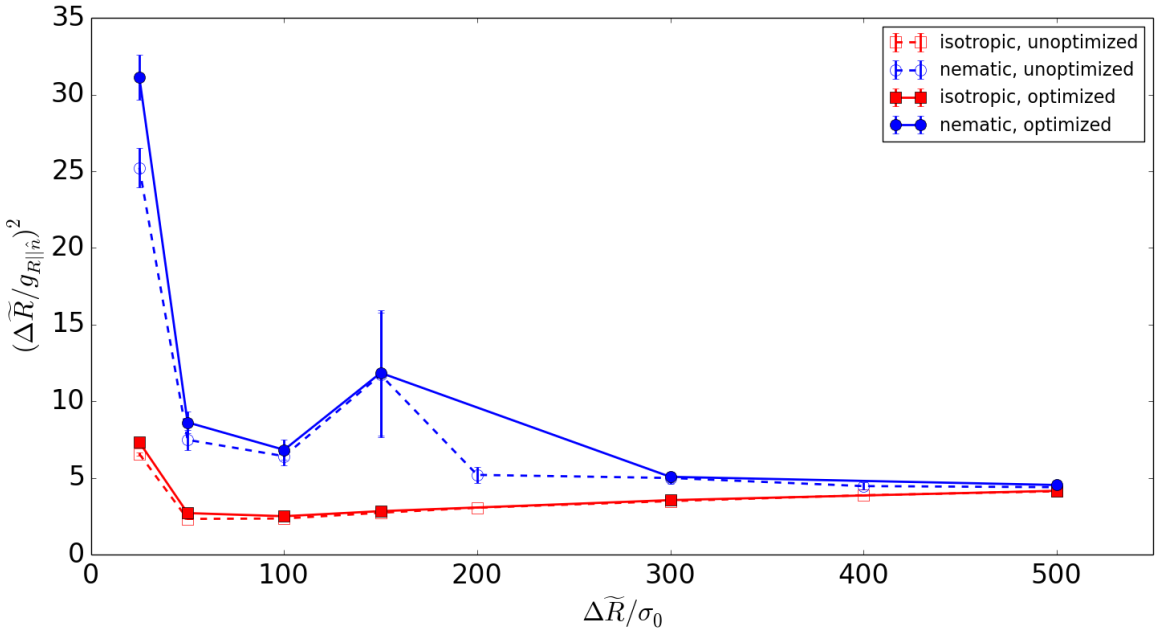

Figure 14: Convergence of rotational geodesic lengths parallel to director with respect to $\Delta\widetilde{R}$.

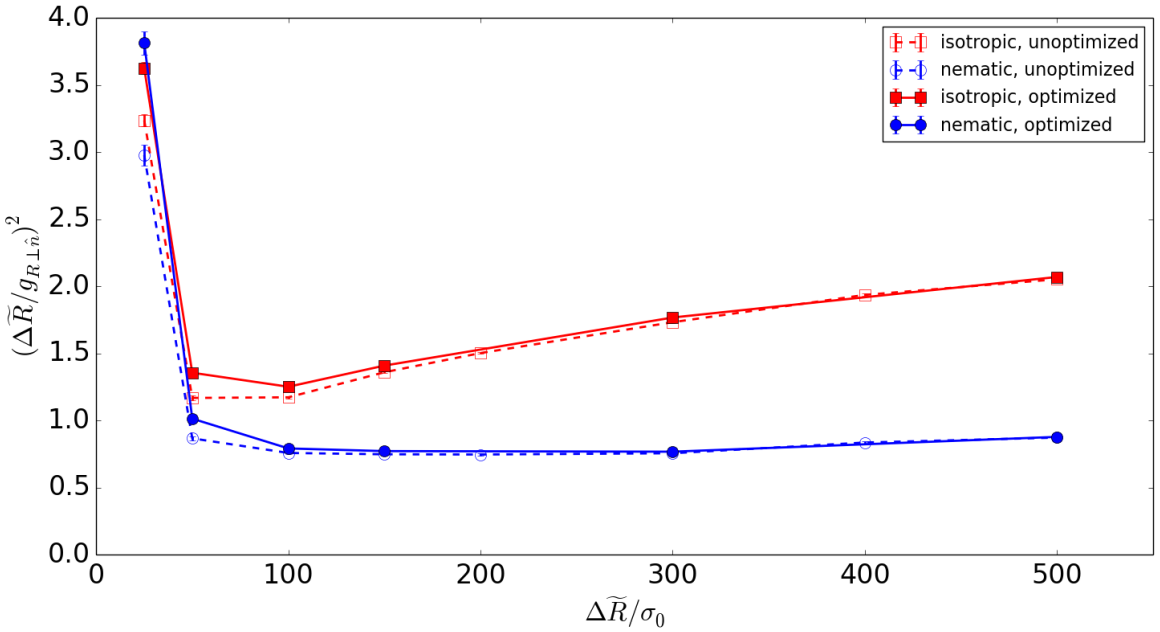

Figure 15: Convergence of rotational geodesic lengths perpendicular to director with respect to $\Delta\widetilde{R}$.

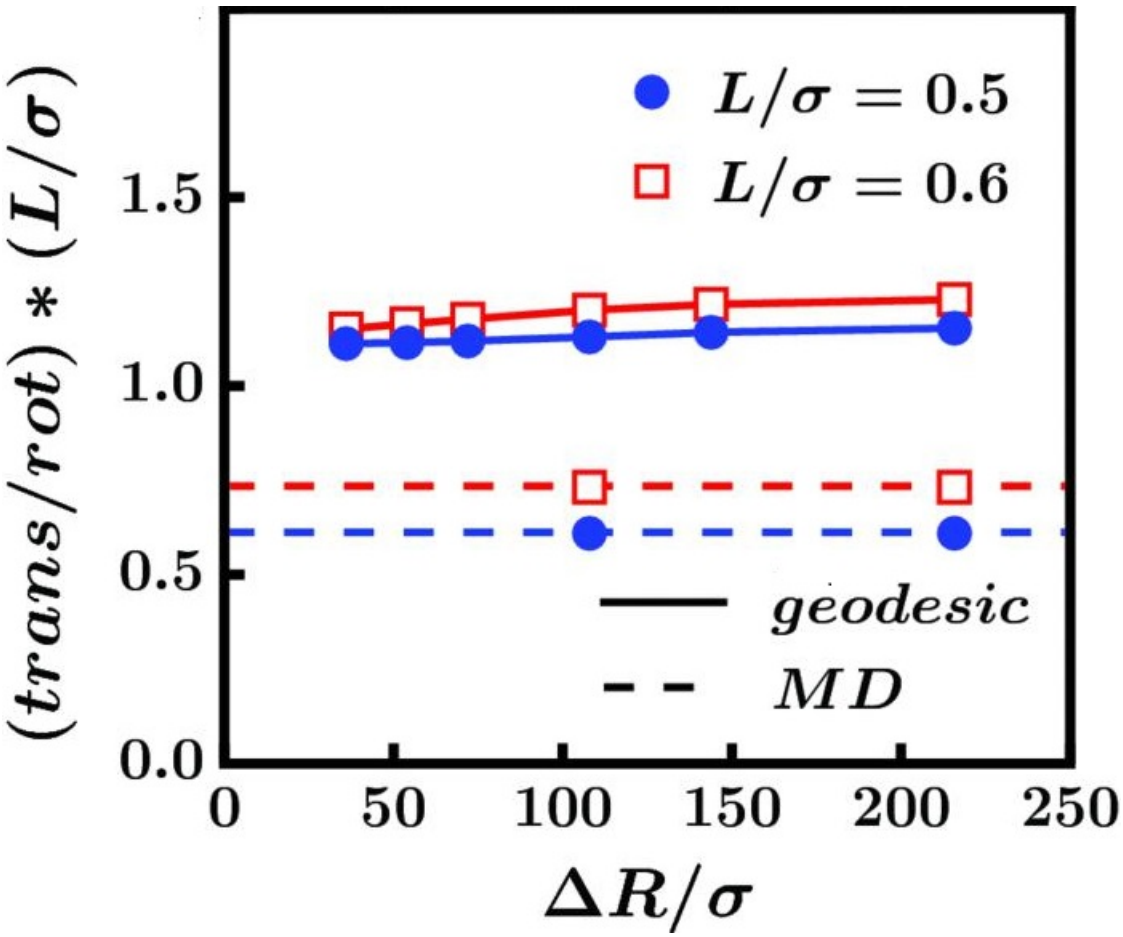

Figure 16: Translational-to-rotational geodesic ratio, normalized by bond length, for diatomic molecules of bond lengths $L = 0.5\sigma$ and $L = 0.6\sigma$. Modified from [2].

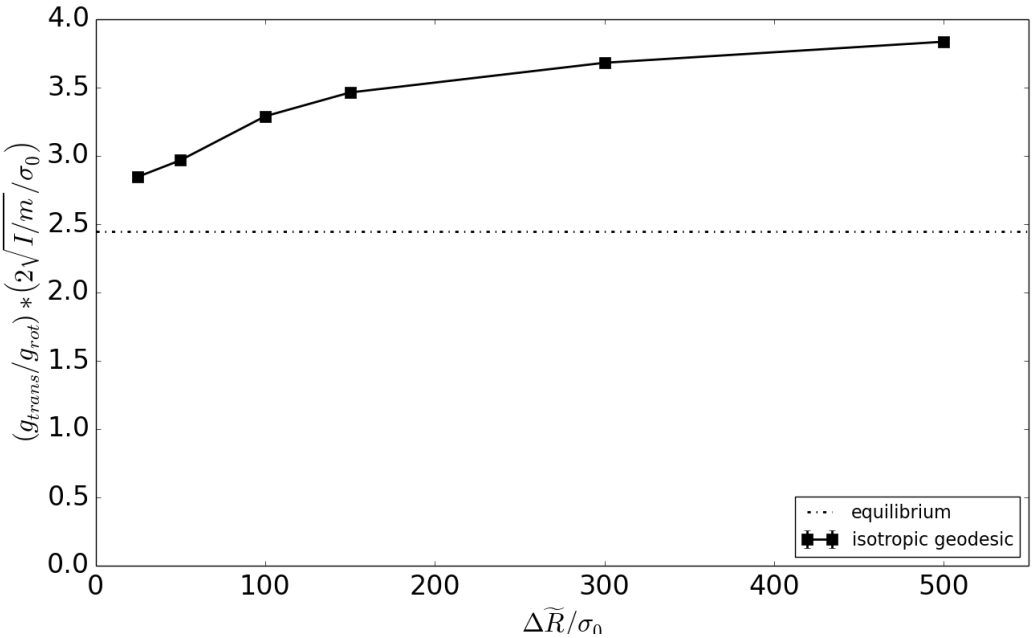

Figure 17: Translational-to-rotational geodesic ratio, normalized by an effective "bond length" $2\sqrt{I/m}$, for isotropic Gay-Berne molecules. In both this figure and the above figure, the ratio of translational to rotational length is greater than that of the equilibrium prediction ($= 2 * \sqrt{3/2}$.)

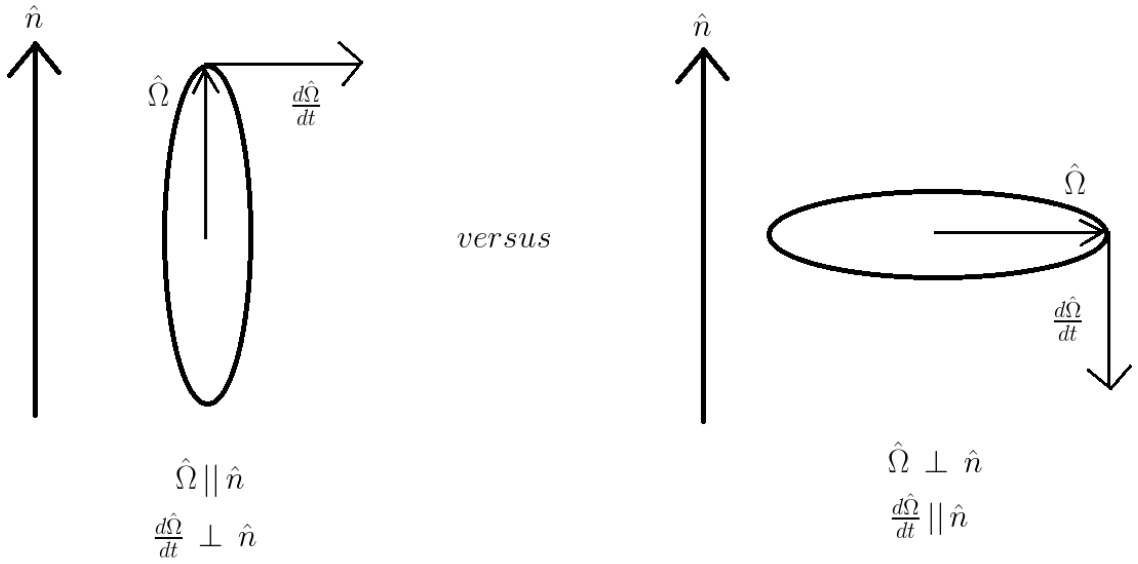

Figure 18: An ellipsoidal molecule with different orientations with respect to the director. As can be seen, when $d\hat{\Omega}/dt$ is perpendicular to the director, the orientation vector is aligned with the director, and when $d\hat{\Omega}/dt$ is parallel to the director, the orientation vector is perpendicular to the director.

6 Conclusion

We have discovered that our formulation of a geodesic analysis of liquid crystal formers was lacking a key piece of physics: constraining the system to stay in a single phase. This was demonstrated by showing that the order parameter of a system travelling along a geodesic from one nematic-phase endpoint to another decays to an isotropic value. To remedy this problem, we are working on creating an algorithm to constrain the order parameter to maintain a particular value along the geodesic. We also saw that the behavior of the isotropic-phase Gay-Berne system is similar to that of a diatomic liquid previously studied [1]. This is reassuring - it confirms that the motional motifs previously suggested for diatomics hold for other linear molecules as well.

7 Acknowledgements

I greatly thank Professor Stratt for his guidance and scientific discussions. I also thank the other members of the Stratt group for their help, especially Vale Cofer-Shabica, with whom I had extensive discussions and who was always willing to help me with computational issues.

Appendices

A Molecular Dynamics Simulation

A.1 Introduction

I wrote a program in C to perform molecular dynamics simulations of the liquid-crystal forming Gay-Berne fluid. The Gay-Berne model exhibits isotropic liquid, nematic liquid crystal, and smectic liquid crystal phases. Here, I report the results of simulations of the isotropic liquid phase and the nematic liquid crystal phase. These results include measurements of various thermodynamic, dynamic, and structural quantities of the two different phases under consideration.

A.2 Parameters

For both the isotropic and nematic phase simulations, I used the following parameters:

$$\begin{aligned} N &= 256 \\ \delta t &= 0.001\tau \\ T^*_{target} &= 1.00 \\ \sigma_\parallel/\sigma_\perp &= 3 \\ \epsilon_s/\epsilon_e &= 5 \\ \nu &= 1 \\ \mu &= 2 \end{aligned}$$

For the isotropic phase simulation I used $\rho^* = 0.28$, and for the nematic phase simulation I used $\rho^* = 0.34$. These values were selected based on the phase diagram of the Gay-Berne fluid, which can be found in [5].

A.3 Setting Up

A.3.1 Initial Configuration

The Gay-Berne molecules were initialized in an α-FCC lattice configuration at a low density of $\rho^* = 0.10$. The center-of-mass positions of the molecules were placed at each of the lattice sites, and the orientations of each of the molecules were assigned, in the manner prescribed by Allen & Tildesley [12].

A.3.2 Initial Velocities and Angular Velocities

The initial velocities and angular velocities were selected from Gaussian distributions using the Box-Muller method [9] The distribution for the time derivatives of the orientation vectors, and hence the angular velocities, is analogous that that for the center-of-mass velocities:

$$f(\dot{\hat{\Omega}}) = \left(\frac{I}{2\pi k_B T}\right)^{3/2} \exp\left[-\frac{I}{2k_B T}(\dot{\hat{\Omega}} \cdot \dot{\hat{\Omega}})\right]$$

The total center-of-mass linear momentum and angular momentum of the system were set to zero at the beginning of each simulation. The total linear momentum stayed at zero, to six decimal places, throughout the course of the simulations. The total angular momentum, however, fluctuated significantly about zero - this is due to the fact that cubic periodic boundary conditions do not conserve angular momentum [13].

A.3.3 Periodic Boundary Conditions

Periodic boundary conditions were enforced in the following way. The center of the (cubic) simulation box was assigned coordinates of $(0, 0, 0)$, and the length each side of the box was set to be L. If any of the center-of-mass coordinates of a molecule was found to exceed $L/2$, then L was subtracted from that coordinate. If any of the coordinates was found to be less than $-L/2$, then L was added to that coordinate. This procedure was repeated at each time step.

A.3.4 Integrating the Equations of Motion

The equations of motion governing the center-of-mass positions were integrated using the leapfrog algorithm, and those governing the molecular orientations were integrated using Fincham's rotational leapfrog algorithm [13]. The equations governing center-of-mass positions are:

$$\vec{r}(t + \delta t) = \vec{r}(t) + \delta t\, \vec{v}(t + \frac{1}{2}\delta t)$$
$$\vec{v}(t + \frac{1}{2}\delta t) = \vec{v}(t - \frac{1}{2}\delta t) + \delta t\, \vec{a}(t)$$

Here $\vec{r}$ is the center-of-mass position of a molecule, $\vec{v}$ is the center-of-mass velocity, and $\vec{a}$ is the acceleration, given by $\vec{f} = m\vec{a}$. This set of equations was, of course, applied to

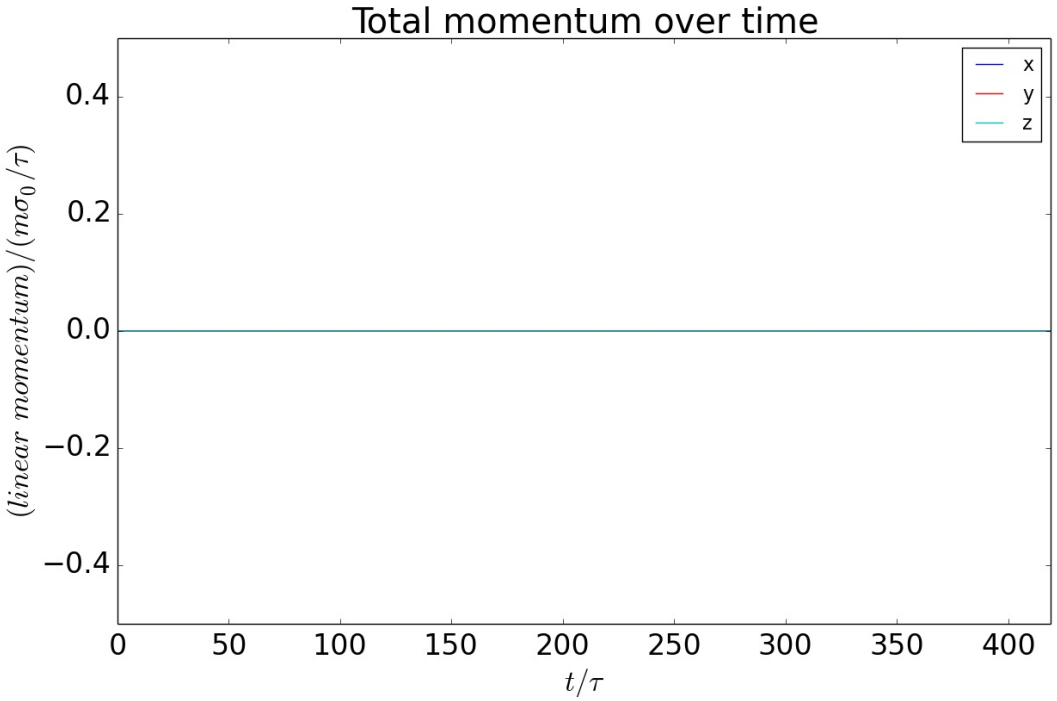

Figure 19: Total momentum of the system over an entire simulation.

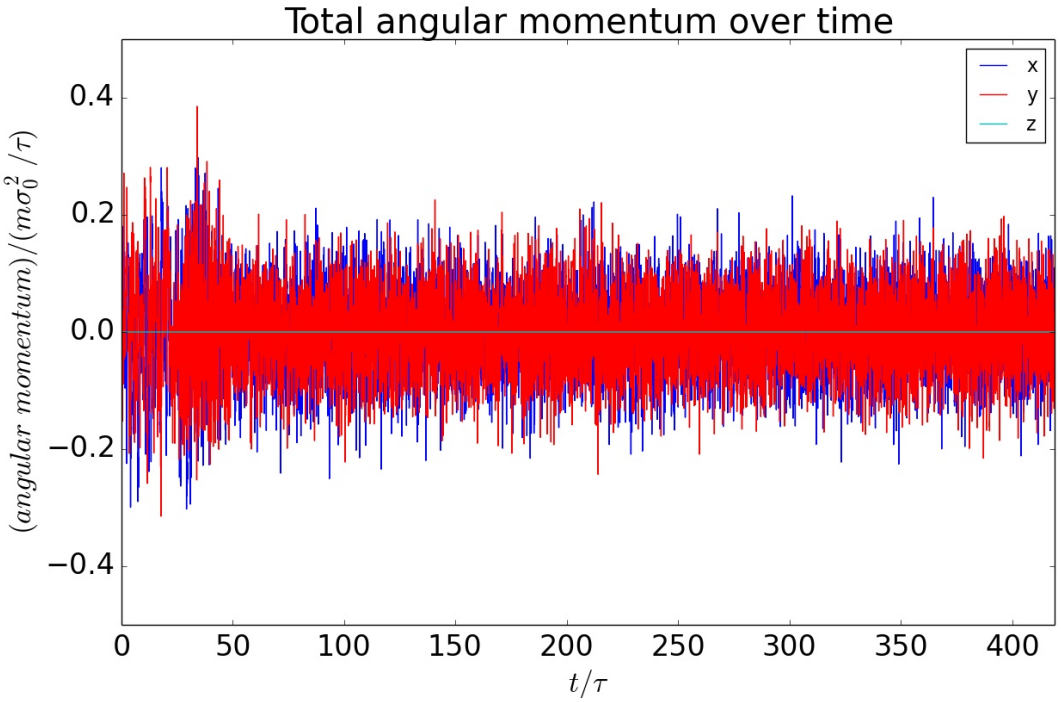

Figure 20: Total angular momentum of the system over an entire simulation. The components are for the body-fixed frame, hence the z component is zero. Larger fluctuations near the beginning of the simulation are due to higher temperature. These plots are for a nematic phase simulation, but those for the isotropic phase are similar.

each molecule at every time step. Note that this algorithm requires knowledge of the velocities only at every half-integer time step. To obtain the velocities at integer time steps, the following formula is used:

$$\vec{v}(t) = \frac{1}{2}(\vec{v}(t - \frac{1}{2}\delta t) + \vec{v}(t + \frac{1}{2}\delta t))$$

The equations governing molecular orientations are given by:

$$\begin{aligned}
\hat{\Omega}(t + \delta t) &= \hat{\Omega}(t) + \delta t\, \dot{\hat{\Omega}}(t + \frac{1}{2}\delta t) \\
\dot{\hat{\Omega}}(t + \frac{1}{2}\delta t) &= \dot{\hat{\Omega}}(t - \frac{1}{2}\delta t) + \delta t \vec{g}^{\perp}(t)/I - 2[\dot{\hat{\Omega}}(t - \frac{1}{2}\delta t) \cdot \hat{\Omega}(t)]\hat{\Omega}(t) \\
\vec{g}^{\perp} &= \vec{g} - (\vec{g} \cdot \hat{\Omega})\hat{\Omega}
\end{aligned}$$

Here $\hat{\Omega}$ is the molecular orientation, $\dot{\hat{\Omega}}$ is the time derivative of the molecular orientation, and $\vec{g}$ is the "auxiliary torque," defined by:

$$\tau = \hat{\Omega} \times \vec{g}$$

At each time step, $\vec{a}(t)$ and $\vec{g}(t)$ must be calculated, using the formulas:

$$\begin{aligned}
\vec{a} &= -\frac{1}{m}\frac{\partial U}{\partial \vec{r}} \\
\vec{g} &= -\frac{\partial U}{\partial \hat{\Omega}}
\end{aligned}$$

Expressions for these quantities for the Gay-Berne potential are derived in Appendix A.8.

A cutoff radius of $L/2$ was used for the simulations, and the minimum image convention was employed. It was necessary to re-normalize the orientation vectors at each time step. If the vectors were not re-normalized, their magnitudes would gradually drift, resulting in a loss of energy conservation.

A.4 Equilibration into different phases

A number of steps are necessary to take the system from its initial configuration to a final, equilibrated configuration in the appropriate phase. These steps are as follows:

1) Melting: Sample the initial velocities and angular velocities from a high-temperature ($T^* = 5.00$) distribution, and allow the system to relax for 25τ. This allows the system to "melt" from its initial lattice configuration.

2) Compression: Compress the system, by increasing the density in small increments ($\rho^*_{new} = \rho^*_{old} + 0.005$) every 0.1τ, until the final density is reached. During this time, rescale the velocities and angular velocities to $T^* = 3.00$ (approximately the temperature to which the system relaxes as it melts.) This prevents the system's temperature from becoming extremely high due to the compression. To rescale the velocities, I applied the following formula to each molecule:

$$v_{new} = \left(\frac{T_{target}}{T_{system}}\right)^{1/2} v_{old}$$

I also applied an identical formula to the time derivatives of the molecular orientation vectors.

3) Cooling: Rescale the velocities and angular velocities every 1τ in small[6] temperature increments ($T^*_{new} = T^*_{old} - 0.1$) until the desired temperature is reached. Continue to rescale the velocites and angular velocities to the desired temperature for another 10τ. Allow the system to relax for 50τ, then do another period of rescaling, every τ for 10τ.[7]

4) Equilibration: Allow the system to relax for 200τ. That this is a sufficient amount of time for relaxation is demonstrated in Figs. 21 and 22.

After the system has finished equilibrating, data is collected for 100τ. Since we sample only every $10\delta t$ to avoid correlations in the data, this corresponds to averaging over 10000 configurations.

A.5 Thermodynamic Quantities

I calculated the following thermodynamic quantities in the isotropic and nematic phases: total, potential, and translational and rotational kinetic energies; translational and rotational temperature; pressure; the orientational order parameter, S; and, in the nematic phase, the (absolute value of) the components of the director. Here, I report the average values and standard deviations of these quantities.

A.5.1 Reported Errors

All the reported errors are in the form of standard (RMS) deviations. The standard deviation of an observable A is defined as:

$$\sqrt{\langle \delta A^2 \rangle} = \sqrt{\langle (A - \langle A \rangle)^2 \rangle}$$

Where $\langle A \rangle$ denotes the time (or ensemble) average of A.

A.5.2 Average Values

All averages were taken over 10000 configurations. I shall first give mathematical definitions for all of the quantities under consideration. Let $\vec{r}_i$ denote the center-of-mass position of the ith molecule, $\vec{v}_i$ the center-of-mass velocity of the ith molecule, $\hat{\Omega}_i$ the orientation of the ith molecule, $\dot{\hat{\Omega}}_i$ the time derivative of the orientation vector of the ith molecule, and $\vec{\omega}_i \, (= \hat{\Omega}_i \times \dot{\hat{\Omega}}_i)$ the angular velocity of the ith molecule. Then we have:

[6] The temperature increments can be significantly larger than the ones I used here. It should be fine to use something like $T^*_{new} = T^*_{old} - 1.0$.

[7] The reason for this rescaling scheme is that when equilibrating into the nematic phase, if the system is cooled and then rescaling is applied for just a few τ, the system's kinetic energy will slowly rise while the potential energy will slowly fall (while the total energy stays constant) for several tens of τ. After this period of time the kinetic and potential energies no longer change.

$$
\begin{aligned}
U &= \sum_i \sum_{j>i} u(\vec{r}, \hat{\Omega}_i, \hat{\Omega}_j) \\
K_{trans} &= \frac{1}{2} m \sum_{i=1}^{N} \vec{v}_i \cdot \vec{v}_i \\
K_{rot} &= \frac{1}{2} I \sum_{i=1}^{N} \dot{\hat{\Omega}}_i \cdot \dot{\hat{\Omega}}_i \\
E &= U + K_{trans} + K_{rot} \\
T_{trans} &= \frac{2}{3Nk_B} K_{trans} = \frac{m}{3Nk_B} \sum_{i=1}^{N} \vec{v}_i \cdot \vec{v}_i \\
T_{rot} &= \frac{1}{k_B} K_{rot} = \frac{I}{2k_B} \sum_{i=1}^{N} \dot{\hat{\Omega}}_i \cdot \dot{\hat{\Omega}}_i \\
p &= \rho k_B T + \frac{1}{3V} \sum_{i=1}^{N} \vec{r}_i \cdot \vec{f}_i
\end{aligned}
$$

Note that in the definition of pressure I wrote T with no subscript - this is because the translational and rotational temperatures should, and do, agree, and so I denote their common value as T. Note also that I am using $\dot{\hat{\Omega}} \cdot \dot{\hat{\Omega}}$ instead of $\vec{\omega} \cdot \vec{\omega}$ above. It is permissible to do this because $\dot{\hat{\Omega}} \cdot \dot{\hat{\Omega}} = \vec{\omega} \cdot \vec{\omega}$.[8]

The (instantaneous) order parameter can be defined in terms of the director $\hat{n}$ as:

$$
S = \frac{1}{N} \sum_{i=1}^{N} \frac{3}{2} \cos^2 \theta_i - \frac{1}{2}
$$

where $\theta_i = \hat{\Omega}_i \cdot \hat{n}$. However, we do have not the director *a priori*. We can alternatively calculate S as the largest eigenvalue of the Q-tensor:

$$
\overleftrightarrow{Q} = \frac{1}{2N} \sum_{i=1}^{N} (3\hat{\Omega}_i \hat{\Omega}_i - \mathbb{1})
$$

Which does not require the value of the director. In fact, the director is obtained as the eigenvector corresponding to the largest eigenvalue of this tensor. To calculate the eigenvalues and eigenvectors, I used code freely available from the GNU Scientific Library [10].[9]

One way to check that the Q-tensor is being calculated properly is to make sure that the trace of the tensor is zero (see Appendix A.9 for a proof.) Reassuringly, it was found that the trace of the tensor was zero, to an accuracy of 6 decimal places.

[8] Proof: since $\vec{\omega} = \hat{\Omega} \times \dot{\hat{\Omega}}$, we have $\vec{\omega} \cdot \vec{\omega} = (\hat{\Omega} \times \dot{\hat{\Omega}}) \cdot (\hat{\Omega} \times \dot{\hat{\Omega}}) = (\hat{\Omega} \cdot \hat{\Omega})(\dot{\hat{\Omega}} \cdot \dot{\hat{\Omega}}) - (\hat{\Omega} \cdot \dot{\hat{\Omega}})^2$. But $\hat{\Omega}$ and $\dot{\hat{\Omega}}$ are orthogonal, so the second term is zero. Also, $\hat{\Omega} \cdot \hat{\Omega} = 1$, so we have the result $\hat{\omega} \cdot \hat{\omega} = \dot{\hat{\Omega}} \cdot \dot{\hat{\Omega}}$.

[9] To make sure that the code worked, I checked that it gave the correct results for a simple matrix, for which eigenvectors and eigenvalues could be easily calculated analytically.

Average Values in the Isotropic phase, $\rho^* = 0.28$								
	U^*/N	K_T^*/N	K_R^*/N	E^*/N	T_T^*	T_R^*	p^*	S
$\langle A \rangle$	-2.80	1.48	0.99	-0.3211	0.99	0.99	2.3	0.12
$\sqrt{\langle \delta A^2 \rangle}$	0.0549	0.0573	0.0526	0.000232	0.0382	0.0526	0.142	0.0494

Average Values in the Nematic phase, $\rho^* = 0.34$								
	U^*/N	K_T^*/N	K_R^*/N	E^*/N	T_T^*	T_R^*	p^*	P_2
$\langle A \rangle$	-3.33	1.50	1.01	-0.824	1.00	1.01	5.0	0.77
$\sqrt{\langle \delta A^2 \rangle}$	0.0628	0.0624	0.0557	0.000307	0.0416	0.0557	0.201	0.0207

Average Absolute Values of the Nematic Director			
	n_x	n_y	n_z
$\langle A \rangle$	0.12	0.987	0.07
$\sqrt{\langle \delta A^2 \rangle}$	0.0569	0.00574	0.0477

A.5.3 A Note on Energy Conservation

Initially, I tried using 108 molecules in my simulations. However, I discovered an energy conservation problem that was caused by using this few molecules. The Gay-Berne potential is quite close to zero by about $r = 4.0\sigma_0$; however, the densities at which we are studying gay-berne molecules necessitate simulation box lengths of around $7\sigma_0$ (so that $L/2 \approx 3.5\sigma_0$) for 108 molecules. In other words, the potential was being cut off before going to zero, leading to a lack of energy conservation. Using the next largest number of molecules that an FCC lattice in a cubic box can accomodate, 256, resulted in energy conservation to within parts in 10^4. Thus the minimum number of Gay-Berne molecules that should be used in a cubic box, starting from an FCC lattice, at densities of around $\rho^* = 0.3$, is 256.

A.6 Structural Quantities

The values of the orientational order parameter and the director give some insight into the structure of the phase, but in order to understand the local structure it is necessary to calculate the radial distribution function.

A.6.1 Radial Distribution Function

The radial distribution function is given by:

$$g(r) = \frac{V}{N^2} \left\langle \sum_i \sum_{j \neq i} \delta(\vec{r} - \vec{r}_{ij}) \right\rangle$$

Where $\vec{r}_{ij}$ refers to the vector between the center-of-mass positions of molecules i and j. Note that this formula does not take the orientations of the molecules into account. It is possible to define distribution functions which do take into account the orientations of the molecules, but here I shall simply use this "orientationally-averaged" function.

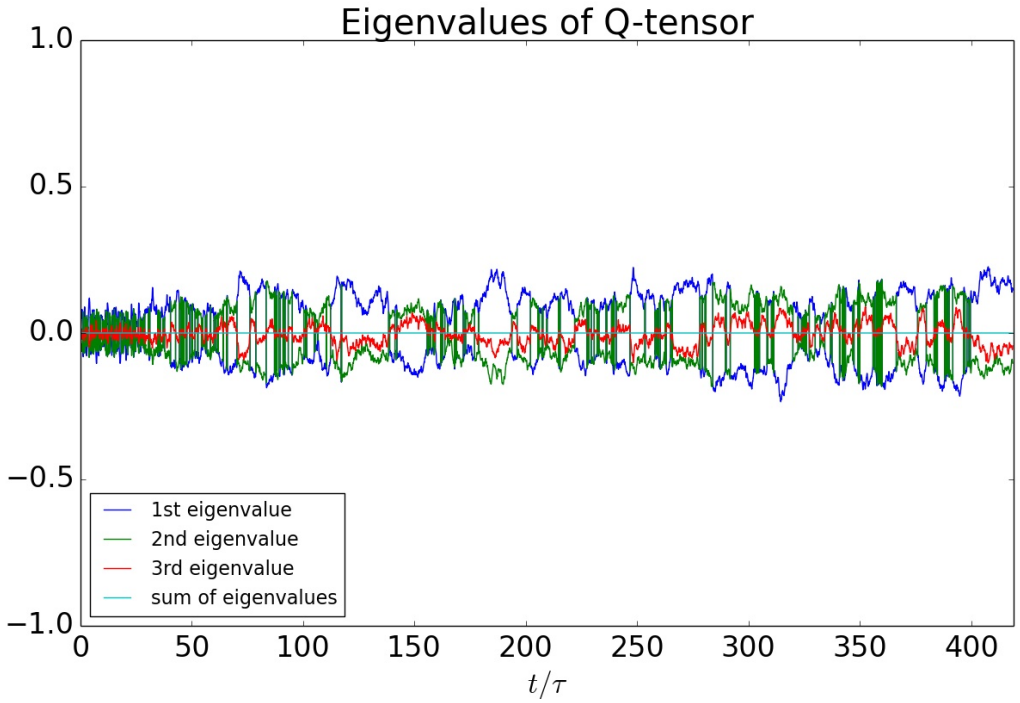

Figure 21: Eigenvalues of the Q-tensor, and sum of these eigenvalues, in the isotropic phase. In this figure and in Fig. 22, time starts from the initial FCC lattice configuration. From $t = 0$ to approximately $t = 130\tau$, the system is heated, compressed, and cooled. The system equilibrates over the next 200τ. The fact that the order parameter is stable over this time is evidence that this is sufficient time for equilibration.

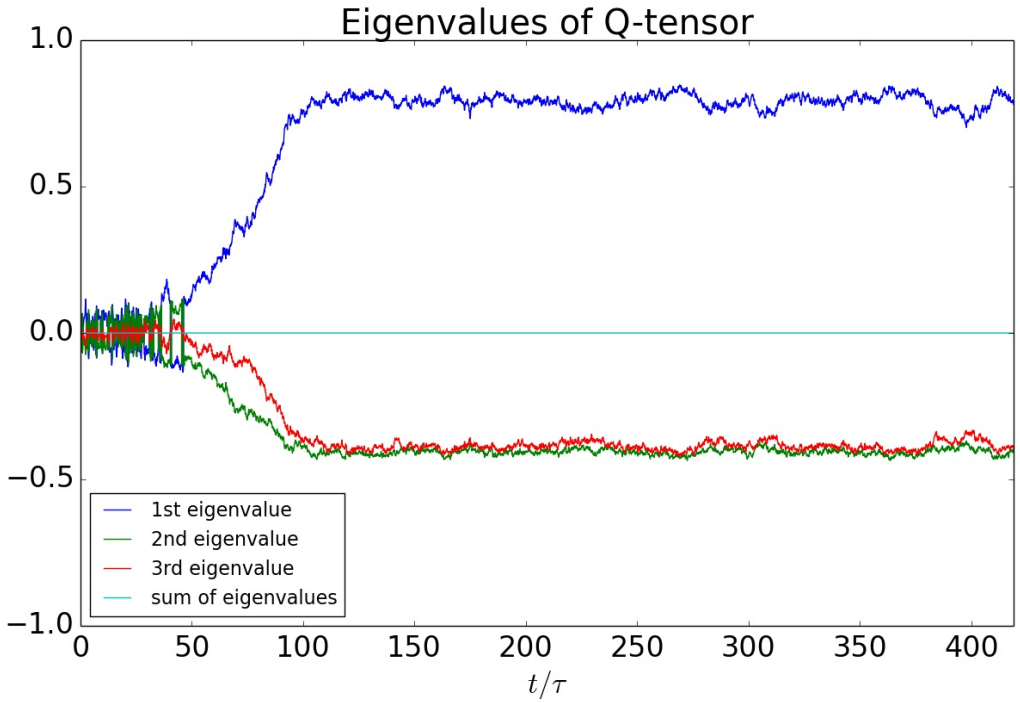

Figure 22: Eigenvalues of the Q-tensor, and sum of these eigenvalues, in the nematic phase. The largest eigenvalue is the order parameter, S.

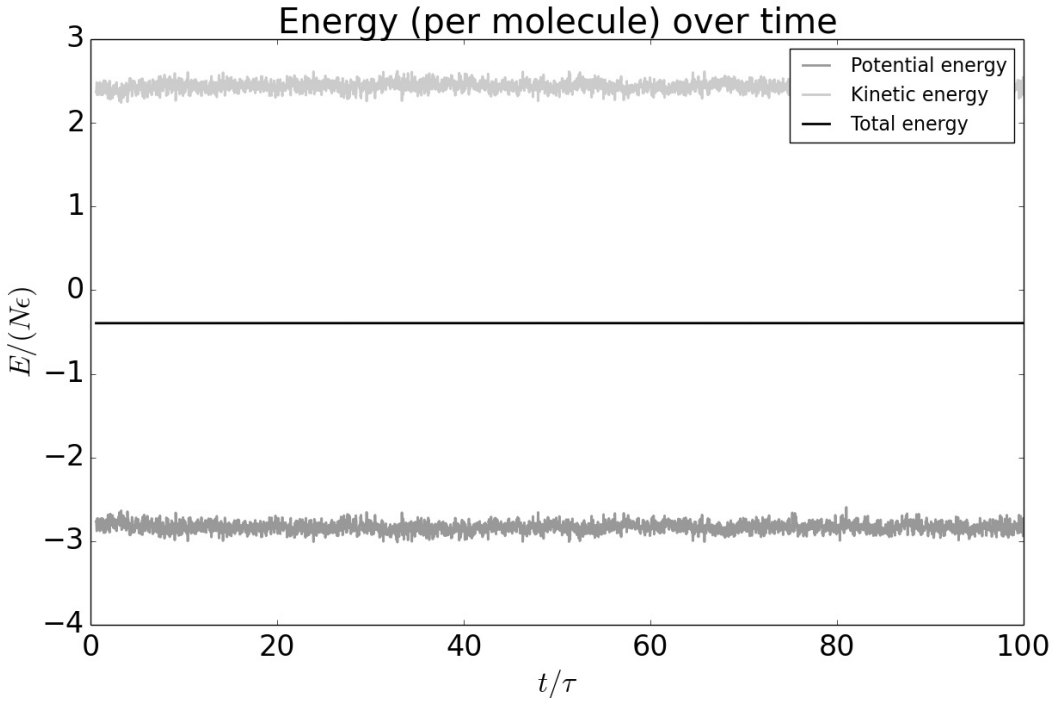

Figure 23: Potential, total kinetic, and total energies in the isotropic phase, during the data collection phase of the simulation.

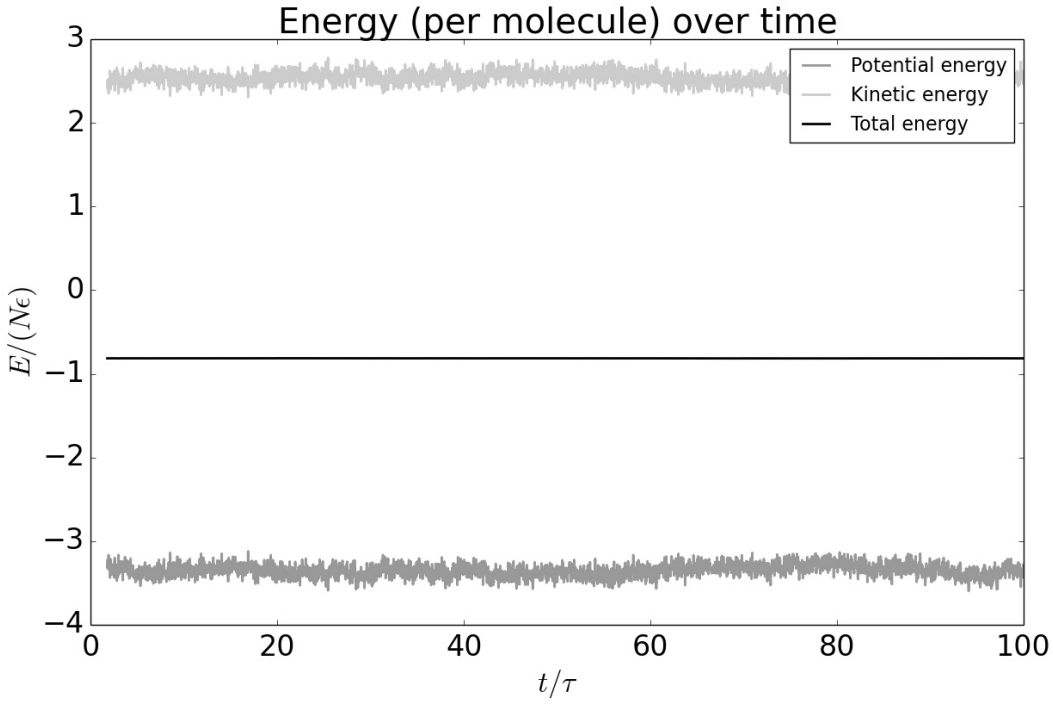

Figure 24: Potential, total kinetic, and total energies in the nematic phase, during the data collection phase of the simulation.

The radial distribution function can be understood as the probability, averaged over all molecules, of finding a molecule in a spherical shell defined by the radii r and $r + \delta r$, where r defines the distance away from some given molecule. This probability is then normalized by the same probability for an ideal gas. An algorithm for computing $g(r)$ is outlined in [14].

A.6.2 Nearest Neighbors

The number of nearest neighbors of an "average" molecule can be calculated as an integral of $g(r)$:

$$\begin{aligned} N_{1st\,shell} &= \rho \int_{r<1st\,min} d\vec{r} g(r) \\ &= 4\pi\rho \int_{r<1st\,min} dr r^2 g(r) \end{aligned}$$

The integration was performed using (the extended) Simpson's rule (see [15].) To find the first minimum, start from the fist nonzero value of $g(r)$. Consider a (discretized) distance r_i. If $g(r_i) > g(r_{i+1})$ and $g(r_i) > g(r_{i-1})$, then we have found the first minimum. Otherwise, look at r_{i+1} and repeat the procedure.

I obtained the following values for the number of nearest neighbors:

Isotropic	Nematic
$N_{neighbors} \approx 5.49$	$N_{neighbors} \approx 5.65$

For both the isotropic and nematic phases, at similar densities, we see that the number of nearest neighbors is around 6. This is markedly different from the value of 12 which is found for simple atomic liquids. It seems likely that this is due to the elongation of the Gay-Berne molecules making it harder to pack as many of them close together.

A.7 Dynamical Quantities

The dynamics of the Gay-Berne fluid was probed using correlation functions. The correlation function of two observables, A and B, is given by:

$$\begin{aligned} C_{AB}(t) &= \langle A(0)B(t)\rangle \\ &= \lim_{T\to\infty} \frac{1}{T} \int_0^T dt' A(t')B(t+t') \end{aligned}$$

It is straightforward to discretize this quantity, as discussed in [14]. When $A = B$, we have an *auto*correlation function. Autocorrelation functions are related to transport coefficients by so-called *Green-Kubo relations*.

We can also define a normalized correlation function:

$$c_{AB}(t) = \frac{\langle A(0)B(t)\rangle}{\langle A(0)B(0)\rangle}$$

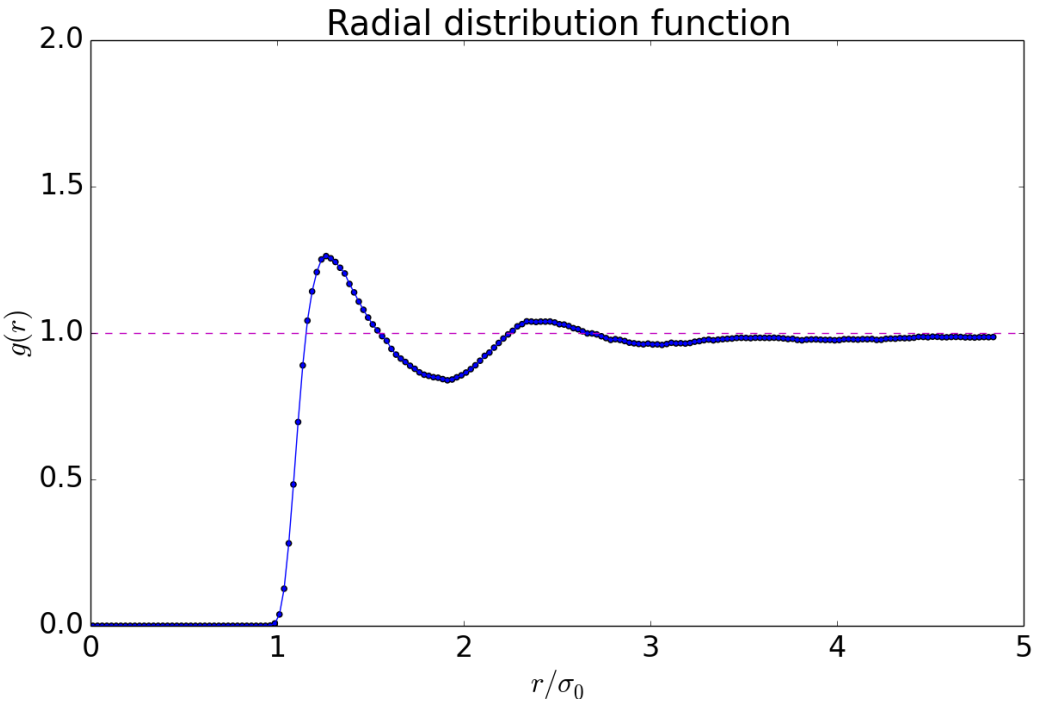

Figure 25: Radial distribution function in the isotropic phase.

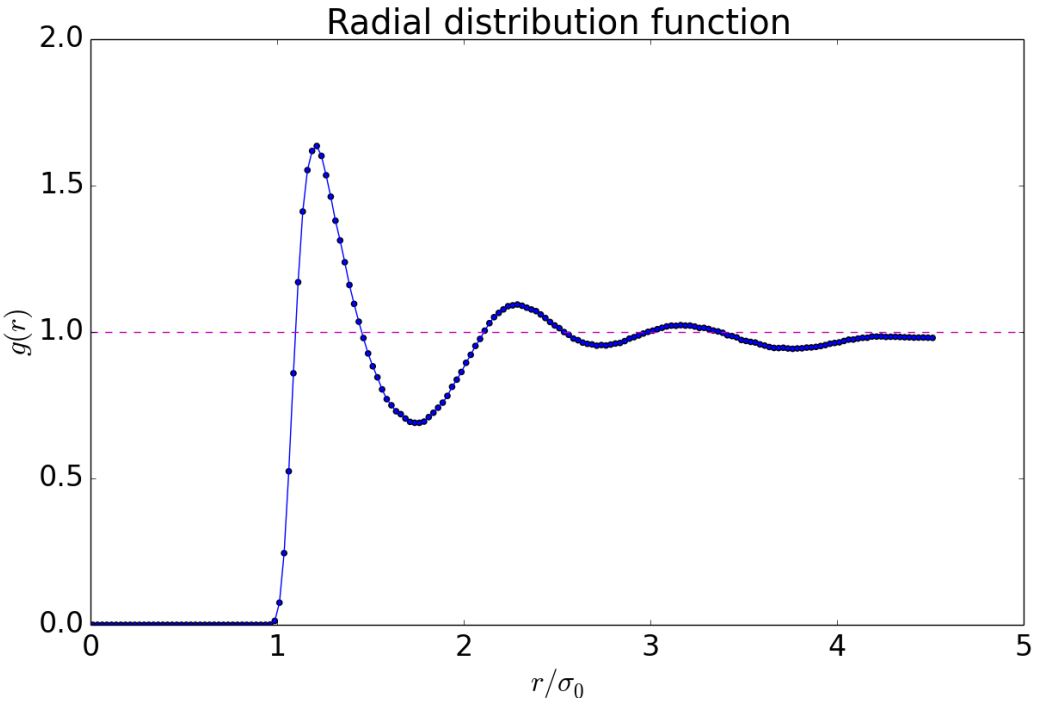

Figure 26: Radial distribution function in the nematic phase.

The plots in this section are all of normalized correlation functions. Values of the correlation functions were calculated every $10\delta t$, and each of these values was averaged over 9000 configurations and over all 256 molecules. All the integrations necessary to calculate the diffusion coefficients were done using Simpson's rule.

A.7.1 Velocity Autocorrelation Function

The velocity autocorrelation function is given by:

$$C_{vv}(t) = \langle \vec{v}(0) \cdot \vec{v}(t) \rangle$$

A Green-Kubo relation [16] allows us to use this correlation function to calculate a translational diffusion coefficient:

$$D_T = \frac{1}{3} \int_0^\infty \langle \vec{v}(0) \cdot \vec{v}(t) \rangle dt$$

In the nematic phase, where there is a preferred direction of orientation, we can calculate translational diffusion coefficients parallel and perpendicular to the director:

$$D_T^{\parallel} = \frac{1}{3} \int_0^\infty \langle \vec{v}(0) \cdot \hat{n}\hat{n} \cdot \vec{v}(t) \rangle dt$$
$$D_T^{\perp} = \frac{1}{3} \int_0^\infty \langle \vec{v}(0) \cdot (\mathbb{1} - \hat{n}\hat{n}) \cdot \vec{v}(t) \rangle dt$$

Here $\hat{n}\hat{n}$ is the director dyad, obtained by taking the "outer product" of $\hat{n}$ with itself, and $\mathbb{1}$ is the unit tensor. I obtained the following values for the translational diffusion coefficients:

Isotropic	Nematic
$D_T^* \approx 0.109$	$D_T^* \approx 0.0518$
	$D_T^{*\parallel} \approx 0.0366$
	$D_T^{*\perp} \approx 0.0152$

As expected, the translational diffusion coefficient is smaller in the denser and more ordered nematic phase. Also, it is apparent from that translational diffusion is easier in the direction of the director than in directions perpendicular to the director.

A.7.2 Orientation Autocorrelation Function

The rank l orientation autocorrelation functions are defined as:

$$C^l(t) = \langle P_l(\hat{\Omega}(0) \cdot \hat{\Omega}(t)) \rangle$$

We shall employ the second-rank function here, because this function is insensitive to whether the orientation vectors are pointing "North" or "South:" it treats both directions as representing the same symmetry axis.

$$\begin{aligned} C^2(t) &= \langle P_2(\hat{\Omega}(0) \cdot \hat{\Omega}(t)) \rangle \\ &= \left\langle \frac{3}{2}(\hat{\Omega}(0) \cdot \hat{\Omega}(t))^2 - \frac{1}{2} \right\rangle \end{aligned}$$

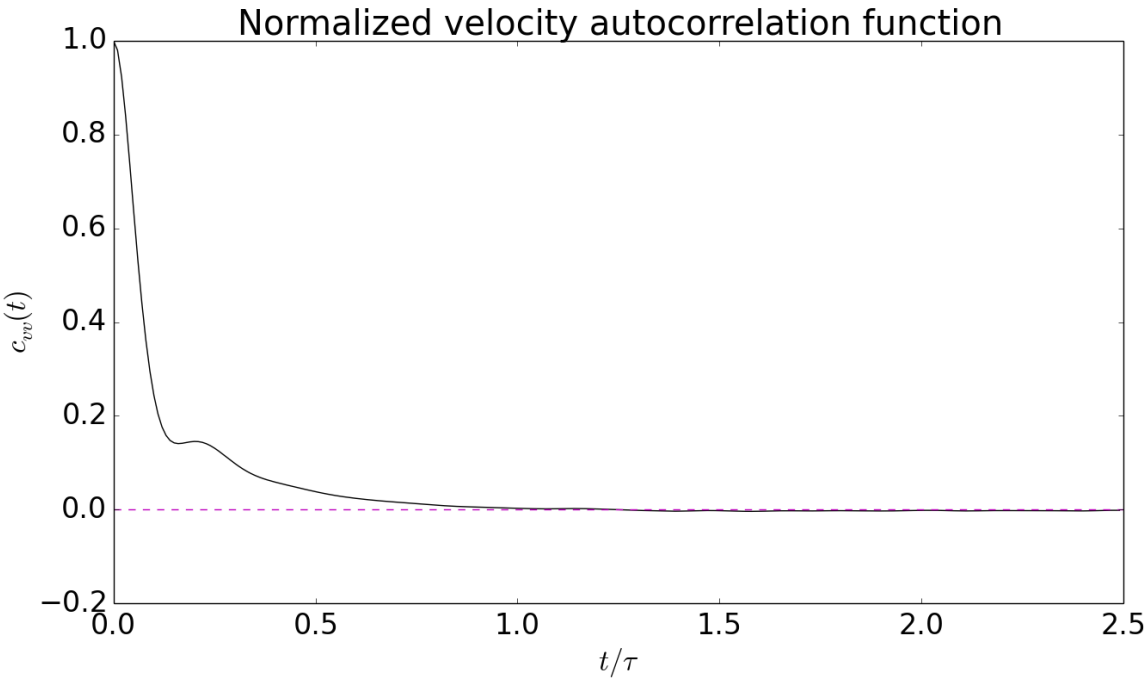

Figure 27: Velocity autocorrelation function in the isotropic phase.

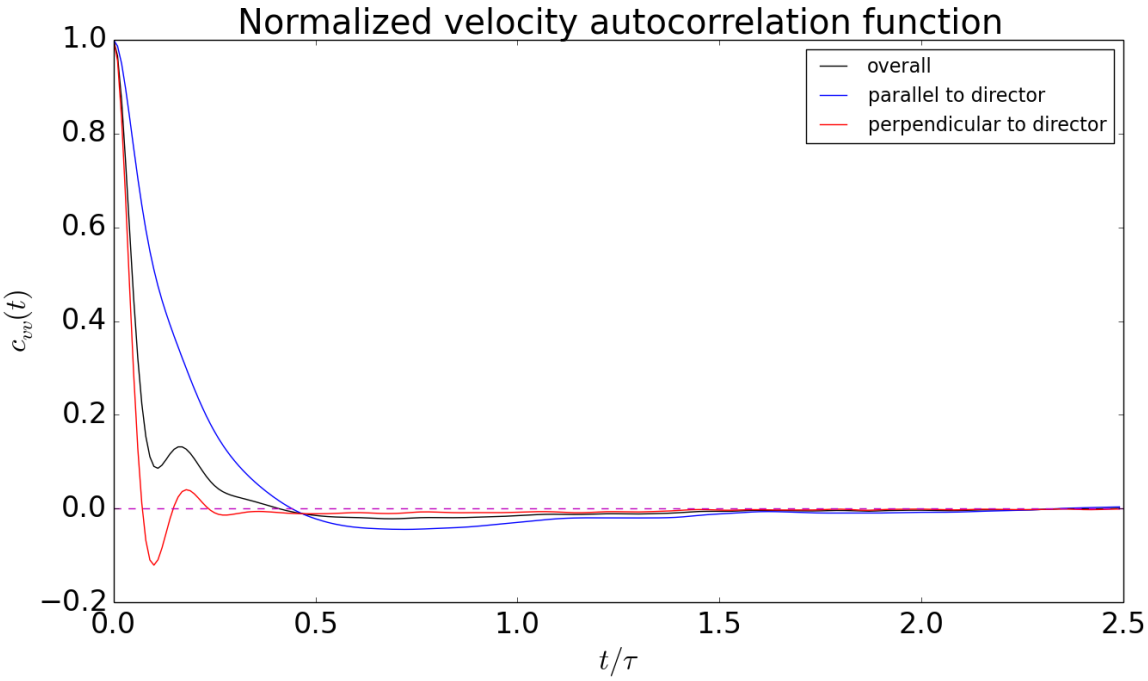

Figure 28: Velocity autocorrelation function in the nematic phase.

This function gives us information about the degree of orientational order in the system. The asymptotic value of this correlation function is the square of the order parameter:

$$\lim_{t\to\infty} C^2(t) = S^2$$

A proof of this can be found in Appendix A.10. From this equation, we see that in a perfectly isotropic system, where the order parameter is zero, the asymptotic value of $C^2(t)$ would be zero. On the other hand, in an anisotropic system where there is a high degree of orientational order, the correlation function will decay to a nonzero value. This is illustrated in the following figures, which show $C^2(t)$ in the isotropic and nematic phases.

A.7.3 Angular Velocity Autocorrelation Function

The angular velocity autocorrelation function is given by:

$$C_{\omega\omega}(t) = \langle \vec{\omega}(0) \cdot \vec{\omega}(t) \rangle$$

A Green-Kubo relation [17] allows us to extract the rotational diffusion constant from $C_{\omega\omega}$:

$$D_R = \frac{1}{2} \int_0^\infty \langle \vec{\omega}(0) \cdot \vec{\omega}(t) \rangle dt$$

We can define an autocorrelation function for each of the degrees of freedom in the body-fixed frame [18]:

$$C^\alpha_{\omega\omega}(t) = \langle \omega^b_\alpha(0) \omega^b_\alpha(t) \rangle$$

Where $\alpha = x, y, z$. Since the Gay-Berne molecules are axially symmetric, $\omega^b_z = 0$, so we only need to consider x and y. By symmetry, the autocorrelation functions in x and y should be identical. With this correlation function in hand, we can define rotational diffusion coefficients for the body fixed x and y:

$$D^\alpha_R = \int_0^\infty \langle \omega^b_\alpha(0) \omega^b_\alpha(t) \rangle \, dt$$

Using the fact that the dot product is invariant to a change of basis, we can write the overal rotational diffusion constant in terms of the body-fixed diffusion constants:

$$\begin{aligned} \langle \vec{\omega}(0) \cdot \vec{\omega}(t) \rangle &= \langle \omega^b_x(0) \omega^b_x(t) \rangle + \langle \omega^b_y(0) \omega^b_y(t) \rangle \\ \implies D_R &= \frac{1}{2}(D^x_R + D^y_R) \end{aligned}$$

An aside: rotational diffusion coefficients are often calculated using the Debye model, which assumes that the orientation vector takes a random walk, with small steps, on the surface of a sphere. However, for nematic liquid crystals is assumption is untenable: the orientation vectors spend most of their time on some small portion of the hypothetical sphere (around the director) and presumably must make large-angle jumps to escape from this region. Thus, we use the angular velocity autocorrelation function instead. For further discussion on the breakdown of the Debye model, see Stillinger [18].

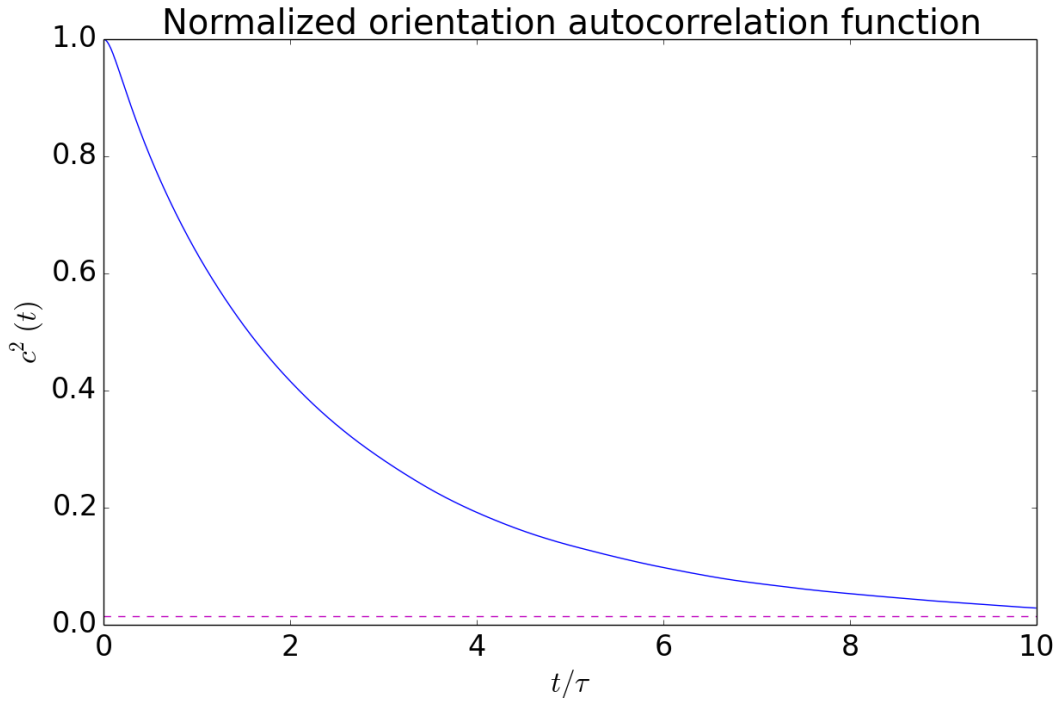

Figure 29: Orientation autocorrelation function in the isotropic phase. The dashed line is the square of the order parameter

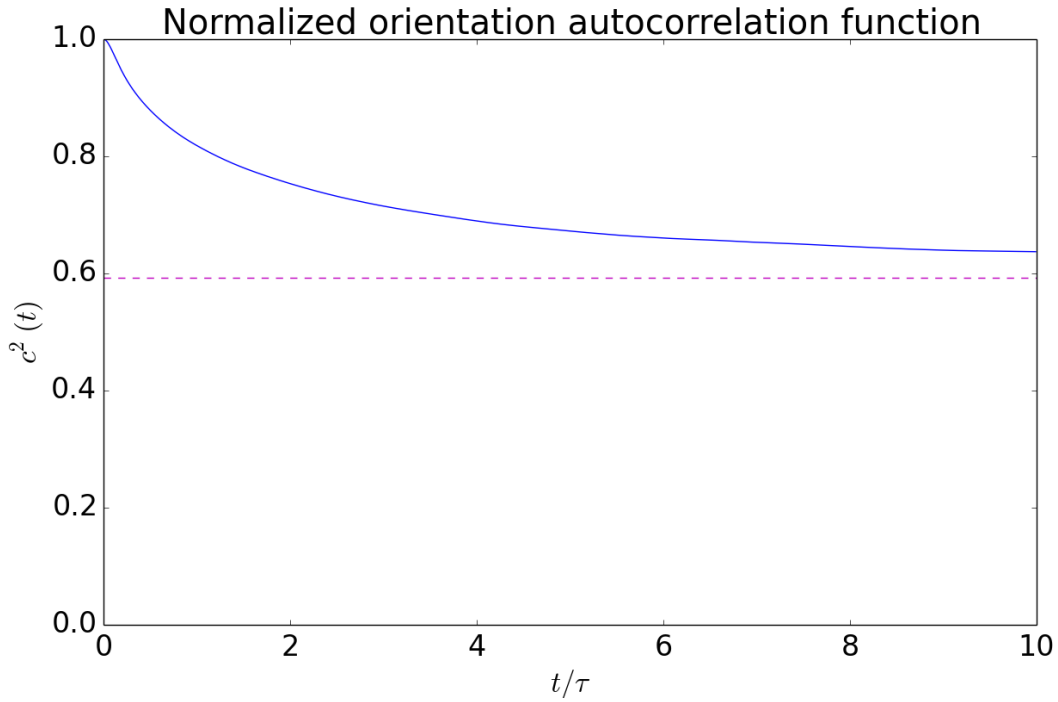

Figure 30: Orientation autocorrelation function in the nematic phase. The dashed line is the square of the order parameter.

To actually calculate the components, ω_α^b, we need to transform the space-fixed vector $\vec{\omega}^s$ into the body-fixed frame. One straightforward way to do this is through Euler angles ([19]). We first rotate the vector through an angle ϕ about the z-axis: ϕ is the angle though which the space-fixed x and y axes are rotated (about z) so that the space fixed y axis lies at a 180 degree angle from the projection of the orientation vector onto the original xy plane. This rotation is performed by multiplying $\vec{\omega}^s$ by the following rotation matrix:

$$\begin{pmatrix} \cos\phi & -\sin\phi & 0 \\ \sin\phi & \cos\phi & 0 \\ 0 & 0 & 1 \end{pmatrix}$$

Next, we rotate the angular velocity vector through an angle θ about the space-fixed x-axis, where θ is the angle between the space-fixed z axis and the orientation vector. This rotation is described by the matrix:

$$\begin{pmatrix} 1 & 0 & 0 \\ 0 & \cos\theta & -\sin\theta \\ 0 & \sin\theta & \cos\theta \end{pmatrix}$$

One would expect that we would be done at this point. However, I found that it was necessary to apply a third rotation, by the angle $-\phi$ about the body-fixed z axis, in order for the rotational diffusion coefficients in x and y to have similar values (which they ought to have.) This is due to the fact that the Gay-Berne molecules are linear and hence symmetric with respect to rotation about the long molecular axis.

The rotational diffusion coefficients are shown below:

Isotropic	Nematic
$D_R^{*x} \approx 0.0560$	$D_R^{*x} \approx 0.00807$
$D_R^{*y} \approx 0.0575$	$D_R^{*y} \approx 0.00955$
$D_R^{*} \approx 0.0568$	$D_R^{*} \approx 0.00881$

As can be seen, for a given phase, the rotational diffusion coefficients in x and y are similar. Also, as expected, the rotational diffusion coefficients are smaller in the denser and more ordered nematic phase than in the isotropic phase.

A.8 Derivation of Gay-Berne Forces and Auxiliary Torques

The calculation of the forces and auxiliary torques on a Gay-Berne molecule involves taking derivatives of the Gay-Berne potential:

$$\begin{aligned} u(\vec{r}, \hat{\Omega}_i, \hat{\Omega}_j) &= 4\epsilon^{\nu}(\hat{\Omega}_i, \hat{\Omega}_j)\epsilon'^{\mu}(\hat{r}, \hat{\Omega}_i, \hat{\Omega}_j) \\ &\times \left[\left(\frac{\sigma_0}{r - \sigma(\hat{r}, \hat{\Omega}_i, \hat{\Omega}_j) + \sigma_0} \right)^{12} - \left(\frac{\sigma_0}{r - \sigma(\hat{r}, \hat{\Omega}_i, \hat{\Omega}_j) + \sigma_0} \right)^{6} \right] \end{aligned}$$

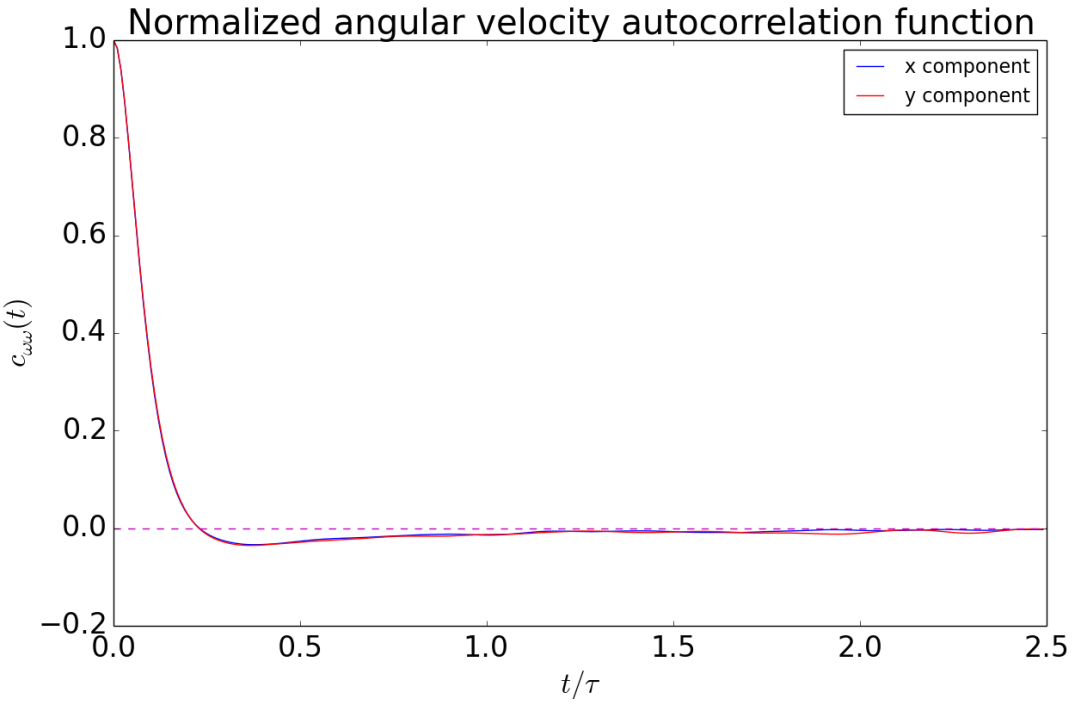

Figure 31: Orientation autocorrelation function in the isotropic phase.

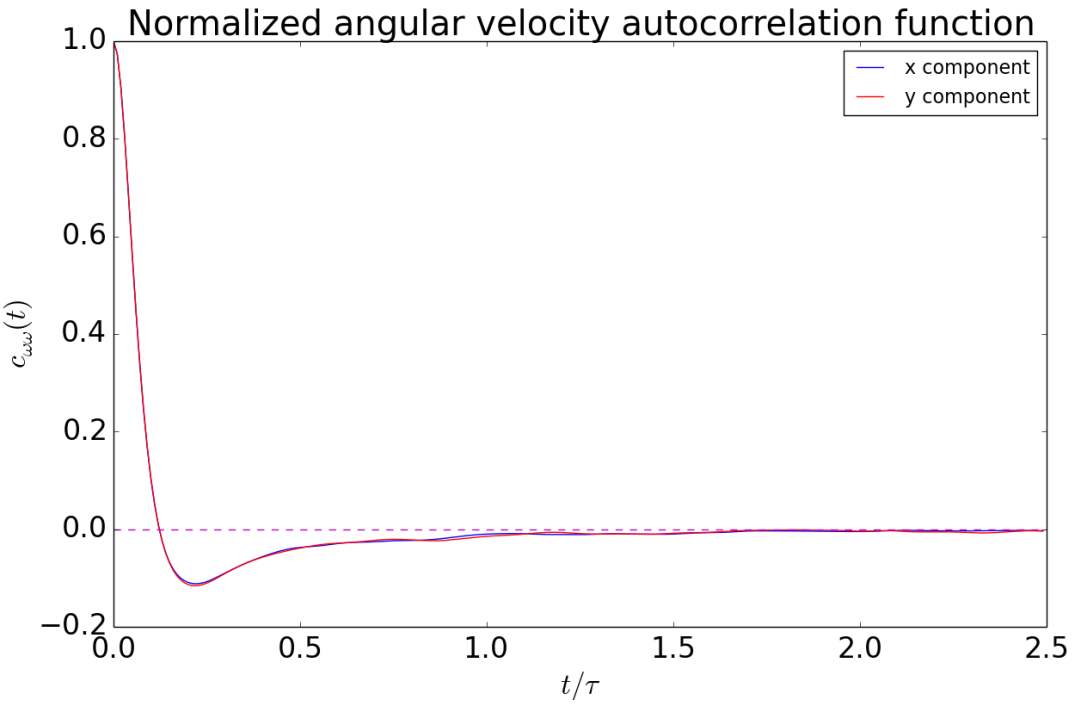

Figure 32: Orientation autocorrelation function in the nematic phase.

Where:

$$\epsilon(\hat{\Omega}_i, \hat{\Omega}_j) = \epsilon_0 \left[1 - \chi^2(\hat{\Omega}_i \cdot \hat{\Omega}_j)\right]^{-1/2}$$

$$\epsilon'(\hat{r}, \hat{\Omega}_i, \hat{\Omega}_j) = 1 - \frac{\chi'}{2}\left[\frac{(\hat{r}\cdot\hat{\Omega}_i + \hat{r}\cdot\hat{\Omega}_j)^2}{1+\chi'(\hat{\Omega}_i\cdot\hat{\Omega}_j)} + \frac{(\hat{r}\cdot\hat{\Omega}_i - \hat{r}\cdot\hat{\Omega}_j)^2}{1-\chi'(\hat{\Omega}_i\cdot\hat{\Omega}_j)}\right]$$

$$\sigma(\hat{r}, \hat{\Omega}_i, \hat{\Omega}_j) = \sigma_0 \left(1 - \frac{\chi}{2}\left[\frac{(\hat{r}\cdot\hat{\Omega}_i + \hat{r}\cdot\hat{\Omega}_j)^2}{1+\chi(\hat{\Omega}_i\cdot\hat{\Omega}_j)} + \frac{(\hat{r}\cdot\hat{\Omega}_i - \hat{r}\cdot\hat{\Omega}_j)^2}{1-\chi(\hat{\Omega}_i\cdot\hat{\Omega}_j)}\right]\right)^{-1/2}$$

For convenience, we shall also define:

$$R = \frac{\sigma_0}{r - \sigma + \sigma_0}$$

The total potential of the system is the sum of the potential energy of the interaction between each pair of molecules. Letting $u_{ij} = u(\vec{r}_{ij}, \hat{\Omega}_i, \hat{\Omega}_j)$,

$$U = \sum_i \sum_{j>i} u_{ij}$$

The force on the i-th molecule is given by:

$$\begin{aligned}\vec{f}_i &= -\frac{\partial U}{\partial \vec{r}_i} \\ &= -\sum_{j\neq i} \frac{\partial}{\partial \vec{r}_i} u_{ij} = -\sum_{j\neq i} \vec{f}_{ij}\end{aligned}$$

Where $\vec{f}_{ij}$ is the force on molecule i due to molecule j. To get the μ-th component of the force on i, , we need the derivative of u_{ij} with respect to the μ-th component of $\vec{r}_i$. Following the suggestion of Allen and Germano [20], we can write the dependencies of u in a more compuationally friendly form:

$$u(\vec{r}, \hat{\Omega}_i, \hat{\Omega}_j) = u(r,\, \hat{r}\cdot\hat{\Omega}_i,\, \hat{r}\cdot\hat{\Omega}_j,\, \hat{\Omega}_i\cdot\hat{\Omega}_j)$$

We can now apply the chain rule. If we have a function $f = f(x_1(t), ..., x_n(t))$,

$$\frac{\partial f}{\partial t} = \sum_{i=1}^{n} \frac{\partial f}{\partial x_i}\frac{\partial x_i}{\partial t}$$

Thus,

$$\begin{aligned}\left(\frac{\partial}{\partial \vec{r}_i} u_{ij}\right)_\mu = {} & \left.\frac{\partial u}{\partial r}\right|_{r_{ij}} \frac{\partial r_{ij}}{\partial r_{i\mu}} + \left.\frac{\partial u}{\partial(\hat{r}\cdot\hat{\Omega}_i)}\right|_{r_{ij}} \frac{\partial(\hat{r}\cdot\hat{\Omega}_i)}{\partial r_{i\mu}} \\ & + \left.\frac{\partial u}{\partial(\hat{r}\cdot\hat{\Omega}_j)}\right|_{r_{ij}} \frac{\partial(\hat{r}\cdot\hat{\Omega}_j)}{\partial r_{i\mu}} + \left.\frac{\partial u}{\partial(\hat{\Omega}_i\cdot\hat{\Omega}_j)}\right|_{r_{ij}} \frac{\partial(\hat{\Omega}_i\cdot\hat{\Omega}_j)}{\partial r_{i\mu}}\end{aligned}$$

For future reference, I will assign the derivatives of u in the above equation, in the order in which they appear, the labels 1), 2), 3) 4). The last term in the above equation is zero, since the orientations do not depend on r, so we have:

$$\left(\frac{\partial}{\partial \vec{r}_i} u_{ij}\right)_\mu = \left.\frac{\partial u}{\partial r}\right|_{r_{ij}} \frac{\partial r_{ij}}{\partial r_{i\mu}} + \left.\frac{\partial u}{\partial(\hat{r}\cdot\hat{\Omega}_i)}\right|_{r_{ij}} \frac{\partial(\hat{r}\cdot\hat{\Omega}_i)}{\partial r_{i\mu}} + \left.\frac{\partial u}{\partial(\hat{r}\cdot\hat{\Omega}_j)}\right|_{r_{ij}} \frac{\partial(\hat{r}\cdot\hat{\Omega}_j)}{\partial r_{i\mu}}$$

We will first evaluate the derivatives that do not depend on u:

$$\begin{aligned}
\frac{\partial r_{ij}}{\partial r_{i\mu}} &= \frac{\partial}{\partial r_{i\mu}} \sqrt{\sum_\nu (r_{i\nu} - r_{j\nu})^2} \\
&= \frac{1}{r_{ij}}(r_{i\mu} - r_{j\mu})
\end{aligned}$$

$$\begin{aligned}
\frac{\partial(\hat{r}_{ij}\cdot\hat{\Omega}_i)}{r_{i\mu}} &= \frac{\partial}{\partial r_{i\mu}} \left(\frac{\vec{r}_{ij}}{r_{ij}}\cdot\hat{\Omega}_i\right) \\
&= \frac{\partial}{\partial r_{i\mu}} \left(\sum_\nu \frac{(r_{i\nu} - r_{j\nu})}{r_{ij}}(\hat{\Omega}_i)_\nu\right) \\
&= \sum_\nu (r_{i\nu} - r_{j\nu})(\hat{\Omega}_i)_\nu \frac{\partial}{\partial r_{i\mu}}\left(\frac{1}{r_{ij}}\right) + \frac{1}{r_{ij}}\frac{\partial}{\partial r_{i\mu}}(r_{i\mu} - r_{j\mu})(\hat{\Omega}_i)_\mu \\
&= (\vec{r}_{ij}\cdot\hat{\Omega}_i)\left(-\frac{1}{r_{ij}^2}\right)\left(\frac{(\vec{r_{ij}})_\mu}{r_{ij}}\right) + \frac{(\hat{\Omega}_i)_\mu}{r_{ij}} \\
&= -(\hat{r}_{ij}\cdot\hat{\Omega}_i)\left(\frac{(\vec{r}_{ij})_\mu}{r_{ij}^2}\right) + \frac{(\hat{\Omega}_i)_\mu}{r_{ij}}
\end{aligned}$$

$$\begin{aligned}
\frac{\partial(\hat{r}_{ij}\cdot\hat{\Omega}_j)}{r_{i\mu}} &= \frac{\partial}{\partial r_{i\mu}} \left(\frac{\vec{r}_{ij}}{r_{ij}}\cdot\hat{\Omega}_j\right) \\
&= \frac{\partial}{\partial r_{i\mu}} \left(\sum_\nu \frac{(r_{i\nu} - r_{j\nu})}{r_{ij}}(\hat{\Omega}_j)_\nu\right) \\
&= \sum_\nu (r_{i\nu} - r_{j\nu})(\hat{\Omega}_j)_\nu \frac{\partial}{\partial r_{i\mu}}\left(\frac{1}{r_{ij}}\right) + \frac{1}{r_{ij}}\frac{\partial}{\partial r_{i\mu}}(r_{i\mu} - r_{j\mu})(\hat{\Omega}_j)_\mu \\
&= (\vec{r}_{ij}\cdot\hat{\Omega}_j)\left(-\frac{1}{r_{ij}^2}\right)\left(\frac{(\vec{r_{ij}})_\mu}{r_{ij}}\right) + \frac{(\hat{\Omega}_j)_\mu}{r_{ij}} \\
&= -(\hat{r}_{ij}\cdot\hat{\Omega}_j)\left(\frac{(\vec{r}_{ij})_\mu}{r_{ij}^2}\right) + \frac{(\hat{\Omega}_j)_\mu}{r_{ij}}
\end{aligned}$$

We thus have an expression for $\vec{f}_i$ for any potential of the form $u(\vec{r}, \hat{\Omega}_i, \hat{\Omega}_j)$:

$$(\vec{f}_i)_\mu = -\sum_{j\neq i} \left.\frac{\partial u}{\partial r}\right|_{r_{ij}} \frac{(\vec{r}_{ij})_\mu}{r_{ij}} + \left.\frac{\partial u}{\partial(\hat{r}\cdot\hat{\Omega}_i)}\right|_{r_{ij}} \left[\frac{(\hat{\Omega}_i)_\mu}{r_{ij}} - \frac{(\vec{r}_{ij})_\mu(\hat{r}_{ij}\cdot\hat{\Omega}_i)}{r_{ij}^2}\right] + \left.\frac{\partial u}{\partial(\hat{r}\cdot\hat{\Omega}_j)}\right|_{r_{ij}} \left[\frac{(\hat{\Omega}_j)_\mu}{r_{ij}} - \frac{(\vec{r}_{ij})_\mu(\hat{r}_{ij}\cdot\hat{\Omega}_j)}{r_{ij}^2}\right]$$

Now we just need the derivatives of the Gay-Berne potential:

1)

$$\begin{aligned}
\frac{\partial u}{\partial r} &= \frac{\partial}{\partial r}\left(4\epsilon^\nu \epsilon'^\mu \left[R^{12} - R^6\right]\right) \\
&= 4\epsilon^\nu \epsilon'^\mu \frac{\partial}{\partial r}\left(R^{12} - R^6\right) \\
&= 4\epsilon^\nu \epsilon'^\mu \left(12R^{11} - 6R^5\right)\frac{\partial}{\partial r}R \\
&= 4\epsilon^\nu \epsilon'^\mu \left(12R^{11} - 6R^5\right)\left(-\frac{\sigma_0}{(r-\sigma+\sigma_0)^2}\right) \\
&= 24\epsilon^\nu \epsilon'^\mu \sigma_0^{-1}\left(R^7 - 2R^{13}\right)
\end{aligned}$$

2)

$$\begin{aligned}
\frac{\partial u}{\partial(\hat{r}\cdot\hat{\Omega}_i)} &= \frac{\partial}{\partial(\hat{r}\cdot\hat{\Omega}_i)}\left(4\epsilon^\nu \epsilon'^\mu \left(R^{12} - R^6\right)\right) \\
&= 4\epsilon^\nu \frac{\partial}{\partial(\hat{r}\cdot\hat{\Omega}_i)}\left(\epsilon'^\mu \left(R^{12} - R^6\right)\right) \\
&= 4\mu\epsilon^\nu \epsilon'^{\mu-1}\frac{\partial\epsilon'}{\partial(\hat{r}\cdot\hat{\Omega}_i)}\left(R^{12} - R^6\right) \\
&\quad + 24\epsilon^\nu \epsilon'^\mu \sigma_0^{-1}\left(2R^{13} - R^7\right)\frac{\partial\sigma}{\partial(\hat{r}\cdot\hat{\Omega}_i)}
\end{aligned}$$

Where:

$$\begin{aligned}
\frac{\partial \epsilon'}{\partial(\hat{r}\cdot\hat{\Omega}_i)} &= \frac{\partial}{\partial(\hat{r}\cdot\hat{\Omega}_i)}\left(1-\frac{\chi'}{2}\left[\frac{(\hat{r}\cdot\hat{\Omega}_i+\hat{r}\cdot\hat{\Omega}_j)^2}{1+\chi'(\hat{\Omega}_i\cdot\hat{\Omega}_j)}+\frac{(\hat{r}\cdot\hat{\Omega}_i-\hat{r}\cdot\hat{\Omega}_j)^2}{1-\chi'(\hat{\Omega}_i\cdot\hat{\Omega}_j)}\right]\right)\\
&= -\frac{\chi'}{2}\left(\frac{2(\hat{r}\cdot\hat{\Omega}_i+\hat{r}\cdot\hat{\Omega}_j)}{1+\chi'(\hat{\Omega}_i\cdot\hat{\Omega}_j)}+\frac{2(\hat{r}\cdot\hat{\Omega}_i-\hat{r}\cdot\hat{\Omega}_j)}{1-\chi'(\hat{\Omega}_i\cdot\hat{\Omega}_j)}\right)\\
&= -\chi'\left(\frac{\hat{r}\cdot\hat{\Omega}_i+\hat{r}\cdot\hat{\Omega}_j}{1+\chi'(\hat{\Omega}_i\cdot\hat{\Omega}_j)}+\frac{\hat{r}\cdot\hat{\Omega}_i-\hat{r}\cdot\hat{\Omega}_j}{1-\chi'(\hat{\Omega}_i\cdot\hat{\Omega}_j)}\right)
\end{aligned}$$

$$\begin{aligned}
\frac{\partial \sigma}{\partial(\hat{r}\cdot\hat{\Omega}_i)} &= \frac{\partial}{\partial(\hat{r}\cdot\hat{\Omega}_i)}\left(\sigma_0\left(1-\frac{\chi}{2}\left[\frac{(\hat{r}\cdot\hat{\Omega}_i+\hat{r}\cdot\hat{\Omega}_j)^2}{1+\chi(\hat{\Omega}_i\cdot\hat{\Omega}_j)}+\frac{(\hat{r}\cdot\hat{\Omega}_i-\hat{r}\cdot\hat{\Omega}_j)^2}{1-\chi(\hat{\Omega}_i\cdot\hat{\Omega}_j)}\right]\right)^{-1/2}\right)\\
&= -\frac{1}{2}\sigma_0\left(\frac{\sigma}{\sigma_0}\right)^3\left(-\frac{\chi}{2}\left(\frac{2(\hat{r}\cdot\hat{\Omega}_i+\hat{r}\cdot\hat{\Omega}_j)}{1+\chi(\hat{\Omega}_i\cdot\hat{\Omega}_j)}+\frac{2(\hat{r}\cdot\hat{\Omega}_i-\hat{r}\cdot\hat{\Omega}_j)}{1-\chi(\hat{\Omega}_i\cdot\hat{\Omega}_j)}\right)\right)\\
&= \frac{\chi}{2}\frac{\sigma^3}{\sigma_0^2}\left(\frac{\hat{r}\cdot\hat{\Omega}_i+\hat{r}\cdot\hat{\Omega}_j}{1+\chi(\hat{\Omega}_i\cdot\hat{\Omega}_j)}+\frac{\hat{r}\cdot\hat{\Omega}_i-\hat{r}\cdot\hat{\Omega}_j}{1-\chi(\hat{\Omega}_i\cdot\hat{\Omega}_j)}\right)
\end{aligned}$$

3)

$$\begin{aligned}
\frac{\partial u}{\partial(\hat{r}\cdot\hat{\Omega}_j)} &= \frac{\partial}{\partial(\hat{r}\cdot\hat{\Omega}_j)}\left(4\epsilon^\nu\epsilon'^\mu\left(R^{12}-R^6\right)\right)\\
&= 4\epsilon^\nu\frac{\partial}{\partial(\hat{r}\cdot\hat{\Omega}_j)}\left(\epsilon'^\mu\left(R^{12}-R^6\right)\right)\\
&= 4\mu\epsilon^\nu\epsilon'^{\mu-1}\frac{\partial\epsilon'}{\partial(\hat{r}\cdot\hat{\Omega}_j)}\left(R^{12}-R^6\right)\\
&\quad + 24\epsilon^\nu\epsilon'^\mu\sigma_0^{-1}\left(2R^{13}-R^7\right)\frac{\partial\sigma}{\partial(\hat{r}\cdot\hat{\Omega}_j)}
\end{aligned}$$

Where:

$$\begin{aligned}
\frac{\partial \epsilon'}{\partial(\hat{r}\cdot\hat{\Omega}_j)} &= \frac{\partial}{\partial(\hat{r}\cdot\hat{\Omega}_j)}\left(1-\frac{\chi'}{2}\left[\frac{(\hat{r}\cdot\hat{\Omega}_i+\hat{r}\cdot\hat{\Omega}_j)^2}{1+\chi'(\hat{\Omega}_i\cdot\hat{\Omega}_j)}+\frac{(\hat{r}\cdot\hat{\Omega}_i-\hat{r}\cdot\hat{\Omega}_j)^2}{1-\chi'(\hat{\Omega}_i\cdot\hat{\Omega}_j)}\right]\right) \\
&= -\frac{\chi'}{2}\left(\frac{2(\hat{r}\cdot\hat{\Omega}_i+\hat{r}\cdot\hat{\Omega}_j)}{1+\chi'(\hat{\Omega}_i\cdot\hat{\Omega}_j)}-\frac{2(\hat{r}\cdot\hat{\Omega}_i-\hat{r}\cdot\hat{\Omega}_j)}{1-\chi'(\hat{\Omega}_i\cdot\hat{\Omega}_j)}\right) \\
&= -\chi'\left(\frac{\hat{r}\cdot\hat{\Omega}_i+\hat{r}\cdot\hat{\Omega}_j}{1+\chi'(\hat{\Omega}_i\cdot\hat{\Omega}_j)}-\frac{\hat{r}\cdot\hat{\Omega}_i-\hat{r}\cdot\hat{\Omega}_j}{1-\chi'(\hat{\Omega}_i\cdot\hat{\Omega}_j)}\right)
\end{aligned}$$

$$\begin{aligned}
\frac{\partial \sigma}{\partial(\hat{r}\cdot\hat{\Omega}_j)} &= \frac{\partial}{\partial(\hat{r}\cdot\hat{\Omega}_j)}\left(\sigma_0\left(1-\frac{\chi}{2}\left[\frac{(\hat{r}\cdot\hat{\Omega}_i+\hat{r}\cdot\hat{\Omega}_j)^2}{1+\chi(\hat{\Omega}_i\cdot\hat{\Omega}_j)}+\frac{(\hat{r}\cdot\hat{\Omega}_i-\hat{r}\cdot\hat{\Omega}_j)^2}{1-\chi(\hat{\Omega}_i\cdot\hat{\Omega}_j)}\right]\right)^{-1/2}\right) \\
&= -\frac{1}{2}\frac{\sigma^3}{\sigma_0^2}\left(-\frac{\chi}{2}\left(\frac{2(\hat{r}\cdot\hat{\Omega}_i+\hat{r}\cdot\hat{\Omega}_j)}{1+\chi(\hat{\Omega}_i\cdot\hat{\Omega}_j)}-\frac{2(\hat{r}\cdot\hat{\Omega}_i-\hat{r}\cdot\hat{\Omega}_j)}{1-\chi(\hat{\Omega}_i\cdot\hat{\Omega}_j)}\right)\right) \\
&= \frac{\chi}{2}\frac{\sigma^3}{\sigma_0^2}\left(\frac{\hat{r}\cdot\hat{\Omega}_i+\hat{r}\cdot\hat{\Omega}_j}{1+\chi(\hat{\Omega}_i\cdot\hat{\Omega}_j)}-\frac{\hat{r}\cdot\hat{\Omega}_i-\hat{r}\cdot\hat{\Omega}_j}{1-\chi(\hat{\Omega}_i\cdot\hat{\Omega}_j)}\right)
\end{aligned}$$

Thus, we have completely specified an arbitrary (Cartesian) component of the force on any one Gay-Berne molecule due to all the other molecules.

Our next task is to calculate the torque. The torque on the ith molecule is given by:

$$\vec{\tau}_i = \hat{\Omega}_i \times \vec{g}_i$$

The quantity $\vec{g}_i$ is called the *auxiliary torque* on molecule i. It is a generalized force (which comes from taking a derivative of the Lagrangian with respect to a generalized coordinate) given by:

$$\vec{g}_i = -\frac{\partial U}{\partial \hat{\Omega}_i} = -\sum_{j\neq i}\frac{\partial}{\partial \hat{\Omega}_i}u_{ij} = -\sum_{j\neq i}\vec{g}_{ij}$$

where $\vec{g}_{ij}$ is the auxiliary torque on molecule i due to molecule j. We wish to calculate the μth component of this gradient. Again, we will rewrite u:

$$u(\vec{r},\hat{\Omega}_i,\hat{\Omega}_j) = u(r,\hat{r}\cdot\hat{\Omega}_i,\hat{r}\cdot\hat{\Omega}_j,\hat{\Omega}_i\cdot\hat{\Omega}_j)$$

and apply the chain rule:

$$\begin{aligned}
\left(\frac{\partial}{\partial\hat{\Omega}_i}u_{ij}\right)_\mu &= \left.\frac{\partial u}{\partial r}\right|_{r_{ij}}\frac{\partial r_{ij}}{\partial(\hat{\Omega}_i)_\mu}+\left.\frac{\partial u}{\partial(\hat{r}\cdot\hat{\Omega}_i)}\right|_{r_{ij}}\frac{\partial(\hat{r}\cdot\hat{\Omega}_i)}{\partial(\hat{\Omega}_i)_\mu} \\
&\quad+\left.\frac{\partial u}{\partial(\hat{r}\cdot\hat{\Omega}_j)}\right|_{r_{ij}}\frac{\partial(\hat{r}\cdot\hat{\Omega}_j)}{\partial(\hat{\Omega}_i)_\mu}+\left.\frac{\partial u}{\partial(\hat{\Omega}_i\cdot\hat{\Omega}_j)}\right|_{r_{ij}}\frac{\partial(\hat{\Omega}_i\cdot\hat{\Omega}_j)}{\partial(\hat{\Omega}_i)_\mu}
\end{aligned}$$

The first and third terms of this expression are zero, since r_{ij} does not depend on the orientations and since the orientation of the jth molecule does not depend on the orientation of the ith molecule. So we have:

$$\left(\frac{\partial}{\partial\hat{\Omega}_i}u_{ij}\right)_\mu = \left.\frac{\partial u}{\partial(\hat{r}\cdot\hat{\Omega}_i)}\right|_{r_{ij}} \frac{\partial(\hat{r}\cdot\hat{\Omega}_i)}{\partial(\hat{\Omega}_i)_\mu} + \left.\frac{\partial u}{\partial(\hat{\Omega}_i\cdot\hat{\Omega}_j)}\right|_{r_{ij}} \frac{\partial(\hat{\Omega}_i\cdot\hat{\Omega}_j)}{\partial(\hat{\Omega}_i)_\mu}$$

Let's evaluate the derivatives that don't depend on u:

$$\begin{aligned}
\frac{\partial(\hat{r}_{ij}\cdot\hat{\Omega}_i)}{\partial(\hat{\Omega}_i)_\mu} &= \frac{\partial}{\partial(\hat{\Omega}_i)_\mu}\frac{1}{r_{ij}}\sum_\nu (r_{i\nu}-r_{j\nu})(\hat{\Omega}_i)_\nu \\
&= \frac{r_{i\mu}-r_{j\mu}}{r_{ij}} \\
&= (\hat{r}_{ij})_\mu \\
\frac{\partial(\hat{\Omega}_i\cdot\hat{\Omega}_j)}{\partial(\hat{\Omega}_i)_\mu} &= \frac{\partial}{\partial(\hat{\Omega}_i)_\mu}\sum_\nu (\hat{\Omega}_i)_\nu(\hat{\Omega}_j)_\nu \\
&= (\hat{\Omega}_j)_\mu
\end{aligned}$$

So,

$$\boxed{(\vec{g}_i)_\mu = -\sum_{j\neq i}\left[\left.\frac{\partial u}{\partial(\hat{r}\cdot\hat{\Omega}_i)}\right|_{r_{ij}}(\hat{r}_{ij})_\mu + \left.\frac{\partial u}{\partial(\hat{\Omega}_i\cdot\hat{\Omega}_j)}\right|_{r_{ij}}(\hat{\Omega}_j)_\mu\right]}$$

We calculated the derivative u that appears in the first term of the expression above previously, for the force calculation, so it remains to calculate the derivative which appears in the second term:

4)

$$\begin{aligned}
\frac{\partial u}{\partial(\hat{\Omega}_i\cdot\hat{\Omega}_j)} &= \frac{\partial}{\partial(\hat{\Omega}_i\cdot\hat{\Omega}_j)}\left(4\epsilon^\nu\epsilon'^\mu\left(R^{12}-R^6\right)\right) \\
&= 4\left(R^{12}-R^6\right)\frac{\partial}{\partial(\hat{\Omega}_i\cdot\hat{\Omega}_j)}(\epsilon^\nu\epsilon'^\mu) + 4\epsilon^\nu\epsilon'^\mu\frac{\partial}{\partial(\hat{\Omega}_i\cdot\hat{\Omega}_j)}\left(R^{12}-R^6\right) \\
&= 4\left(R^{12}-R^6\right)\left(\nu\epsilon^{\nu-1}\epsilon'^\mu\frac{\partial\epsilon}{\partial(\hat{\Omega}_i\cdot\hat{\Omega}_j)} + \mu\epsilon^\nu\epsilon'^{\mu-1}\frac{\partial\epsilon'}{\partial(\hat{\Omega}_i\cdot\hat{\Omega}_j)}\right) \\
&+ 24\sigma_0^{-1}\epsilon^\nu\epsilon'^\mu\left(2R^{13}-R^7\right)\frac{\partial\sigma}{\partial(\hat{\Omega}_i\cdot\hat{\Omega}_j)}
\end{aligned}$$

Where:

$$\begin{aligned}
\frac{\partial \epsilon}{\partial(\hat{\Omega}_j \cdot \hat{\Omega}_i)} &= \frac{\partial}{\partial(\hat{\Omega}_i \cdot \hat{\Omega}_j)} \epsilon_0 \left[1 - \chi^2 (\hat{\Omega}_i \cdot \hat{\Omega}_j)^2\right]^{-1/2} \\
&= -\frac{\epsilon_0}{2} \left[1 - \chi^2 (\hat{\Omega}_i \cdot \hat{\Omega}_j)^2\right]^{-3/2} \left(-2\chi^2 (\hat{\Omega}_i \cdot \hat{\Omega}_j)\right) \\
&= \chi^2 \frac{\epsilon^3}{\epsilon_0^2} (\hat{\Omega}_i \cdot \hat{\Omega}_j)
\end{aligned}$$

$$\begin{aligned}
\frac{\partial \epsilon'}{\partial(\hat{\Omega}_i \cdot \hat{\Omega}_j)} &= \frac{\partial}{\partial(\hat{\Omega}_i \cdot \hat{\Omega}_j)} \left(1 - \frac{\chi'}{2} \left[\frac{(\hat{r} \cdot \hat{\Omega}_i + \hat{r} \cdot \hat{\Omega}_j)^2}{1 + \chi'(\hat{\Omega}_i \cdot \hat{\Omega}_j)} - \frac{(\hat{r} \cdot \hat{\Omega}_i - \hat{r} \cdot \hat{\Omega}_j)^2}{1 - \chi'(\hat{\Omega}_i \cdot \hat{\Omega}_j)}\right]\right) \\
&= \frac{\chi'^2}{2} \left[\left(\frac{\hat{r} \cdot \hat{\Omega}_i + \hat{r} \cdot \hat{\Omega}_j}{1 + \chi'(\hat{\Omega}_i \cdot \hat{\Omega}_j)}\right)^2 - \left(\frac{\hat{r} \cdot \hat{\Omega}_i - \hat{r} \cdot \hat{\Omega}_j}{1 - \chi'(\hat{\Omega}_i \cdot \hat{\Omega}_j)}\right)^2\right]
\end{aligned}$$

$$\begin{aligned}
\frac{\partial \sigma}{\partial(\hat{\Omega}_i \cdot \hat{\Omega}_j)} &= \frac{\partial}{\partial(\hat{\Omega}_i \cdot \hat{\Omega}_j)} \left(\sigma_0 \left(1 - \frac{\chi}{2} \left[\frac{(\hat{r} \cdot \hat{\Omega}_i + \hat{r} \cdot \hat{\Omega}_j)^2}{1 + \chi(\hat{\Omega}_i \cdot \hat{\Omega}_j)} + \frac{(\hat{r} \cdot \hat{\Omega}_i - \hat{r} \cdot \hat{\Omega}_j)^2}{1 - \chi(\hat{\Omega}_i \cdot \hat{\Omega}_j)}\right]\right)^{-1/2}\right) \\
&= -\frac{1}{2} \frac{\sigma^3}{\sigma_0^2} \frac{\partial}{\partial(\hat{\Omega}_i \cdot \hat{\Omega}_j)} \left(1 - \frac{\chi}{2} \left[\frac{(\hat{r} \cdot \hat{\Omega}_i + \hat{r} \cdot \hat{\Omega}_j)^2}{1 + \chi(\hat{\Omega}_i \cdot \hat{\Omega}_j)} + \frac{(\hat{r} \cdot \hat{\Omega}_i - \hat{r} \cdot \hat{\Omega}_j)^2}{1 - \chi(\hat{\Omega}_i \cdot \hat{\Omega}_j)}\right]\right) \\
&= -\frac{1}{2} \frac{\sigma^3}{\sigma_0^2} \left(-\frac{\chi^2}{2} \left[-\left(\frac{\hat{r} \cdot \hat{\Omega}_i + \hat{r} \cdot \hat{\Omega}_j}{1 + \chi(\hat{\Omega}_i \cdot \hat{\Omega}_j)}\right)^2 + \left(\frac{\hat{r} \cdot \hat{\Omega}_i - \hat{r} \cdot \hat{\Omega}_j}{1 - \chi(\hat{\Omega}_i \cdot \hat{\Omega}_j)}\right)^2\right]\right) \\
&= \frac{\chi^2}{4} \frac{\sigma^3}{\sigma_0^2} \left[\left(\frac{\hat{r} \cdot \hat{\Omega}_i - \hat{r} \cdot \hat{\Omega}_j}{1 - \chi(\hat{\Omega}_i \cdot \hat{\Omega}_j)}\right)^2 - \left(\frac{\hat{r} \cdot \hat{\Omega}_i + \hat{r} \cdot \hat{\Omega}_j}{1 + \chi(\hat{\Omega}_i \cdot \hat{\Omega}_j)}\right)^2\right]
\end{aligned}$$

By Newton's third law, the force on molecule i due to molecule j is the negative of the force on j due to i. However, the auxiliary torques don't work this way. To get the μth component of the auxiliary torque on molecule j due to molecule i, we switch the indices i and j in the equation for the auxiliary torque:

$$\boxed{(\vec{g}_{ji})_\mu = \left.\frac{\partial u}{\partial(\hat{r} \cdot \hat{\Omega}_j)}\right|_{r_{ij}} (\hat{r}_{ij})_\mu + \left.\frac{\partial u}{\partial(\hat{\Omega}_i \cdot \hat{\Omega}_j)}\right|_{r_{ij}} (\hat{\Omega}_i)_\mu}$$

We have thus completely specified the Gay-Berne forces and auxiliary torques.

A.9 Proof that the Q-tensor is Traceless

The Q-tensor is defined as:

$$\overleftrightarrow{Q} = \frac{1}{2N} \sum_{i=1}^{N} (3\hat{\Omega}_i \hat{\Omega}_i - \mathbb{1})$$

We wish to show that $\mathrm{Tr}\,\overleftrightarrow{Q} = 0$. Consider the diagonal elements of $\overleftrightarrow{Q}$:

$$Q_{\alpha\alpha} = \frac{1}{2N} \sum_{i=1}^{N} (3(\hat{\Omega}_i)_\alpha (\hat{\Omega}_i)_\alpha - 1)$$

To get the trace, we just sum over α:

$$\begin{aligned}\mathrm{Tr}\overleftrightarrow{Q} &= \sum_{\alpha} Q_{\alpha\alpha} \\ &= \frac{1}{2N}\sum_{i=1}^{N}\sum_{\alpha}(3(\hat{\Omega}_i)_\alpha(\hat{\Omega}_i)_\alpha - 1) \\ &= \frac{1}{2N}\sum_{i=1}^{n}\left(3\sum_{\alpha}((\hat{\Omega}_i)_\alpha(\hat{\Omega}_i)_\alpha) - 3\right)\end{aligned}$$

But $\sum_\alpha((\hat{\Omega}_i)_\alpha(\hat{\Omega}_i)_\alpha)$ is just $\hat{\Omega}_i \cdot \hat{\Omega}_i$, which is 1. So,

$$\begin{aligned}\mathrm{Tr}\overleftrightarrow{Q} &= \frac{1}{2N}\sum_{i=1}^{N}(3(1) - 3) \\ &= 0\end{aligned}$$

A.10 Derivation of the Asymptotic Value of $C^2(t)$

We wish to show that:

$$\lim_{t\to\infty}\langle P_2(\hat{\Omega}(0)\cdot\hat{\Omega}(t))\rangle = S^2$$

Where $S = \langle P_2(\cos\theta)\rangle = \langle P_2(\hat{n}\cdot\hat{\Omega})\rangle$. Do do this, first note that we can rewrite the correlation function using the addition theorem for spherical harmonics:

$$\begin{aligned}\langle P_2(\hat{\Omega}(0)\cdot\hat{\Omega}(t))\rangle &= \left\langle \frac{4\pi}{5}\sum_{m=-2}^{2} Y_2^m(\hat{\Omega}(0)Y_2^{*m}(\hat{\Omega}(t))\right\rangle \\ &= \frac{4\pi}{5}\sum_{m=-2}^{2}\langle Y_2^m(\hat{\Omega}(0))Y_2^{*m}(\hat{\Omega}(t))\rangle\end{aligned}$$

Now, using the fact that $\lim_{t\to\infty}\langle A(0)B(t)\rangle = \langle A\rangle\langle B\rangle$,

$$\lim_{t\to\infty}\langle P_2(\hat{\Omega(0)}\cdot\hat{\Omega}(t))\rangle = \frac{4\pi}{5}\sum_{m=-2}^{2}\langle Y_2^m(\hat{\Omega}_1)\rangle\langle Y_2^{*m}(\hat{\Omega}_2)\rangle$$

We have let $\hat{\Omega}(0) = \hat{\Omega}_1$, $\hat{\Omega}(t) = \hat{\Omega}_2$ because these orientations are uncorrelated as $t\to\infty$. Next, we can write out the ensemble averages in a director-fixed coordinate system, with the director taken to be the z-axis:

$$\langle Y_2^m(\hat{\Omega}_1)\rangle = \frac{\int_0^{2\pi}\int_0^{\pi} d\phi_1 d\theta_1 (-1)^m\sqrt{\frac{5}{4\pi}\frac{(2-m)!}{(2+m)!}}\sin\theta_1 P_2^m(\cos\theta_1)e^{im\phi_1}f(\theta_1,\phi_1)}{\int_0^{2\pi}\int_0^{\pi} d\phi_1 d\theta_1 \sin\theta_1 f(\theta_1,\phi_1)}$$

$$\langle Y_2^{*m}(\hat{\Omega}_2)\rangle = \frac{\int_0^{2\pi}\int_0^{\pi} d\phi_2 d\theta_2 (-1)^m\sqrt{\frac{5}{4\pi}\frac{(2-m)!}{(2+m)!}}\sin\theta_2 P_2^m(\cos\theta_2)e^{-im\phi_2}f(\theta_2,\phi_2)}{\int_0^{2\pi}\int_0^{\pi} d\phi_2 d\theta_2 \sin\theta_2 f(\theta_2,\phi_2)}$$

Where $\theta_i = \arccos(\hat{n} \cdot \hat{\Omega}_i)$. Now, we make the assumption that $f(\theta_i, \phi_i) = f(\theta_i)$. That is, we assume that the distribution of orientation vectors along the azimuth is uniform. Then we have:

$$\langle Y_2^m(\hat{\Omega}_1)\rangle = \frac{\int_0^{2\pi}\int_0^{\pi} d\phi_1 d\theta_1 (-1)^m \sqrt{\frac{5}{4\pi}\frac{(2-m)!}{(2+m)!}} \sin\theta_1 P_2^m(\cos\theta_1) e^{im\phi_1} f(\theta_1)}{\int_0^{2\pi}\int_0^{\pi} d\phi_1 d\theta_1 \sin\theta_1 f(\theta_1)}$$

$$\langle Y_2^{*m}(\hat{\Omega}_2)\rangle = \frac{\int_0^{2\pi}\int_0^{\pi} d\phi_2 d\theta_2 (-1)^m \sqrt{\frac{5}{4\pi}\frac{(2-m)!}{(2+m)!}} \sin\theta_2 P_2^m(\cos\theta_2) e^{-im\phi_2} f(\theta_2)}{\int_0^{2\pi}\int_0^{\pi} d\phi_2 d\theta_2 \sin\theta_2 f(\theta_2)}$$

Let's evaluate the ϕ integrals. We have:

$$\frac{\int_0^{2\pi} d\phi_i e^{\pm im\phi_i}}{\int_0^{2\pi} d\phi_i}$$

If $m = 0$, $e^{\pm im\phi_i} = 1$, so:

$$\frac{\int_0^{2\pi} d\phi_i (1)}{\int_0^{2\pi} d\phi_i} = 1$$

But if $m \neq 0$,

$$\begin{aligned}
\frac{\int_0^{2\pi} d\phi_i e^{\pm im\phi_i}}{\int_0^{2\pi} d\phi_i} &= \frac{1}{2\pi}\frac{1}{(\pm im)}(e^{\pm im\phi_i})\Big|_0^{2\pi} \\
&= \frac{1}{2\pi}\frac{1}{(\pm im)}(1-1) \\
&= 0
\end{aligned}$$

Thus, in the sum $\sum_{m=-2}^{2}\langle Y_2^m(\hat{\Omega}_1)\rangle\langle Y_2^{*m}(\hat{\Omega}_2)\rangle$, every term with $m \neq 0$ vanishes. So we have:

$$\begin{aligned}
\lim_{t\to\infty}\langle P_2(\hat{\Omega}(0)\cdot\hat{\Omega}(t))\rangle = \frac{4\pi}{5} &\left(\frac{\int_0^{\pi} d\theta_1 \sqrt{\frac{5}{4\pi}} \sin\theta_1 P_2^0(\cos\theta_1) f(\theta_1)}{\int_0^{\pi} d\theta_1 \sin\theta_1 f(\theta_1)}\right) \\
&\times \left(\frac{\int_0^{\pi} d\theta_2 \sqrt{\frac{5}{4\pi}} \sin\theta_2 P_2^0(\cos\theta_2) f(\theta_2)}{\int_0^{\pi} d\theta_2 \sin\theta_2 f(\theta_2)}\right)
\end{aligned}$$

Note that since $P_l^m(x) = (-1)^m(1-x^2)^{m/2}\frac{d^m}{dx^m}(P_l(x))$, we have $P_l^0(x) = P_l(x)$. Using this fact, and moving the square root constants out of the integrals to cancel the prefactor,

$$\begin{aligned}
\lim_{t\to\infty}\langle P_2(\hat{\Omega}(0)\cdot\hat{\Omega}(t))\rangle = &\left(\frac{\int_0^{\pi} d\theta_1 \sin\theta_1 P_2(\cos\theta_1) f(\theta_1)}{\int_0^{\pi} d\theta_1 \sin\theta_1 f(\theta_1)}\right) \\
&\times \left(\frac{\int_0^{\pi} d\theta_2 \sin\theta_2 P_2(\cos\theta_2) f(\theta_2)}{\int_0^{\pi} d\theta_2 \sin\theta_2 f(\theta_2)}\right)
\end{aligned}$$

The terms being multiplied are just ensemble averages of $P(\cos\theta_i)$:

$$\lim_{t\to\infty}\langle P_2(\hat{\Omega}(0)\cdot\hat{\Omega}(t))\rangle = \langle P_2(\cos\theta_1)\rangle\langle P_2(\cos\theta_2)\rangle$$

But θ_i is just the angle between the director and the orientation vector of some molecule, and the ensemble average $\langle P_2(\cos\theta_i)\rangle$ should be the same regardless of the choice of $\hat{\Omega}_i$. So we can write, for some orientation vector $\hat{\Omega}$ and angle $\theta = \hat{n}\cdot\hat{\Omega}$,

$$\lim_{t\to\infty}\langle P_2(\hat{\Omega}(0)\cdot\hat{\Omega}(t))\rangle = \langle P_2(\cos\theta)\rangle^2 = S^2$$

B Efficacy of Monte Carlo Optimization

One measure of the efficacy of the Monte Carlo optimization is the ratio of the unoptimized to optimized total path lengths. A plot of this ratio for different values of endpoint separation is shown in Fig. 33. The closer the value of this ratio to 1, of course, the less the paths lengths were shortened by optimization. As the plot shows, optimization changed this ratio very little.

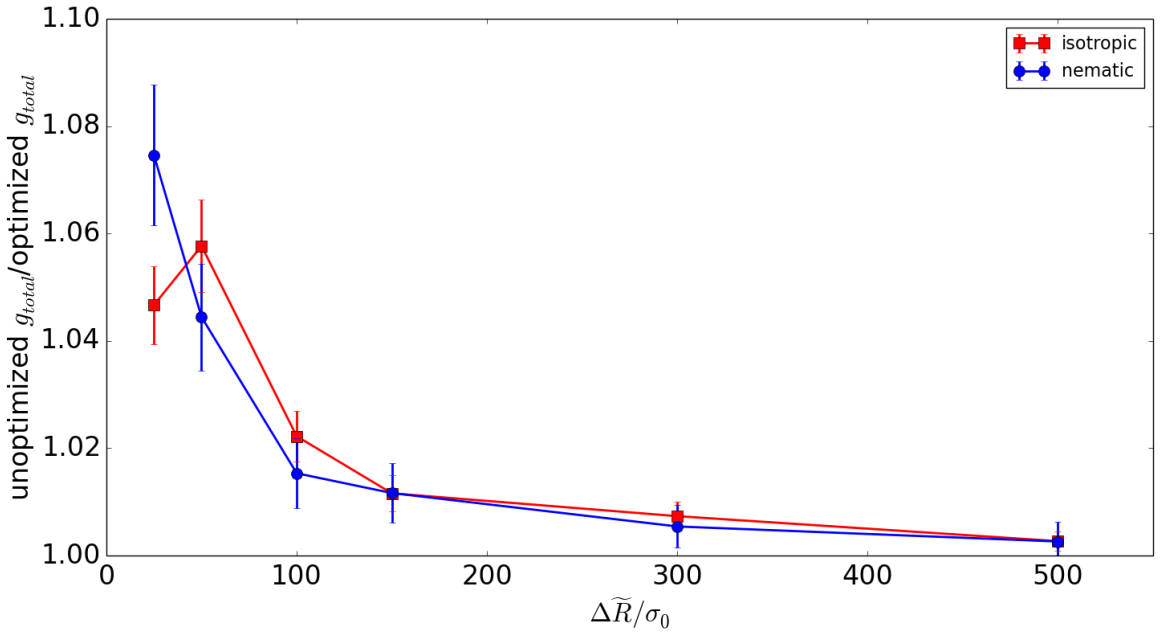

Figure 33: Ratio of unoptimized to optimized total geodesic path length.

We also considered the number of MC trials that failed to successfully locate a path, and the number of successfully-found paths that resulted in an acceptance move (i.e., were shorter than the current shortest path.) The results for different values of endpoint separation are shown in the table below. As can be seen, as the endpoint separation increases, more trials fail to locate paths, and fewer paths result in acceptance moves. The geodesics at large $\Delta\widetilde{R}$ are thus not very well-optimized.

endpoint separation (σ_0)	failed trials, isotropic	acceptance moves, isotropic
25	0.000	4.641
50	0.224	2.661
100	1.516	1.210
150	2.526	0.842
300	3.510	0.608
500	3.917	0.367

endpoint separation (σ_0)	failed trials, nematic	acceptance moves, nematic
25	0.000	4.785
50	0.569	1.828
100	2.655	0.793
150	4.758	0.452
300	6.615	0.393
500	6.432	0.309

Table 1: Average number of failed trials and acceptance moves versus endpoint separation, out of 10 trials per geodesic. The averages are taken over the numbers endpoint pairs indicated in Chapter 5.2 of this thesis.

C Derivation of Rotational Diffusion Green's Function

We wish to come up with a "classical" expression for the rotational diffusion Green's function - that is, one which can be written in terms of integrals rather than sums. The rotational diffusion equation is given by [21]:

$$\frac{\partial G}{\partial t} = D_R \nabla^2 G$$

where $G = G(\hat{\Omega}_i \to \hat{\Omega}_f, t)$, D_R is the rotational diffusion constant, and ∇^2 is the angular part of the Laplacian in spherical coordinates:

$$\nabla^2 = \frac{1}{\sin\theta}\frac{\partial}{\partial\theta}\left(\sin\theta\frac{\partial}{\partial\theta}\right) + \frac{1}{\sin^2\theta}\frac{\partial^2}{\partial\phi^2}$$

The solution to this equation is given by [21]:

$$G(\hat{\Omega}_i \to \hat{\Omega}_f, t) = \sum_{l=0}^{\infty} \frac{2l+1}{4\pi} P_l(\hat{\Omega}_i \cdot \hat{\Omega}_f) e^{-l(l+1)D_R t}$$

Where P_l is the l-th order Legendre polynomial, and $\hat{\Omega}_i \cdot \hat{\Omega}_f = \cos\theta$. For a short time step (δt), this is:

$$G(\hat{\Omega}_t \to \hat{\Omega}_{t+\delta t}, \delta t) = \sum_{l=0}^{\infty} \frac{2l+1}{4\pi} P_l(\hat{\Omega}_t \cdot \hat{\Omega}_{t+\delta t}) e^{-l(l+1)D_R \delta t}$$

To start, let us examine P_l for short times. We know that for short times, $x \equiv \hat{\Omega}_t \cdot \hat{\Omega}_{t+\delta t} \approx 1$. Taylor expanding $P_l(x)$ about $x = 1$,

$$\begin{aligned} P_l(x) &= 1 + \frac{l(l+1)}{2}(x-1) + \mathcal{O}(x-1)^2 \\ &= 1 - \frac{l(l+1)}{2}(1-x) + \mathcal{O}(1-x)^2 \end{aligned}$$

since ([22]) $P_l'(x=1) = l(l+1)/2$. We also know that $1 - \hat{\Omega}_t \cdot \hat{\Omega}_{t+\delta t} = (\hat{\Omega}_{t+\delta t} - \hat{\Omega}_t)^2/2$. Substituting this fact into the above expression for P_l, and substituting *that* into the expression for the Green's function, we obtain:

$$G(\hat{\Omega}_t \to \hat{\Omega}_{t+\delta t}, \delta t) = \frac{1}{4\pi} \sum_{l=0}^{\infty} (2l+1) \left[1 - \frac{l(l+1)}{4} (\hat{\Omega}_{t+\delta t} - \hat{\Omega}_t)^2 + \dots \right] e^{-l(l+1) D_R \delta t}$$

Now we make the classical approximation that $D_R \delta t$ is small. This allows us to write the sum over the angular momentum "quantum number" as an integral:

$$G(\hat{\Omega}_t \to \hat{\Omega}_{t+\delta t}, \delta t) \approx \frac{1}{4\pi} \int_0^{\infty} dx \left[1 - \frac{x}{4} (\hat{\Omega}_{t+\delta t} - \hat{\Omega}_t)^2 + \dots \right] e^{-x D_R \delta t}$$

where:

$$\begin{aligned} x &= l(l+1) \\ \sum_{l=0}^{\infty} (2l+1) f[l(l+1)] &\to \int_0^{\infty} dx f(x) \end{aligned}$$

Note the similarity of this approximation to that of the classical limit of the quantum mechanical partition function of the rigid rotor [23]. Now the integral in the Green's function is easily evaluated. Using the facts that:

$$\begin{aligned} \int_0^{\infty} e^{-\alpha x} dx &= \frac{1}{\alpha} \\ \int_0^{\infty} x e^{-\alpha x} dx &= -\frac{d}{d\alpha} \left(\frac{1}{\alpha} \right) = \frac{1}{\alpha^2} \end{aligned}$$

(where $\alpha = D_R \delta t$), we have:

$$\begin{aligned} G(\hat{\Omega}_t \to \hat{\Omega}_{t+\delta t}, \delta t) &= \frac{1}{4\pi D_R \delta t} - \frac{1}{4\pi} \frac{(\hat{\Omega}_{t+\delta t} - \hat{\Omega}_t)^2}{4} \frac{1}{(D_R \delta t)^2} + \dots \\ &= \frac{1}{4\pi D_R \delta t} \left[1 - \frac{(\hat{\Omega}_{t+\delta t} - \hat{\Omega}_t)^2}{4 D_R \delta t} + \dots \right] \\ &= \frac{1}{4\pi D_R \delta t} \exp \left[- \frac{(\hat{\Omega}_{t+\delta t} - \hat{\Omega}_t)^2}{4 D_R \delta t} + \dots \right] \end{aligned}$$

Neglecting higher-order terms, the exponent can be written as:

$$- \frac{1}{4 D_R} \frac{(\hat{\Omega}_{t+\delta t} - \hat{\Omega}_t)^2}{(\delta t)^2} \delta t$$

Our short-time Green's function is then:

$$G(\hat{\Omega}_t \to \hat{\Omega}_{t+\delta t}, \delta t) = \frac{1}{4\pi D_R \delta t} \exp\left[-\frac{1}{4D_R}\left(\frac{\hat{\Omega}_{t+\delta t} - \hat{\Omega}_t}{\delta t}\right)^2 \delta t\right]$$

Now, we really want to find an expression for the *finite*-time rotational diffusion Green's function. Say that we want to find the Green's function for diffusing from $\hat{\Omega}_i$ to $\hat{\Omega}_f$ in a time t. Let us divide the time interval into P parts, so that $t = P\delta t$. Then, following [24], the finite-time Green's function can be written in terms of the product of short-time Green's functions:

$$G(\hat{\Omega}_i \to \hat{\Omega}_f, t) = \int d\hat{\Omega}_1 \cdots \int d\hat{\Omega}_{P-1} \left(\frac{1}{4\pi D_R \delta t}\right)^{P+1} \exp\left[-\frac{1}{4D_R}\sum_{k=0}^{P-1}\left(\frac{\hat{\Omega}_{k+1} - \hat{\Omega}_k}{\delta t}\right)^2 \delta t\right]$$

Taking the limit as $P \to \infty$, $\delta t \to 0$, the integrals over the $\hat{\Omega}_k$ become a path integral, the sum in the exponential becomes a time integral, and the ratio $(\hat{\Omega}_{k+1} - \hat{\Omega}_k)/\delta t$ becomes a derivative $d\hat{\Omega}/d\tau$, yielding:

$$G(\hat{\Omega}_i \to \hat{\Omega}_f, t) = \int_{\hat{\Omega}_i, 0}^{\hat{\Omega}_f, t} \mathcal{D}[\hat{\Omega}(\tau)] \exp\left[-\frac{1}{4D_R}\int_0^t \left(\frac{d\hat{\Omega}}{d\tau}\right)^2 d\tau\right]$$

where the normalization has been absorbed into the path integral measure $\mathcal{D}$.

D Derivation of Rotational Diffusion Constant in terms of Geodesic Length

To derive an expression for the rotational diffusion constant in terms of the rotational geodesic length, we compare two equivalent expressions for the rotational diffusion Green's function. One expression involves the phenomenological rotational diffusion constant. From the previous section, we know that, if we make the "classical" approximation that D_R is small, we can write the rotational diffusion Green's function as:

$$\begin{aligned} G(\hat{\Omega}_i \to \hat{\Omega}_f, t) &= \frac{1}{4\pi D_R t} \exp\left[-\frac{1}{4D_R}\frac{(\hat{\Omega}_f - \hat{\Omega}_i)^2}{t}\right] \\ &= \frac{1}{4\pi D_R t} \exp\left[-\frac{2(1 - \cos\Delta\psi)}{4D_R t}\right] \\ &= \frac{1}{4\pi D_R t} \exp\left[-\frac{2(\frac{1}{2}(\Delta\psi)^2 + \cdots)}{4D_R t}\right] \\ &= \frac{1}{4\pi D_R t} \exp\left[-\frac{(\Delta\psi)^2 + \cdots}{4D_R t}\right] \end{aligned}$$

But we also know that in the slow diffusion limit, the path that dominates the path-integral expression for the Green's function is going to be the geodesic. Thus we want to find a way to write the integral in the Green's function exponential in terms of the geodesic length. We do this by considering a simple, prototypical case. Consider the

rotational diffusion of an linear molecule of length $2\sqrt{I/m}$ around a circular obstacle, as shown in Fig. 34. The geodesic path from point 1 to point 2 can be broken into two separate components: free motion and motion along the boundary of the obstacle.

Free Motion

Let us consider evaluating the action integral for the free segments of the path. We know that the molecule's orientation vector's path can be written as a SLERP (spherical linear interpolation) formula [1]:

$$\hat{\Omega}(\tau) = \hat{\Omega}(0)\frac{\sin\Delta\psi(1-\tau/t)}{\sin\Delta\psi} + \hat{\Omega}(t)\frac{\sin\Delta\psi(\tau/t)}{\sin\Delta\psi}$$
$$0 \le \tau \le t$$

where $\hat{\Omega}(0)\cdot\hat{\Omega}(t) = \cos\Delta\psi$. The time derivative of $\hat{\Omega}$ is:

$$\frac{d\hat{\Omega}(\tau)}{d\tau} = \frac{\Delta\psi}{t}\left[-\hat{\Omega}(0)\frac{\cos\Delta\psi(1-\tau/t)}{\sin\Delta\psi} + \hat{\Omega}(t)\frac{\cos\Delta\psi(\tau/t)}{\sin\Delta\psi}\right]$$

Now we can evaluate the square of the derivative. To clean things up a bit, let:

$$\sin\Delta\psi = s \quad \cos\Delta\psi = c$$
$$\sin\Delta\psi(\tau/t) = S \quad \cos\Delta\psi(\tau/t) = C$$

Using this notation and the fact that $\cos(\alpha-\beta) = \cos\alpha\cos\beta + \sin\alpha\sin\beta$, we can write the derivative as:

$$\frac{d\hat{\Omega}(\tau)}{d\tau} = \frac{\Delta\psi}{ts}\left[-\hat{\Omega}(0)(cC+sS) + C\hat{\Omega}(\tau)\right]$$

Taking the square,

$$\begin{aligned}
\left(\frac{d\hat{\Omega}(\tau)}{d\tau}\right)^2 &= \frac{(\Delta\psi)^2}{t^2s^2}\left[(cC+sS)^2 + C^2 - 2cC(cC+sS)\right] \\
&= \frac{(\Delta\psi)^2}{t^2s^2}\left[c^2C^2 + s^2S^2 + 2cCsS + C^2 - 2c^2C^2 - 2cCsS\right] \\
&= \frac{(\Delta\psi)^2}{t^2s^2}\left[s^2S^2 - c^2C^2 + C^2\right] \\
&= \frac{(\Delta\psi)^2}{t^2s^2}\left[sS^2 + C^2(1-c^2)\right] \\
&= \frac{(\Delta\psi)^2}{t^2s^2}\left[s^2(S^2+C^2)\right] \\
&= \frac{(\Delta\psi)^2}{t^2s^2}(s^2) \\
&= \left(\frac{\Delta\psi}{t}\right)^2
\end{aligned}$$

Now we can perform the action integral:

$$\frac{1}{4D_R}\int_0^t \left(\frac{d\hat{\Omega}}{d\tau}\right)^2 d\tau = \frac{1}{4D_R}\int_0^t (\Delta\psi/t)^2 d\tau = \frac{(\Delta\psi)^2}{4D_R t}$$

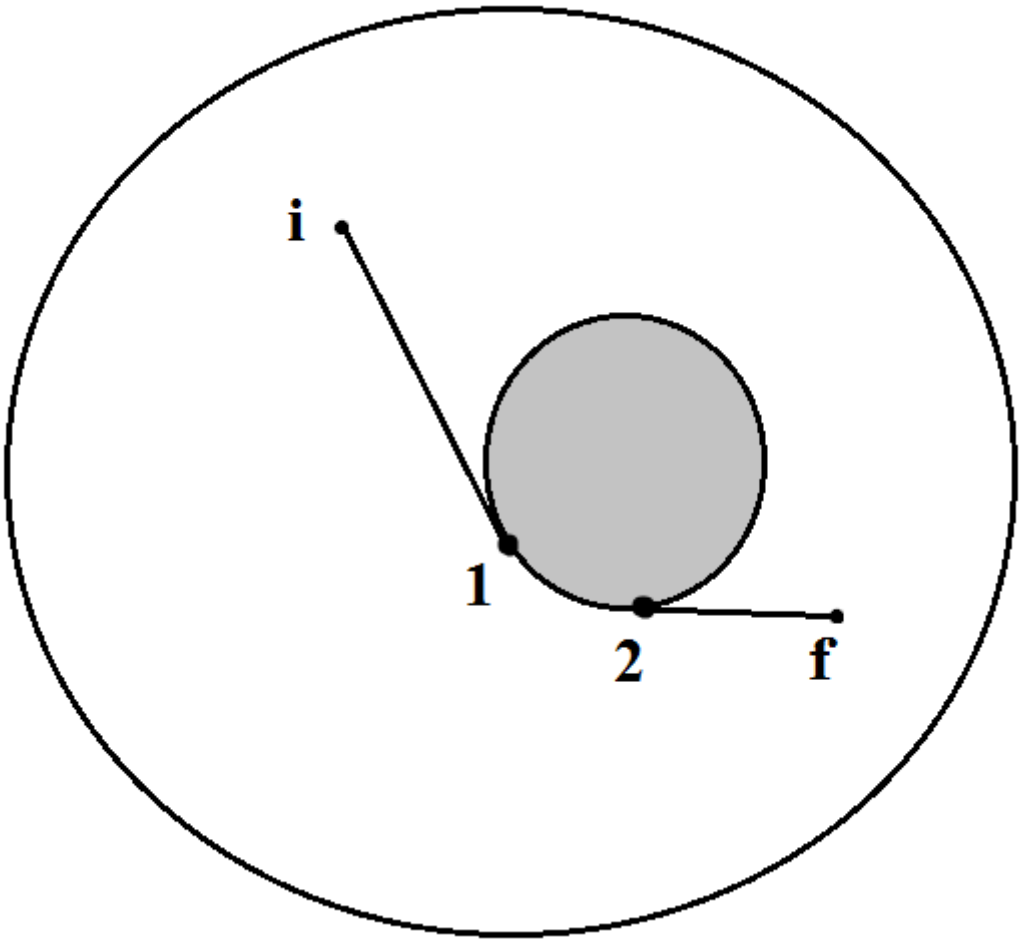

Figure 34: The motion of the linear molecule consists of free motion ($i \to 1$ and $2 \to f$) and motion along the boundary ($1 \to 2$).

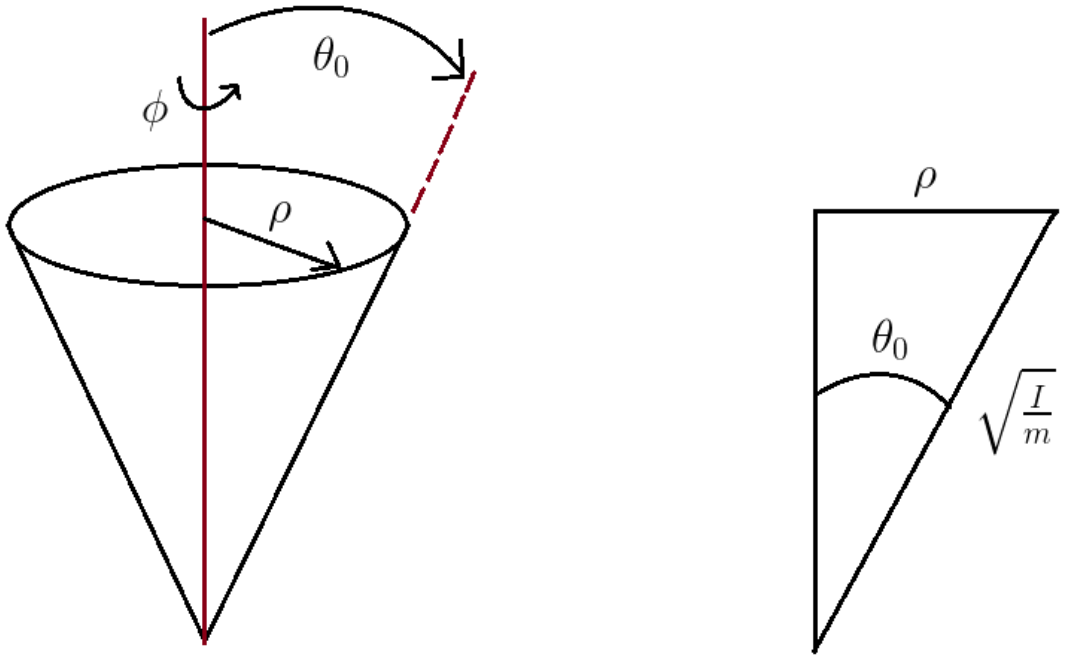

Figure 35: Motion of the linear molecule along the boundary. From the diagram, $\rho = \sqrt{I/m}\sin\theta_0$.

Now, note that the free segment geodesic is just the arc length traversed by the molecule, $g = \Delta\psi\sqrt{I/m}$. Solving for $\Delta\psi$ and plugging into the above expression, we obtain:

$$\frac{1}{4D_R}\int_0^t \left(\frac{d\hat{\Omega}}{d\tau}\right)^2 d\tau = \frac{g^2}{4(I/m)D_R t}$$

Motion Along Boundary

We assume that the molecule travels by an azimuthal angle $\Delta\phi$ along the boundary, at a constant polar angle (relative to a vector "normal" to the circular boundary) of θ_0, as shown in Fig. 35. Then we have:

$$\hat{\Omega}(\tau) = \begin{pmatrix} \sin\theta_0\cos\phi(\tau) \\ \sin\theta_0\sin\phi(\tau) \\ \cos\theta_0 \end{pmatrix}$$
$$\phi(\tau) = \phi_1 + (\tau/t)\Delta\phi$$

Thus,

$$\frac{d\hat{\Omega}}{d\tau} = \begin{pmatrix} -\sin\phi(t) \\ \cos\phi(t) \\ 0 \end{pmatrix} \sin\theta_0 \frac{d\phi}{d\tau}$$
$$\frac{d\phi}{d\tau} = \frac{\Delta\phi}{t}$$

And so,

$$\left(\frac{d\hat{\Omega}}{d\tau}\right)^2 = (\sin^2\phi + \cos^2\phi)\sin^2\theta_0(\Delta\phi/t)^2$$
$$= \sin^2\theta_0(\Delta\phi/t)^2$$

Now, the geodesic length is just the arc length traced out on the circular boundary, $g = \rho\Delta\psi = \sqrt{I/m}\sin\theta_0\Delta\psi$. Thus,

$$\sin^2\theta_0 = \frac{g^2}{(I/m)(\Delta\phi)^2}$$

Finally, then, the action integral is:

$$\frac{1}{4D_R}\int_0^t \left(\frac{d\hat{\Omega}}{d\tau}\right)^2 d\tau = \frac{g^2}{4(I/m)D_R t}$$

So the value of the action integral along the boundary is the same as that along the free segments.

Now, for this geodesic, the rotational diffusion constant is not the "true," phenomenological diffusion constant, but rather a "bare" diffusion constant - what the phenomenological diffusion constant would be in the low-density (essentially free motion) limit. Let

us denote this "reference" diffusion constant $D_R^{(0)}$. Equating the exponentials for the two different Green's function expressions, we have:

$$\frac{g^2}{4(I/m)D_R^{(0)}t} = \frac{(\Delta\psi)^2}{4D_R t}$$

From which we finally obtain an expression for the rotational diffusion constant, relative to a reference constant, in terms of the rotational geodesic length:

$$\boxed{\frac{D_R}{D_R^{(0)}} = \frac{\frac{I}{m}(\Delta\psi)^2}{g^2}}$$

E Derivation of of Equilibrium Predictions of Geodesic Length Ratios

E.1 l_T/l_R

We know that $l \sim \sqrt{K}$, where K is the kinetic energy. By the equipartition theorem [23], for a linear molecule, the translational kinetic energy is $\frac{3}{2}k_BT$ and the rotational kinetic energy is k_BT. Thus,

$$\begin{aligned}\frac{l_T}{l_R} &= \sqrt{\frac{\frac{3}{2}k_BT}{k_BT}} \\ &= \sqrt{\frac{3}{2}}\end{aligned}$$

E.2 $l_{z_b}/l_{x_b,y_b}$

Since z_b is one degree of freedom, it is associated with a kinetic energy of $\frac{1}{2}k_BT$, and x_b, y_b together possess a kinetic energy of k_BT. Thus the contour length ratio is:

$$\begin{aligned}\frac{l_{z_b}}{l_{x_b,y_b}} &= \sqrt{\frac{\frac{1}{2}k_BT}{k_BT}} \\ &= \frac{1}{\sqrt{2}}\end{aligned}$$

E.3 $l_{R||\hat{n}}/l_{R\perp\hat{n}}$

This derivation is less straightforward than for the previous ratios. To start, we need to compute the rotational partition function. The rotational Hamiltonian for a linear molecule is:

$$H = \frac{1}{2I}\left(p_\theta^2 + \frac{p_\phi^2}{\sin^2\theta}\right)$$

We *define* the partition function to be:

$$\begin{aligned} Q &= \int_{-\infty}^{\infty}\int_{-\infty}^{\infty}\int_{0}^{\pi}\int_{0}^{2\pi} dp_\theta\, dp_\phi\, d\theta\, d\phi\, e^{-\beta H} \\ &= \int_{-\infty}^{\infty}\int_{-\infty}^{\infty}\int_{0}^{\pi}\int_{0}^{2\pi} dp_\theta\, dp_\phi\, d\theta\, d\phi\, e^{-\frac{\beta}{2I}\left(p_\theta^2+\frac{p_\phi^2}{\sin^2\theta}\right)} \end{aligned}$$

The ϕ integration is trivial, just yielding a factor of 2π. Next we perform the p_θ and p_ϕ integrals, which are just Gaussian integrals:

$$\begin{aligned} Q &= 2\pi\int_{-\infty}^{\infty}\int_{-\infty}^{\infty}\int_{0}^{\pi} dp_\theta\, dp_\phi\, d\theta e^{-\frac{\beta}{2I}\left(p_\theta^2+\frac{p_\phi^2}{\sin^2\theta}\right)} \\ &= 2\pi\sqrt{\frac{\pi}{\beta/(2I)}}\int_{0}^{\pi}\sqrt{\frac{\pi}{\beta/(2I\sin^2\theta)}} \\ &= 2\pi\left(\frac{2\pi I}{\beta}\right)\int_{0}^{\pi}\sin\theta d\theta \end{aligned}$$

And finally the theta integral:

$$\begin{aligned} Q &= \frac{4\pi^2 I}{\beta}\left(-\cos\theta\right)\Big|_0^\pi \\ &= \frac{8\pi^2 I}{\beta} \end{aligned}$$

Ultimately, we wish to compute the average rotational kinetic energy parallel and perpendicular to the director. Let's start by computing the total average rotational kinetic energy, K. This can be obtained as a logarithmic derivative of the partition function:

$$\begin{aligned} \langle K\rangle &= -\frac{\partial}{\partial\beta}\ln Q \\ &= -\frac{\partial}{\partial\beta}\ln\frac{8\pi^2 I}{\beta} \\ &= -\frac{\partial}{\partial\beta}\left(\ln 8\pi^2 I - \ln\beta\right) \\ &= \frac{1}{\beta} \end{aligned}$$

This is just what we expect from the equipartition theorem; a linear molecule has two rotational degrees of freedom, and so it ought it to have a rotational kinetic energy of $2(\frac{1}{2}k_BT) = k_BT = \beta^{-1}$.

To decompose the rotational kinetic energy into components parallel and perpendicular to the director (or some arbitrary axis, generally), note that we can rewrite the

rotational kinetic energy as:

$$\begin{aligned}
\langle K \rangle &= \left\langle \frac{1}{2} I \frac{d\hat{\Omega}}{dt} \cdot \frac{d\hat{\Omega}}{dt} \right\rangle \\
&= \frac{1}{2} I \left\langle \frac{d\hat{\Omega}}{dt} \cdot \mathbb{1} \cdot \frac{d\hat{\Omega}}{dt} \right\rangle \\
&= \frac{1}{2} I \left\langle \frac{d\hat{\Omega}}{dt} \cdot [(\mathbb{1} - \hat{n}\hat{n}) + (\hat{n}\hat{n})] \cdot \frac{d\hat{\Omega}}{dt} \right\rangle \\
&= \frac{1}{2} I \left\langle \frac{d\hat{\Omega}}{dt} \cdot (\mathbb{1} - \hat{n}\hat{n}) \cdot \frac{d\hat{\Omega}}{dt} \right\rangle + \frac{1}{2} I \left\langle \frac{d\hat{\Omega}}{dt} \cdot \hat{n}\hat{n} \cdot \frac{d\hat{\Omega}}{dt} \right\rangle \\
&= \langle K_{\perp \hat{n}} \rangle + \langle K_{||\hat{n}} \rangle
\end{aligned}$$

In general, we can write an arbitrary unit vector on a sphere, $\hat{n}$, as:

$$\hat{n} = \begin{pmatrix} \sin\theta\cos\phi \\ \sin\theta\sin\phi \\ \cos\theta \end{pmatrix}$$

The $\hat{n}\hat{n}$ dyad is then:

$$\hat{n}\hat{n} = \begin{pmatrix} \sin^2\theta\cos^2\phi & \sin^2\theta\cos\phi\sin\phi & \sin\theta\cos\theta\cos\phi \\ \sin^2\theta\cos\phi\sin\phi & \sin^2\theta\sin^2\phi & \sin\theta\cos\theta\sin\phi \\ \sin\theta\cos\theta\cos\phi & \sin\theta\cos\theta\sin\phi & \cos^2\theta \end{pmatrix}$$

In the isotropic phase, since the choice of axis is immaterial, the dyad can be replaced by its average:

$$\langle \hat{n}\hat{n} \rangle_{iso} = \begin{pmatrix} \langle \sin^2\theta\cos^2\phi \rangle & \langle \sin^2\theta\cos\phi\sin\phi \rangle & \langle \sin\theta\cos\theta\cos\phi \rangle \\ \langle \sin^2\theta\cos\phi\sin\phi \rangle & \langle \sin^2\theta\sin^2\phi \rangle & \langle \sin\theta\cos\theta\sin\phi \rangle \\ \langle \sin\theta\cos\theta\cos\phi \rangle & \langle \sin\theta\cos\theta\sin\phi \rangle & \langle \cos^2\theta \rangle \end{pmatrix}$$

The off-diagonal elements are all zero, since:

$$\begin{aligned}
\int_0^{2\pi} \sin\phi d\phi &= -\cos\phi|_0^{2\pi} = 0 \\
\int_0^{2\pi} \cos\phi d\phi &= \sin\phi|_0^{2\pi} = 0
\end{aligned}$$

Now for the diagonal elements:

$$\begin{aligned}
\langle \sin^2\theta\cos^2\phi \rangle &= \frac{1}{4\pi} \int_0^{\pi} d\theta \int_0^{2\pi} d\phi \sin^3\theta\cos^2\phi \\
&= \frac{1}{4\pi} \int_0^{\pi} \sin^3\theta\, d\theta \int_0^{2\pi} \cos^2\phi\, d\phi
\end{aligned}$$

First the theta integral:

$$\begin{aligned}\int_0^\pi \sin^3\theta d\theta &= \int_0^\pi \sin\theta(1-\cos^2\theta)d\theta \\ &= \int_{-1}^1 1-u^2 du \\ &= (u-\frac{1}{3}u^3)|_{-1}^1 \\ &= \frac{2}{3}-(-1+\frac{1}{3}) \\ &= \frac{4}{3}\end{aligned}$$

Now the phi integral:

$$\begin{aligned}\int_0^{2\pi}\cos^2\phi\, d\phi &= \frac{1}{2}\int_0^{2\pi} 1+\cos 2\phi\, d\phi \\ &= \frac{1}{2}(\phi+\frac{1}{2}\sin 2\phi)|_0^{2\pi} \\ &= \pi\end{aligned}$$

Thus our average is:

$$\langle \sin^2\theta\cos^2\phi\rangle = \frac{4\pi/3}{4\pi} = \frac{1}{3}$$

Similarly, the second diagonal element is:

$$\begin{aligned}\langle \sin^2\theta\sin^2\phi\rangle &= \frac{1}{4\pi}\int_0^\pi \sin^3\theta\, d\theta \int_0^{2\pi}\sin^2\phi\, d\phi \\ &= \frac{1}{4\pi}\left(\frac{4}{3}\right)(\pi) \\ &= \frac{1}{3}\end{aligned}$$

And the last diagonal element:

$$\begin{aligned}\langle \cos^2\theta\rangle &= \frac{1}{2}\int_0^\pi \cos^3\theta d\theta \\ &= \frac{1}{3}\end{aligned}$$

So each diagonal element is 1/3:

$$\langle \hat{n}\hat{n}\rangle_{iso} = \frac{1}{3}\mathbb{1}$$

With this in hand, it is easy to compute the kinetic energy components:

$$\begin{aligned}
\langle K_{||\hat{n}} \rangle &= \frac{1}{2} I \left\langle \frac{d\hat{\Omega}}{dt} \cdot \langle \hat{n}\hat{n} \rangle_{iso} \cdot \frac{d\hat{\Omega}}{dt} \right\rangle \\
&= \frac{1}{2} I \left\langle \frac{d\hat{\Omega}}{dt} \cdot \left(\frac{1}{3} \mathbb{1} \right) \cdot \frac{d\hat{\Omega}}{dt} \right\rangle \\
&= \frac{1}{3} \left(\frac{1}{2} I \left\langle \frac{d\hat{\Omega}}{dt} \cdot \mathbb{1} \cdot \frac{d\hat{\Omega}}{dt} \right\rangle \right) \\
&= \frac{1}{3} \left(\frac{1}{2} I \left\langle \frac{d\hat{\Omega}}{dt} \cdot \frac{d\hat{\Omega}}{dt} \right\rangle \right) \\
&= \frac{1}{3} \langle K \rangle \\
&= \frac{1}{3} k_B T
\end{aligned}$$

And similarly,

$$\begin{aligned}
\langle K_{\perp\hat{n}} \rangle &= \frac{1}{2} I \left\langle \frac{d\hat{\Omega}}{dt} \cdot (\mathbb{1} - \langle \hat{n}\hat{n} \rangle_{iso}) \cdot \frac{d\hat{\Omega}}{dt} \right\rangle \\
&= \frac{1}{2} I \left\langle \frac{d\hat{\Omega}}{dt} \cdot \left(\frac{2}{3} \mathbb{1} \right) \cdot \frac{d\hat{\Omega}}{dt} \right\rangle \\
&= \frac{2}{3} \langle K \rangle \\
&= \frac{2}{3} k_B T
\end{aligned}$$

This result makes sense. It takes three basis vectors to describe 3d space; if the system is isotropic, then if we pick a single arbitrary axis in 3d space, a third of the average kinetic energy will be in that direction.

Since the contour length goes as $\sqrt{K}$, the ratio $l_{R||\hat{n}}/l_{R\perp\hat{n}}$ in the isotropic phase is given by:

$$\boxed{\frac{l_{R||\hat{n}}}{l_{R\perp\hat{n}}} = \sqrt{\frac{K_{||\hat{n}}}{K_{\perp\hat{n}}}} = \sqrt{\frac{k_B T/3}{2k_B T/3}} = \frac{1}{\sqrt{2}}}$$

Now for the nematic phase. First, we shall express $K_{||\hat{n}}$ and $K_{\perp\hat{n}}$ in terms of momenta and coordinates. Pick a coordinate system in which $\hat{n} = \hat{z}$. We can write:

$$\hat{\Omega} = \begin{pmatrix} \sin\theta\cos\phi \\ \sin\theta\sin\phi \\ \cos\theta \end{pmatrix}$$
$$\frac{d\hat{\Omega}}{dt} = \begin{pmatrix} \dot{\theta}\cos\theta\cos\phi - \dot{\phi}\sin\theta\sin\phi \\ \dot{\theta}\cos\theta\sin\phi + \dot{\phi}\sin\theta\cos\phi \\ -\dot{\theta}\sin\theta \end{pmatrix}$$

We can express the parallel kinetic energy as:

$$\begin{aligned} K_{||\hat{n}} &= \frac{1}{2} I \frac{d\hat{\Omega}}{dt} \cdot \hat{z}\hat{z} \cdot \frac{d\hat{\Omega}}{dt} \\ &= \frac{1}{2} I \dot{\theta}^2 \sin^2\theta \\ &= \frac{p_\theta^2 \sin^2\theta}{2I} \end{aligned}$$

Since the total rotational kinetic energy is $K = \frac{1}{2} I(\dot{\theta}^2 + \dot{\phi}^2 \sin^2\theta) = K_{||\hat{n}} + K_{\perp\hat{n}}$,

$$\begin{aligned} K_{\perp\hat{n}} &= \frac{1}{2} I(\dot{\theta}^2 + \dot{\phi}^2 \sin^2\theta) - \frac{1}{2} I \dot{\theta}^2 \sin^2\theta \\ &= \frac{1}{2} I(\dot{\theta}^2 \cos^2\theta + \dot{\phi}^2 \sin^2\theta) \\ &= \frac{1}{2I}\left(p_\theta^2 \cos^2\theta + \frac{p_\phi^2}{\sin^2\theta}\right) \end{aligned}$$

To obtain an average of the kinetic energy, we need a Hamiltonian; for the nematic phase, we will need to include an effective potential in the Hamiltonian. We assume a mean-field potential of the form:

$$U = -\alpha(\hat{n} \cdot \hat{\Omega})^2 = -\alpha\cos^2\theta$$

where α is a parameter that depends on the order parameter. (Up to normalization, this is the Maier-Saupe potential [25].) We can now write down the partition function for the nematic phase:

$$\begin{aligned} Q &= \int_{-\infty}^{\infty}\int_{-\infty}^{\infty}\int_0^{\pi}\int_0^{2\pi} dp_\theta dp_\phi d\theta d\phi \, e^{-\beta H} \\ H &= K + U = \frac{1}{2I}\left(p_\theta^2 + \frac{p_\phi^2}{\sin^2\theta}\right) - \alpha\cos^2\theta \end{aligned}$$

Performing the (trivial) phi integral and the Gaussian momentum integrals,

$$\begin{aligned} Q &= \frac{4\pi^2 I}{\beta}\int_0^{\pi} d\theta \sin\theta \, e^{\beta\alpha\cos^2\theta} \\ &= \frac{4\pi^2 I}{\beta}\int_{-1}^{1} du \, e^{\beta\alpha u^2} \end{aligned}$$

The integral in the above expression is known as *Dawson's integral* [26]. Now we can calculate the average kinetic energies:

$$\begin{aligned}
\langle K_{||\hat{n}} \rangle &= \frac{2\pi}{Q} \int_{-\infty}^{\infty} \int_{-\infty}^{\infty} \int_{0}^{\pi} dp_\theta dp_\phi d\theta \left(\frac{p_\theta^2 \sin^2 \theta}{2I} \right) e^{-\beta H} \\
&= \frac{2\pi^2 I}{\beta^2} \frac{1}{Q} \int_0^\pi d\theta \, \sin^3 \theta \, e^{\beta \alpha \cos^2 \theta} \\
&= \frac{2\pi^2 I}{\beta^2} \frac{1}{Q} \int_0^\pi d\theta \, \sin\theta (1 - \cos^2 \theta) \, e^{\beta \alpha \cos^2 \theta} \\
&= \frac{1}{2\beta} \frac{\int_{-1}^{1} du \, (1-u^2) e^{\beta \alpha u^2}}{\int_{-1}^{1} du \, e^{\beta \alpha u^2}} \\
&= \frac{1}{2\beta} \left(1 - \frac{\int_{-1}^{1} du \, u^2 e^{\beta \alpha u^2}}{\int_{-1}^{1} du \, e^{\beta \alpha u^2}} \right)
\end{aligned}$$

But the second term is just an average of $u^2 = \cos^2 \theta = (\hat{n} \cdot \hat{\Omega})^2$ with respect to the distribution:

$$P(\hat{\Omega}) = \frac{e^{\beta \alpha (\hat{n} \cdot \hat{\Omega})^2}}{\int d\hat{\Omega} \, e^{\beta \alpha (\hat{n} \cdot \hat{\Omega})^2}}$$

And an average with respect to this distribution is equivalent to an average with respect to the phase space distribution, at least for an observable that depends only on theta. To see this, take the phase space average of an observable $A(\theta)$:

$$\langle A \rangle = \frac{\int_{-\infty}^{\infty} \int_{-\infty}^{\infty} \int_0^\pi \int_0^{2\pi} dp_\theta \, dp_\phi \, d\theta \, d\phi \, A(\theta) \, e^{-\beta \left(\frac{p_\theta^2}{2I} + \frac{p_\phi^2}{2I \sin^2 \theta} - \alpha \cos^2 \theta \right)}}{\int_{-\infty}^{\infty} \int_{-\infty}^{\infty} \int_0^\pi \int_0^{2\pi} dp_\theta \, dp_\phi \, d\theta \, d\phi \, e^{-\beta \left(\frac{p_\theta^2}{2I} + \frac{p_\phi^2}{2I \sin^2 \theta} - \alpha \cos^2 \theta \right)}}$$

$$= \frac{\frac{4\pi^2 I}{\beta} \int_0^{2\pi} d\phi \int_0^\pi d\theta \, \sin\theta \, A(\theta) \, e^{\beta \alpha \cos^2 \theta}}{\frac{4\pi^2 I}{\beta} \int_0^{2\pi} d\phi \int_0^\pi d\theta \, \sin\theta \, e^{\beta \alpha \cos^2 \theta}}$$

$$= \frac{\int_0^{2\pi} d\phi \int_0^\pi d\theta \, \sin\theta \, A(\theta) \, e^{\beta \alpha \cos^2 \theta}}{\int_0^{2\pi} d\phi \int_0^\pi d\theta \, \sin\theta \, e^{\beta \alpha \cos^2 \theta}}$$

$$= \frac{\int d\hat{\Omega} \, A(\theta) e^{\beta \alpha (\hat{n} \cdot \hat{\Omega})^2}}{\int d\hat{\Omega} \, e^{\beta \alpha (\hat{n} \cdot \hat{\Omega})^2}}$$

So we have:

$$\langle K_{||\hat{n}} \rangle = \frac{1}{2\beta} (1 - \langle (\hat{n} \cdot \hat{\Omega})^2 \rangle)$$

But recalling the definition of the order parameter,

$$S = \left\langle \frac{3(\hat{n} \cdot \hat{\Omega})^2 - 1}{2} \right\rangle$$

Rearranging,

$$\langle (\hat{n} \cdot \hat{\Omega})^2 \rangle = \frac{2S+1}{3}$$

Plugging this into the formula for the kinetic energy,

$$\begin{aligned}
\langle K_{||\hat{n}} \rangle &= \frac{1}{2\beta} \left(1 - \left(\frac{2S+1}{3} \right) \right) \\
&= \frac{1}{2\beta} \left(\frac{2(1-S)}{3} \right) \\
&= k_B T \left(\frac{1-S}{3} \right)
\end{aligned}$$

The kinetic energy perpendicular to the director is then given by:

$$\begin{aligned}
\langle K_{\perp\hat{n}} \rangle &= \langle K \rangle - \langle K_{||\hat{n}} \rangle \\
&= k_B T - k_B T \left(\frac{1-S}{3} \right) \\
&= k_B T \left(\frac{3-(1-S)}{3} \right) \\
&= k_B T \left(\frac{2+S}{3} \right)
\end{aligned}$$

Finally, we obtain the contour length ratio:

$$\boxed{\frac{l_{R||\hat{n}}}{l_{R\perp\hat{n}}} = \sqrt{\frac{\langle K_{||\hat{n}} \rangle}{\langle K_{\perp\hat{n}} \rangle}} = \sqrt{\frac{1-S}{2+S}}}$$

Notice that we never had to use the fact that the distribution has a Gaussian form - all of the results hold assuming only that the mean-field potential has a form $U(\hat{n} \cdot \hat{\Omega})$ such that $\langle (\hat{n} \cdot \hat{\Omega})^2 \rangle = (2S+1)/3$.

References

[1] Jacobson, D. and Stratt, R.M. "The inherent dynamics of a molecular liquid: Geodesic pathways through the potential energy landscape of a liquid of linear molecules." *J. Chem. Phys.* 140, 174503 (2014).

[2] Frechette, L., Jacobson, D., and Stratt, R.M. "Erratum: "The inherent dynamics of a molecular liquid: Geodesic pathways through the potential energy landscape of a liquid of linear molecules" [J. Chem. Phys. 140, 174503 (2014)]". *J. Chem. Phys.* 141, 209902 (2014).

[3] Chandrasekhar, S. *Liquid Crystals.* 2nd ed. New York: Cambridge University Press, 1992. Chap. 1.

[4] Gay, J.G. and Berne, B.J. "Modification of the overlap potential to mimic a linear site-site potential." *J. Chem. Phys.* 74.6 (1981): 3316-3319.

[5] De Miguel, Enrique, Rull, Luis F., Chalam, Manoj K., and Gubbins, Keith E. "Liquid crystal phase diagram of the Gay-Berne fluid." *Molecular Physics.* 74.2 (1991): 405-424.

[6] Wang, C. and Stratt, R.M. "Global perspectives on the energy landscapes of liquids, supercooled liquids, and glassy systems: The potential energy landscape ensemble." *J. Chem. Phys.* 127, 224503 (2007).

[7] Wang, C. and Stratt, R. M. "Global perspectives on the energy landscapes of liquids, supercooled liquids, and glassy systems: Geodesic pathways through the potential energy landscape." *J. Chem. Phys.* 127, 224504 (2007).

[8] Wiegel, F.W. *Introduction to Path-Integral Methods in Physics and Polymer Science.* Philadelphia: World Scientific Publishing Co Pte Ltd., 1986. Chap. 1.

[9] Allen, M.P. and Tildesley, D.J. *Computer Simulation of Liquids.* New York: Oxford University Press Inc., 1987. Appendix G.

[10] GSL - GNU Scientific Library. http://www.gnu.org/software/gsl/

[11] Random.org. https://www.random.org/

[12] Allen, M.P. and Tildesley, D.J. *Computer Simulation of Liquids.* New York: Oxford University Press Inc., 1987. Chap. 5.

[13] Allen, M.P. and Tildesley, D.J. *Computer Simulation of Liquids.* New York: Oxford University Press Inc., 1987. Chap. 3.

[14] Allen, M.P. and Tildesley, D.J. *Computer Simulation of Liquids.* New York: Oxford University Press Inc., 1987. Chap. 6.

[15] Abramowitz, M. and Stegun, I.A. *Handbook of Mathematical Functions with Formulas, Graphs and Mathematical Tables.* Washington, D.C.: National Bureau of Standards, 1964. Page 886.

[16] Allen, M.P. and Tildesley, D.J. *Computer Simulation of Liquids.* New York: Oxford University Press Inc., 1987. Chap. 2.

[17] Hansen, J. and McDonald, I.R. *Theory of Simple Liquids.* 2nd ed. San Diego, CA: Academic Press Inc., 1986. Chap. 12.

[18] Lombardo, T.G., Debenedetti, P.G., and Stillinger, F.H. "Computational probes of molecular motion in the Lewis-Wahnström model for *ortho*-terphenyl." *J. Chem. Phys.* 125, 175507 (2006).

[19] Goldstein, H. *Classical Mechanics.* 2nd ed. Philippines: Addison-Wesley Publishing Company, Inc., 1980. Chap. 4.

[20] Allen, M.P. and Germano, G. "Expressions for forces and torques in molecular simulations using rigid bodies." *Molecular Physics.* 104.20-21 (2006): 3225-3235.

[21] McQuarrie, D.A. *Statistical Mechanics.* Sausalito, CA: University Science Books, 2000. Chap. 17.

[22] Arfken, G.B. and Weber, H.J. *Mathematical Methods for Physicists.* 4th ed. San Diego: Academic Press, 1995. Chap. 12.

[23] McQuarrie, D.A. *Statistical Mechanics.* Sausalito, CA: University Science Books, 2000. Chap. 7.

[24] Feynman, R.P. and Hibbs, A.R. *Quantum Mechanics and Path Integrals.* New York: McGraw-Hill Companies, Inc., 1965. Chap. 2.

[25] Chandrasekhar, S. *Liquid Crystals.* 2nd ed. New York: Cambridge University Press, 1992. Chap. 2.

[26] Press, W.H., Teukolsky, S.A., Vetterling, W.T., and Flannery, B.P. *Numerical Recipes: The Art of Scientific Computing.* 3rd ed. New York: Cambridge University Press, 1992. Chap. 6.